CTS COMMUNICATIONS LINK CHARACTERIZATION EXPERIMENT TECHNICAL DATA REPORT VOLUME 3

AUGUST 1977

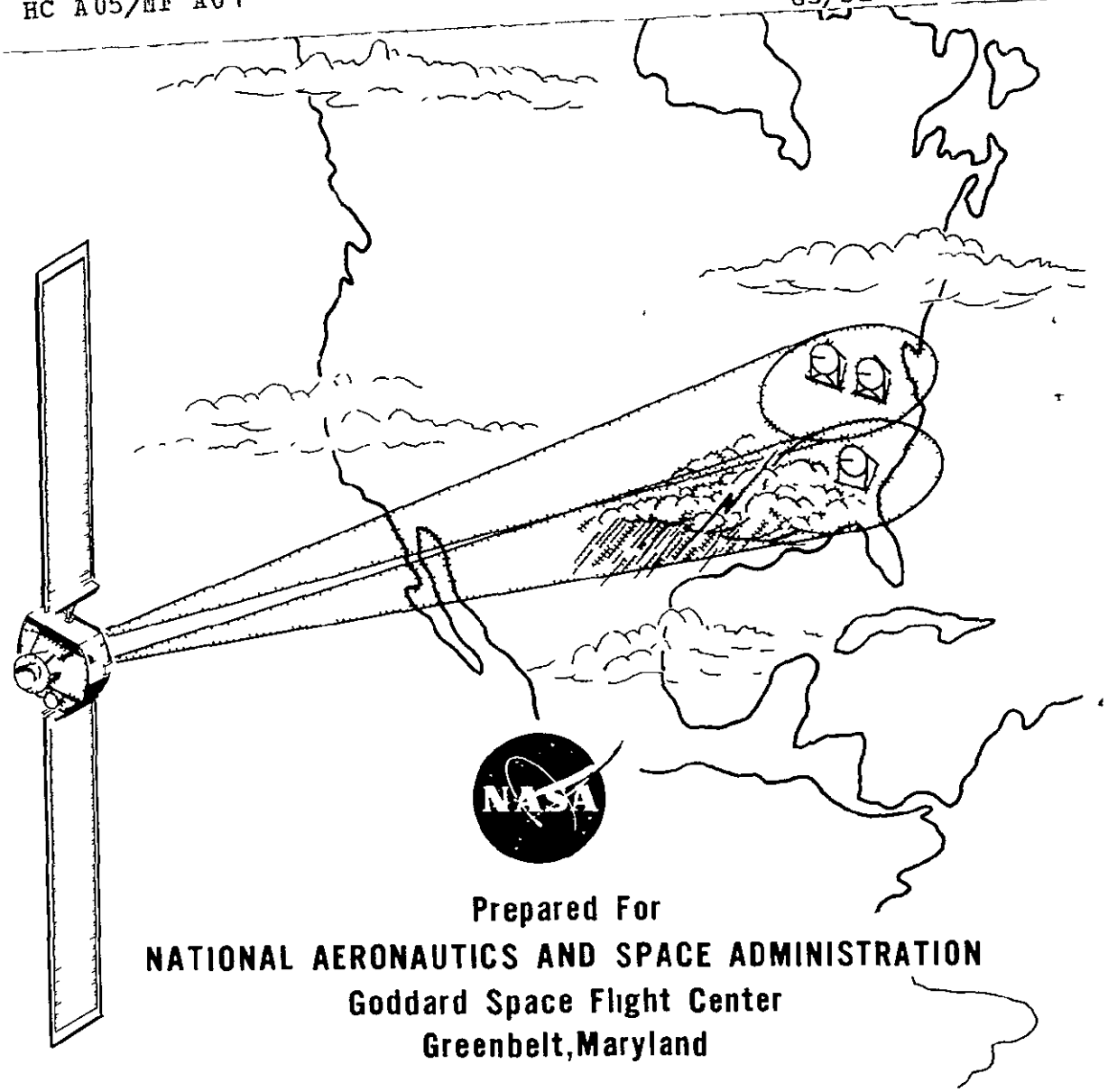

Prepared For

NATIONAL AERONAUTICS AND SPACE ADMINISTRATION

Goddard Space Flight Center

Greenbelt, Maryland

FIS-77-4057

COMMUNICATIONS LINK CHARACTERIZATION EXPERIMENT (CLCE)

Volume 3

TECHNICAL DATA REPORT

CONTRACT NAS 5-20729

AUGUST 1977

WESTINGHOUSE ELECTRIC CORPORATION
Defense & Electronic Systems Corporation
P.O. Box 1693
Baltimore, Maryland 21203

TABLE OF CONTENTS

LIST OF ILLUSTRATIONS

LIST OF APPENDICES (Continued)

LIST OF APPENDICES

LIST OF TABLES

SECTION I
INTRODUCTION

The purpose of this report is to present the results of the data which has been acquired, reduced and analyzed as of June 1977, from the Communications Link Characterization Experiment (CLCE) while utilizing the CTS satellite. Data presented in this report was acquired from the NASA Greenbelt PTF facility and the NASA Rosman Station located in Rosman, North Carolina.

The test data obtained from the Goddard Station consists of long term 11.7 GHz attenuation data and rain rate data obtained from a single rain bucket placed at the base of the receiving antenna. The data was reduced from strip chart recordings in which instantaneous rain rate values and approximate minutely mean attenuation (δ) values were obtained. The time period over which the data was obtained extended from June 1976 through May of 1977. In addition to the propagation experiment the Greenbelt facility is also conducting extensive television tests over the satellite links that include signal-to-noise tests as well as TV performance tests. The results of this extensive testing over the above yearly period will be presented in this report.

The Rosman station was able to obtain a more definitive description of the meteorological environment because on-beam backscatter measurements were obtained from the dual frequency weather radar and rain rate measurements were obtained from 10 tipping buckets rather than one as in the case for the Greenbelt Station. Also a finer resolution of the δ data was obtained because the on-site computer records the data at secondly average values. The data is reduced utilizing a 4 secondly mean.

In Section 2 of the report the long term yearly and worst month propagation data from both stations will be presented for the defined yearly period. In Section 3 the test results of the Goddard Television Experiment will be presented. In Section 4 the data for the continuing path length analysis started in reference (1) will be updated. In Section 5 the progress on the continuing analysis of utilizing the weather radars for attenuation prediction will be given. The concept of the weather radar ratio will be presented. In Section 6 a summary and conclusion for the presented data will be given.

SECTION 2
PROPAGATION DATA

2.1 INTRODUCTION

In this section the yearly and worst month propagation data obtained from both stations will be mainly presented in the form of cumulative distributions. The measurement time sample of the δ data as specified on each of the cumulative plots is the sum of the measurement times for each test run employed in the cumulative distribution. The start time for each test run should be defined as the time in which $\delta > 0$dB. This time is chosen as the time in which rain rate is measured or a measurable value of δ is obtained. The latter criterion is mainly determined by the ability of the system to measure a small amount of attenuation. Hence, the noise characteristics and the resolution capabilities of the measuring device play an important part in detecting small changes in δ. By also utilizing the rain rate factor to define the start time, the time in which the condition of $\delta > 0$dB exists can be determined even if the system is not capable of measuring the small changes in the received signal level.

2.2 GREENBELT PROPAGATION DATA

The data presented for this station was measured over a 12 month period starting in June of 1976 through May of 1977. Over that period the most intense storm occurred on May 6, 1977. A time history of the resulting δ and rain rate data is shown in Figure 2-1. Attenuation values exceeded 30 dB at two points in time where the receiver broke lock. Exact time correspondence between the 185MM/HR rain rate peaks and the δ peaks wasn't obtained. The rain rate peaks tended to lead the δ peaks as shown in figure.

If it is assumed that the path length of the intense storm cell is on the order of 1 km and the peak rain rate within the cell is 185MM/HR then the resulting δ value is only 11.46 dB. To attain a δ of 30 dB the required rain rate value must be 399MM/HR. The time between bucket tips for the 185 MM/HR value is 4.94 seconds and for the 399 MM/HR value it is 2.3 seconds. This small time difference can cause large errors in the determination of the rain rate values in the 200 to 400 range because of the relatively low rain rate chart speed of 6" per hour. Hence, the peak rain rate could have been much higher than the 185 MM/HR value that was computed.

The yearly cumulative distribution for the δ data obtained at the PTF is shown in Figure 2-2. This plot was computed on the basis of the total yearly time between June 1976 to May of 1977. The measurement sample for this data consists of 14, 647 minutes of measured δ values. As shown the peak δ value of 30 dB corresponding to a percentage value of 0.0013% was obtained for the defined year. At the 11.7 GHz frequency an attenuation of 30 dB is an extremely rare event for a ground-to-satellite communication link. The yearly cumulative distribution for rain rate is shown in Figure 2-3. An instantaneous rain rate value of 180 MM/HR was exceeded for .00015% of the time which corresponds to the δ value of 30 dB. Because of the possible large errors in determining large rain rate values the magnitudes of the rain rates below the .001% point are suspect.

Figure 2-4 shows the plots of the cumulative distributions for the long term attenuation and rain rate plots given in Figures 2-2 and 2-3. This type of presentation is used mainly for obtaining δ and rain rate pair values at a given percentage value. The δ cumulative distribution is plotted for the total attenuation measurement time of 14, 647 minutes. The rain rate measurement time was less than the δ time due mainly to the fact that the above time encompasses measurement periods where only overcast skies were present before rain started to actually fall.

Because of this discrepancy, the rain rate cumulative is normalized to the attenuation time.

The "worst month" attenuation (δ) and rain rate statistics for the year of 1976 are given in Figures 2-5 and 2-6 respectively.

Various definitions can be developed for defining "worst" month statistics from data obtained from a number of months. One would involve choosing an arbitrary level of say 5 dB and then defining the "worst" month as the month in which the above level was exceeded for the maximum time percentage of the month. Another criteria would be to choose the month in which the highest δ value was measured. For communication systems with relatively low fade margins, the former criterion is more applicable. Of course, both criteria could be met in a particular month since they are not mutually exclusive.

For the Greenbelt station the month of August fulfills both criteria for the "worst month" statistics in 1976. Attenuation was actually measured for 0.6% of the month. However, if time in which rain was recorded is taken into account the first δ bin would correspond to 1%. The total time in which rain occurred in the elevated beam in which an attenuation measurement was attempted was 351 minutes. The corresponding rain rate cumulative distribution in Figure 2-6 shows measured rain rates on the order of 180 MM/HR occurred during the month.

The worst month statistics obtained to date for 1977 occurred in the month of May. A time history of the resulting peak attenuation values is shown in Figure (2-1). The δ statistics for this month is shown in Figure (2-7) and the corresponding rain rate statistics in Figure (2-8). In comparing Figures (2-5) and (2-7), it is noticed that the attenuation time sample for August was higher (351 minutes versus 227 minutes); however, due to the intense storm that occurred on May 6, the peak attenuation values exceeded 30 dB while in August, δ values greater than 20 dB was measured. For worst month statistics, one storm lasting a few minutes can alter the δ statistics for percentage values less than about 0.05% which corresponds to a time of 22.3 minutes. For the overall time period, the worst month statistics should correspond to May of 1977.

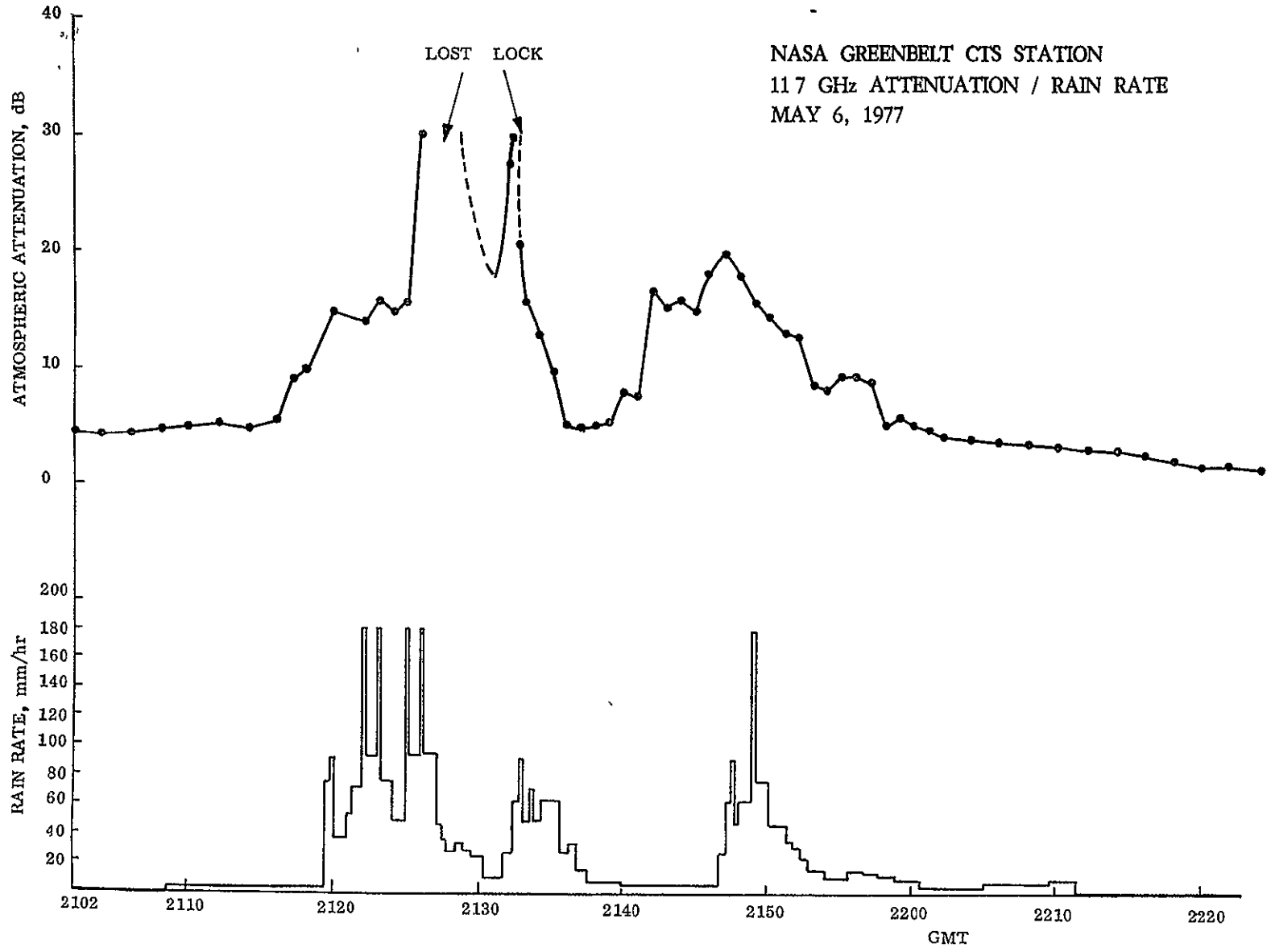

Figure 2-1. Time Plot of 11.7 GHz Attenuation and Rain Rate

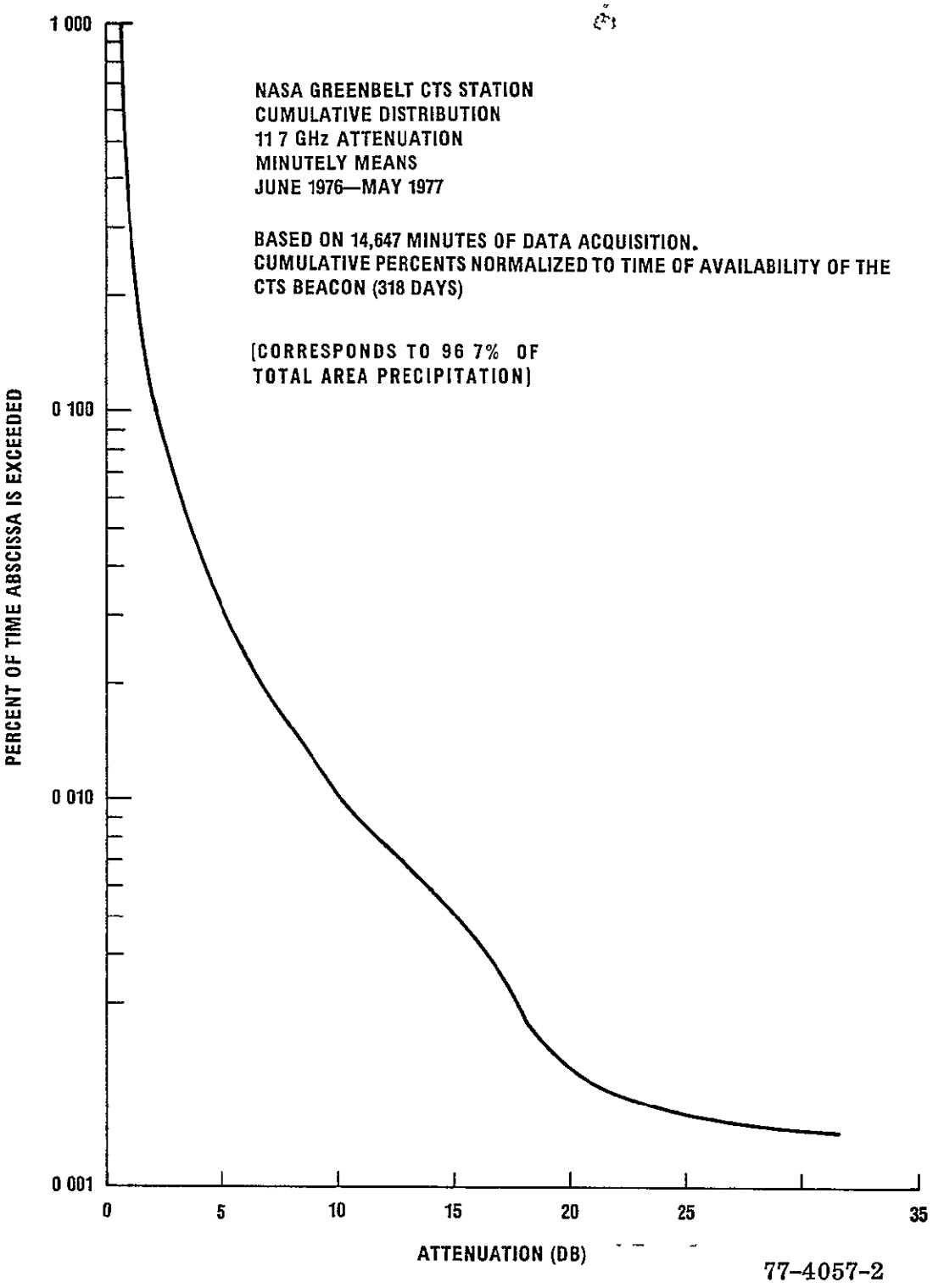

Figure 2-2. Yearly Cumulative Distribution for 11.7 GHz Attenuation Measured at the Greenbelt Station

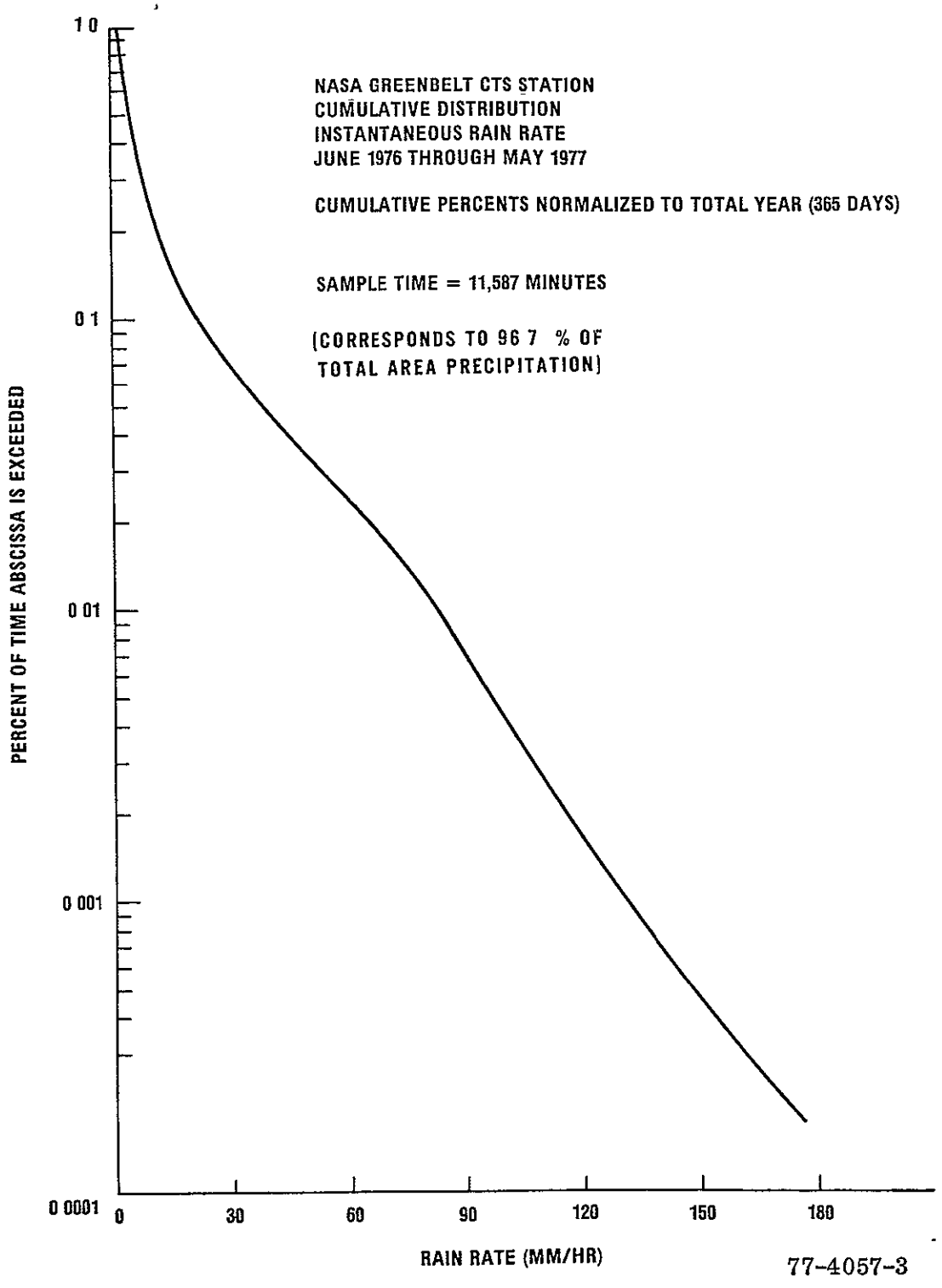

Figure 2-3. Yearly Cumulative Distribution for Rain Rate Measured at the Greenbelt Station

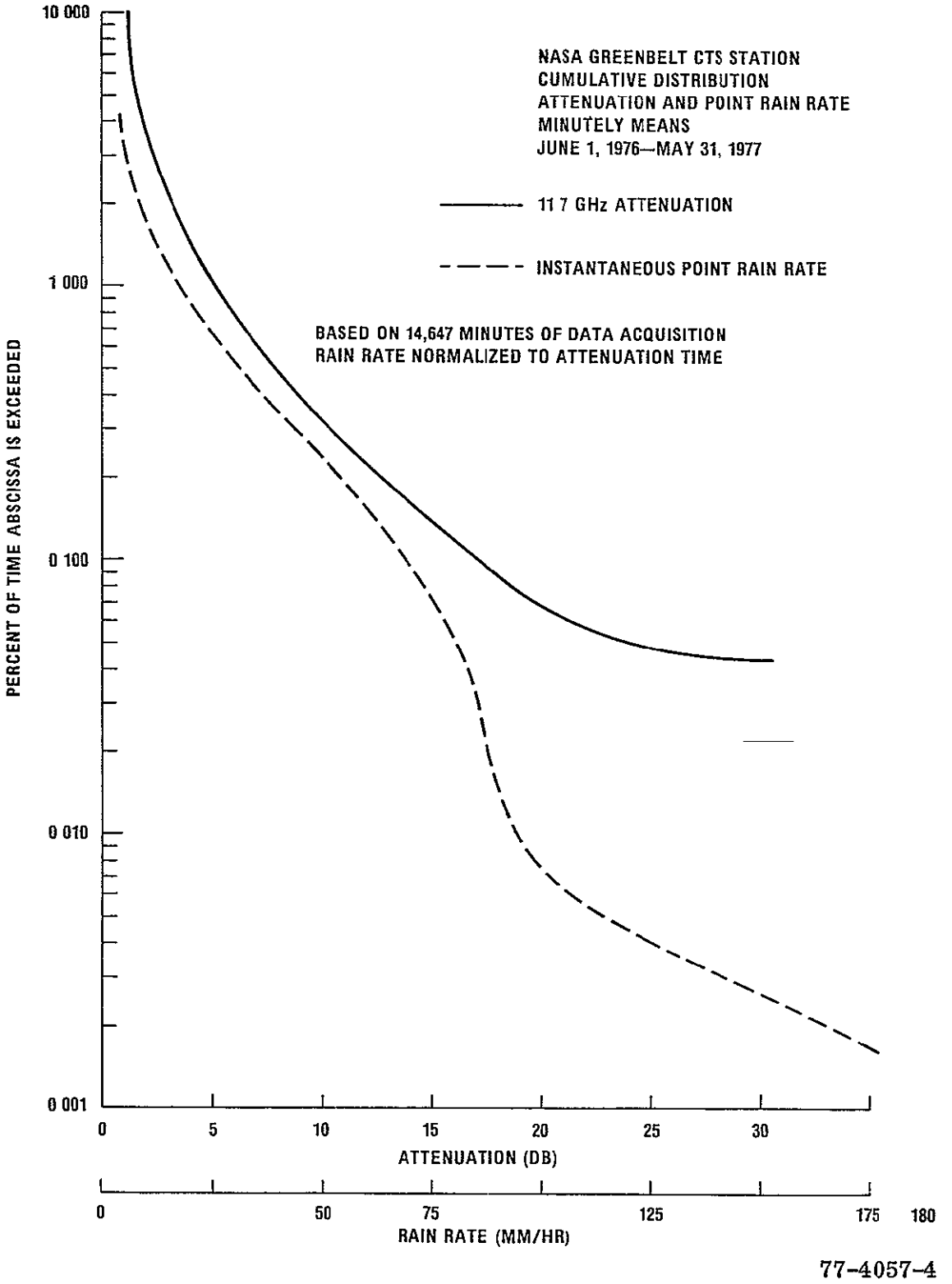

Figure 2-4. Long Term Rain Rate and Attenuation Cumulative Distribution

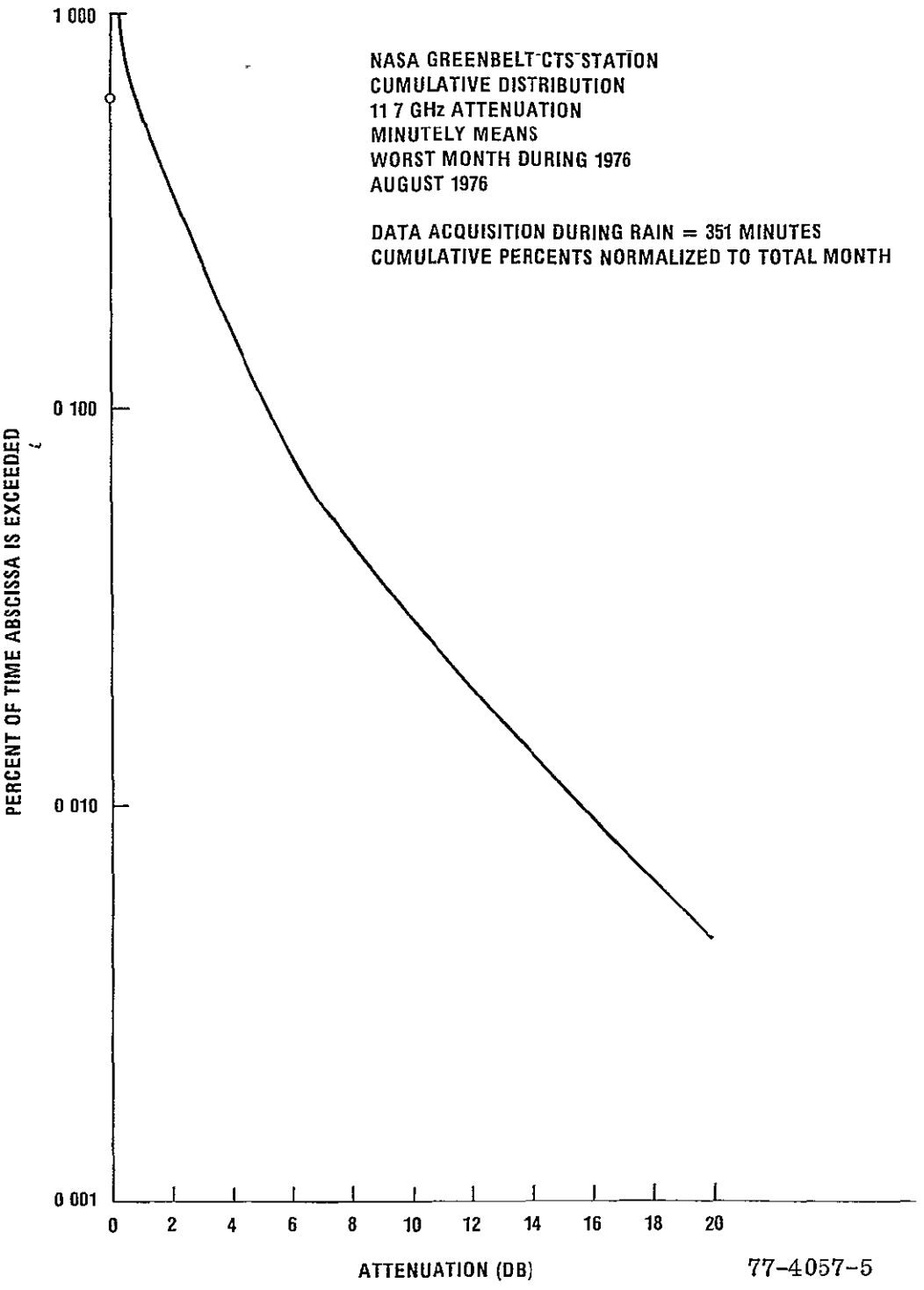

Figure 2-5. Worst Month Attenuation Statistics for 1976 (August) Measured at the Greenbelt Station

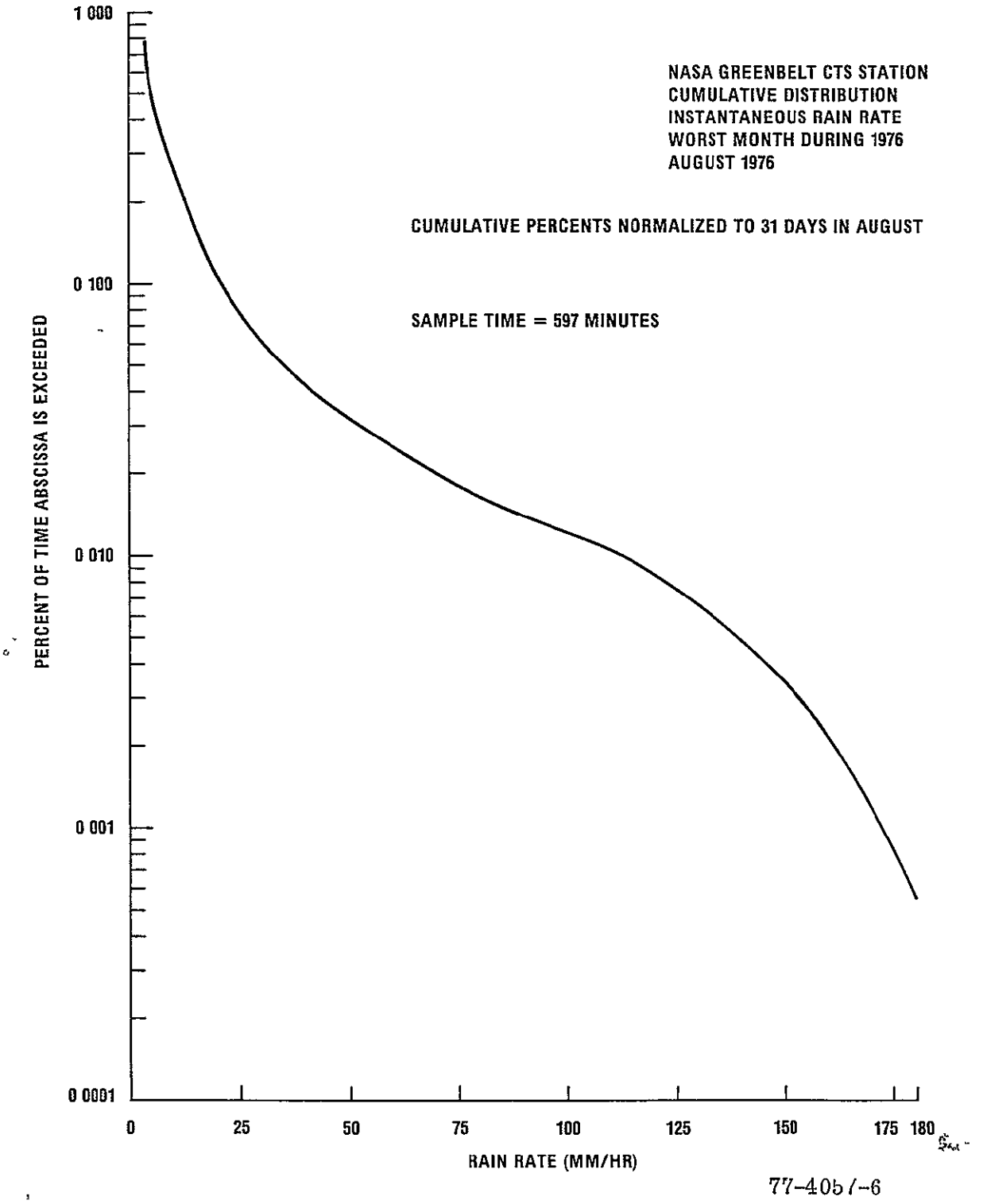

Figure 2-6. Worst Month Rain Rate Statistics (1976) Measured at the Greenbelt Station

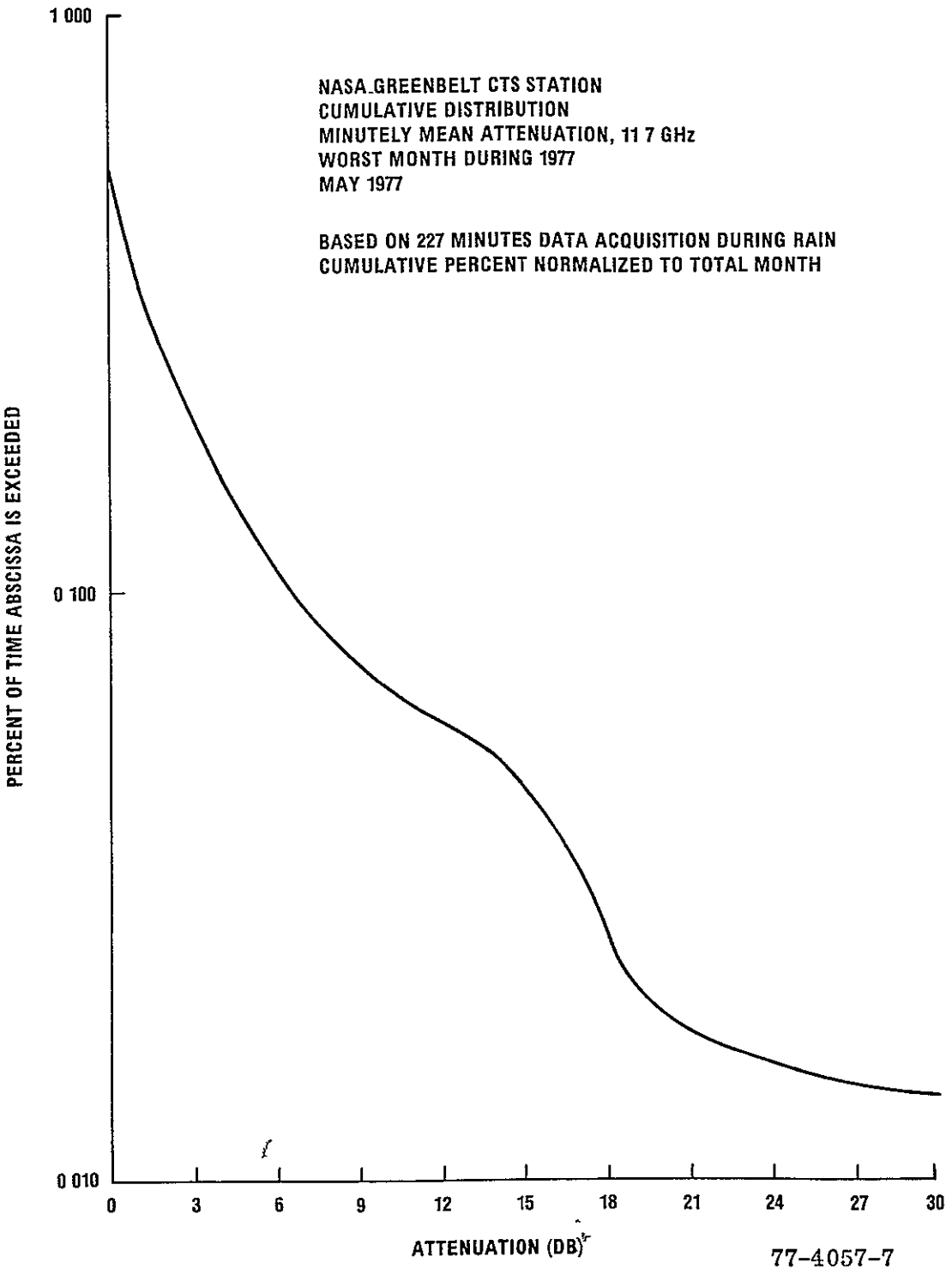

Figure 2-7. Worst Month Attenuation Statistics for 1977 (May) Measured at the Greenbelt Station

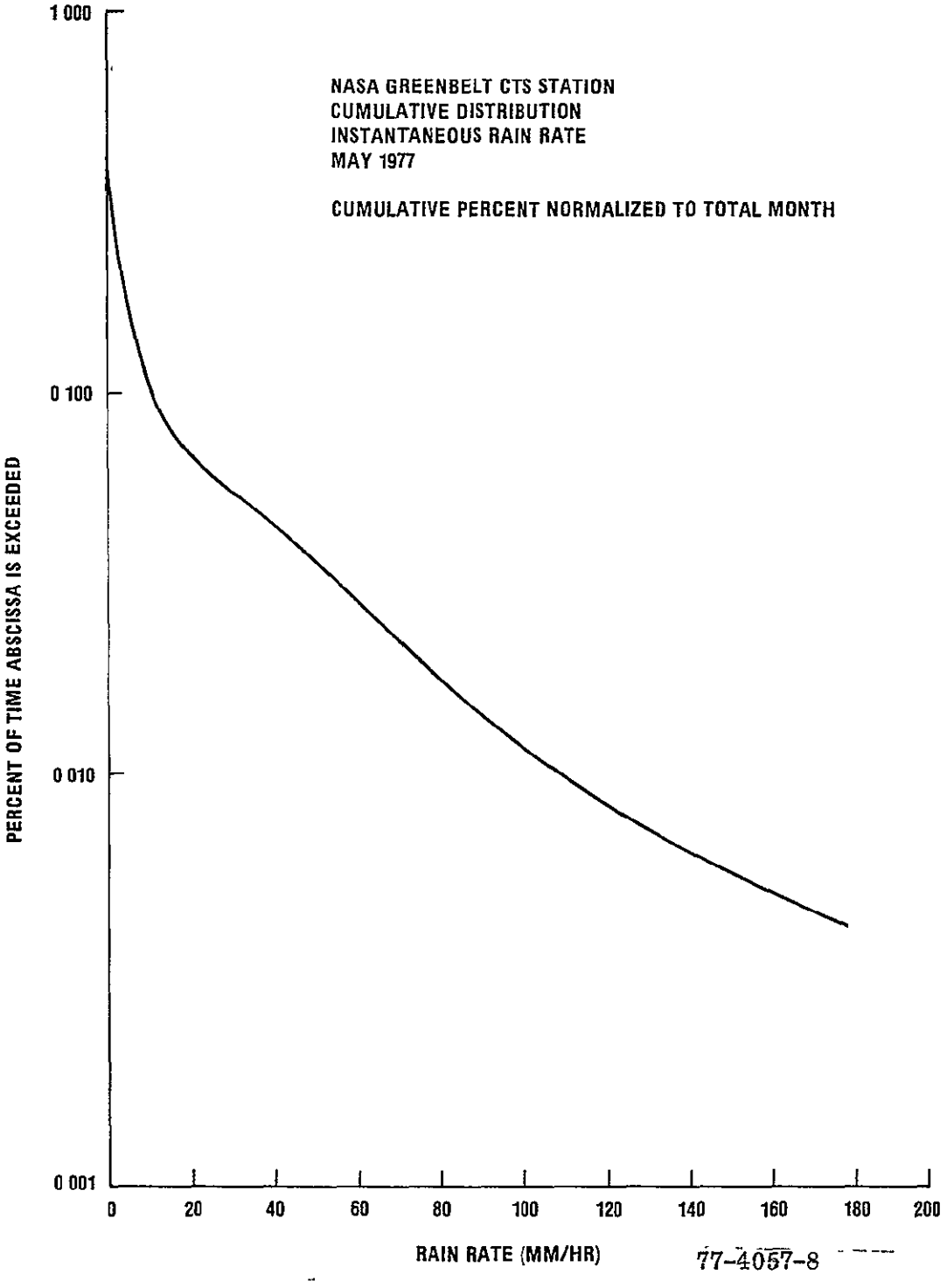

Figure 2-8. Worst Month Rain Rate Statistics for 1977 (May) 1977 Measured at the Greenbelt Station

2.3 ROSMAN PROPAGATION DATA

For the Rosman data four second means are employed for the cumulative distributions of δ and rain rate. Rain rate statistics are presented in the form of a point rain rate defined as the near bucket (NB), (rain bucket that is in close proximity to the main receive antenna) and the ground average (GA), which is the average of the ten tipping buckets placed under the elevated beam. The δ and rain rate cumulative distributions are shown in Figures 2-9 and 2-10, respectively.

As shown in the above figures the sample time for δ is less than the time for the NB which is less than the time for GA. Also, the statistics cover a period of June 1, 1976 to June 30, 1977, a period of 13 months. The larger sample times for rain rate stem from the fact that in certain test runs only the rain rate was measured. The limitations of the point rain rate measurement are shown in comparing the sample times of GA and NB. The point measurement did not measure precipitation for a 1509 minute time period over the overall measurement time.

The rain rate data obtained at Greenbelt was measured from a single rain bucket placed near the receiving antenna and reduced manually from the resulting bucket tips on a strip chart. Therefore, all rain that was collected by the bucket was recorded and analyzed. The reduced amount of data (11, 587 minutes) corresponds to 33.29" of rain which compares to the weather bureau measurement for the same general area of 34.43" of rain. Therefore, the single bucket measurement at Greenbelt was within 96.7% of the measurement taken by the weather bureau. The long term attenuation statistics given in Figure (2-3) is an excellent measure of the values that should be obtained in the Greenbelt area.

For the Rosman station; a computer program is utilized to obtain the 4 secondly mean rain rate statistics. The input to the program are the instantaneous bucket tips recorded on magnetic tape from the ten tipping buckets. The total measured precipitation time for the average of the ten buckets (GA) is 6521 minutes as compared to near bucket (NB) time of 5012 minutes. For the GA time, a total of 18.4" of rain was measured. The weather bureau maintains a measuring device in the town of Rosman and for the 13 month period between June 1, 1976 to July 1, 1977 a total of 82.16" of rain was measured. The Rosman station is located about 8 miles from the town and is about a 1000' higher.

At the Rosman station automated precipitation measurements were only taken over a daily 8 hour working period from June 1, 1976 to March of 1977. From March to July 1 of 1977, measurements were taken over a 24 hour period due to the use of an automated program which initiated the rain rate and attenuation measurements when at least two bucket tips occurred within a 15 minute interval. This interval corresponds to a rain rate of 1 MM/HR. Due mainly to the daily 8 hour measurement period, the measured precipitation only covered 22.4% ($\frac{18.4}{82.16}$) of the total precipitation that fell in the general area.

The rain rate and δ cumulatives for both NB and GA factors are shown in Figures 2-11 and 2-12, respectively. In these cases the rain rate cumulatives were normalized to the attenuation time of 4148 minutes. As previously stated the higher rain rate times are due to measuring rain rate at times that attenuation was not measured. Normalizing to the lower attenuation time essentially assumes that the rain rate distribution in the overall rain rate measurement time and the attenuation time are equivalent.

The "worst month" rain rate and δ statistics for the Rosman station are shown in Figures 2-13 and 2-14 , respectively. For this month the signal was affected by rain for 1.6% of the total monthly time. The sample time for the GA factor is 934 minutes which correspond to a percentage factor relative to the total month's time of 2.2%. Relative to the other months a large amount of rain was recorded and the near peak measurable δ value was 22 dB.

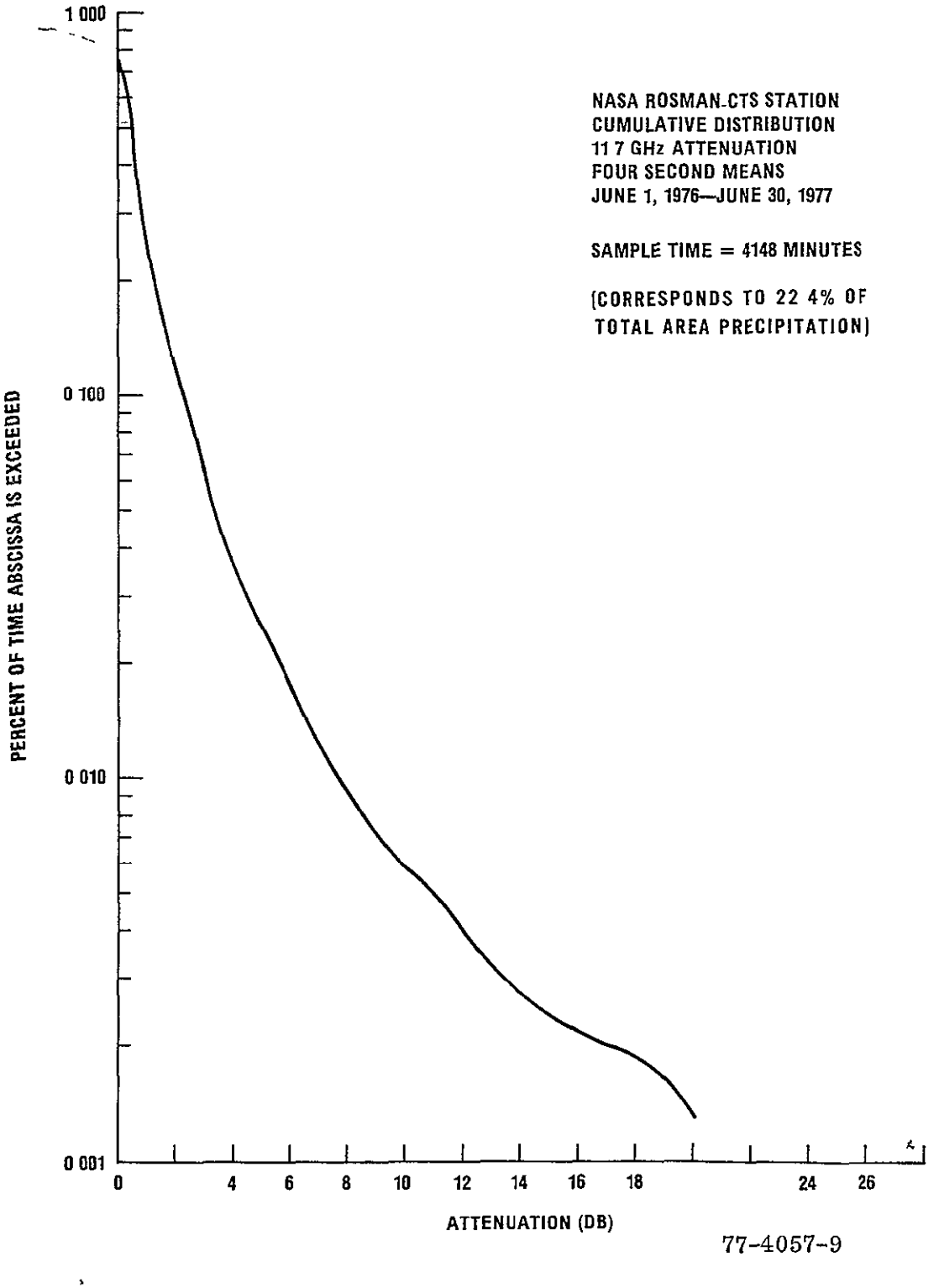

Figure 2-9. Long Term Cumulative Distribution of 11.7 GHz Attenuation Measurement at the Rosman, North Carolina Station

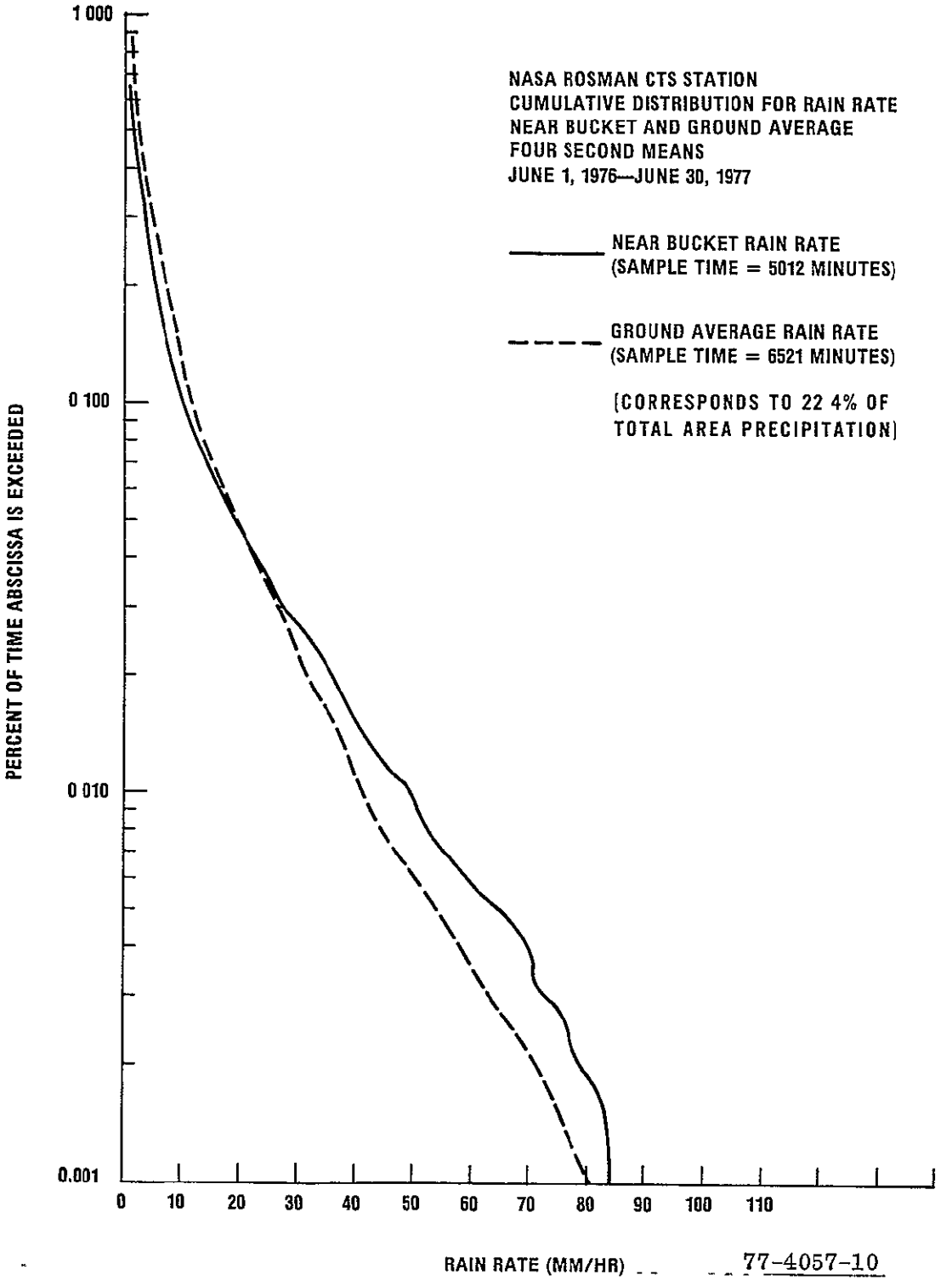

Figure 2-10. Long Term Rain Cumulative Distributions at the Rosman, North Carolina Station

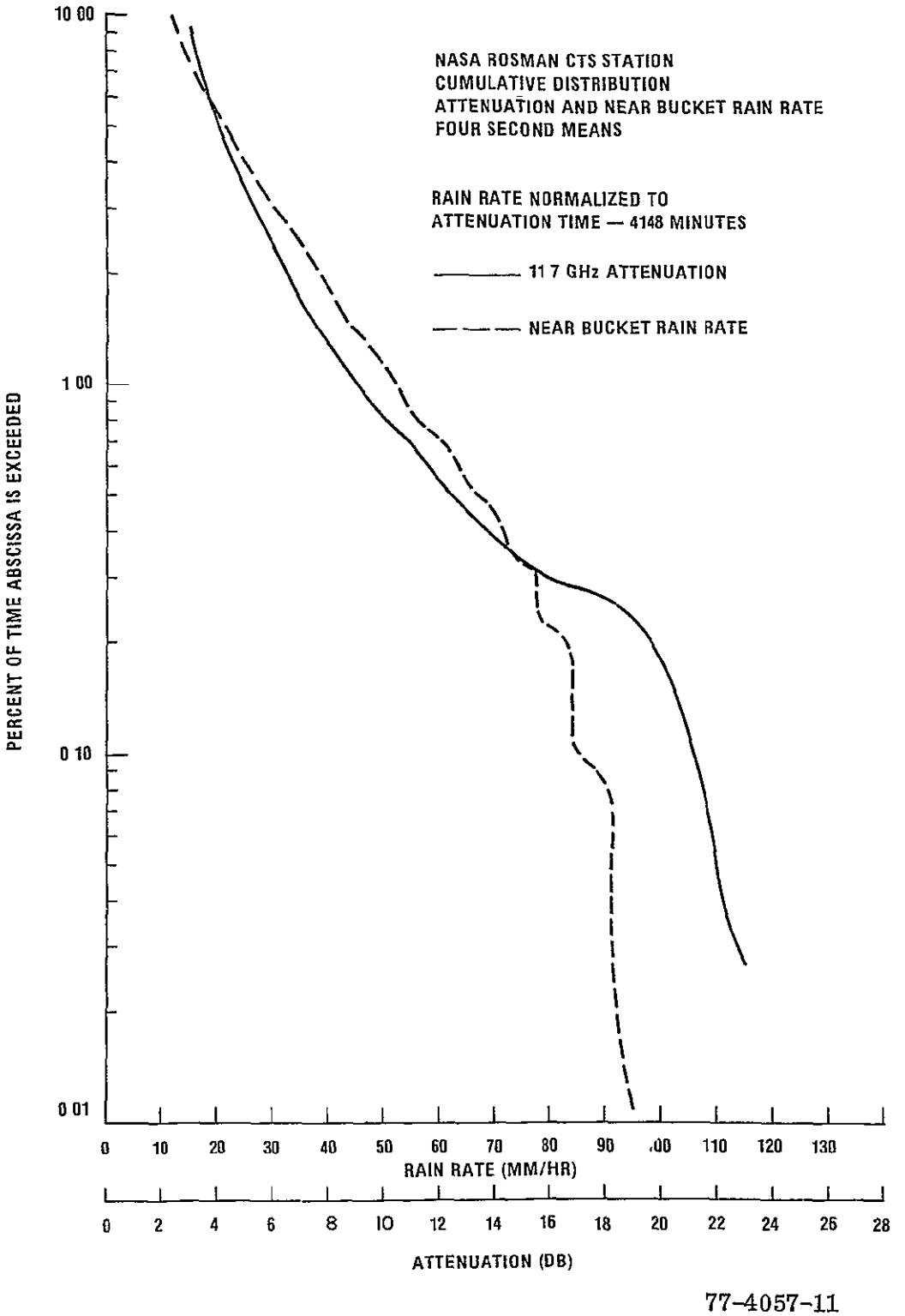

Figure 2-11. Long Term Rain Rate (NB) and Attenuation Distributions at the Rosman, North Carolina Station

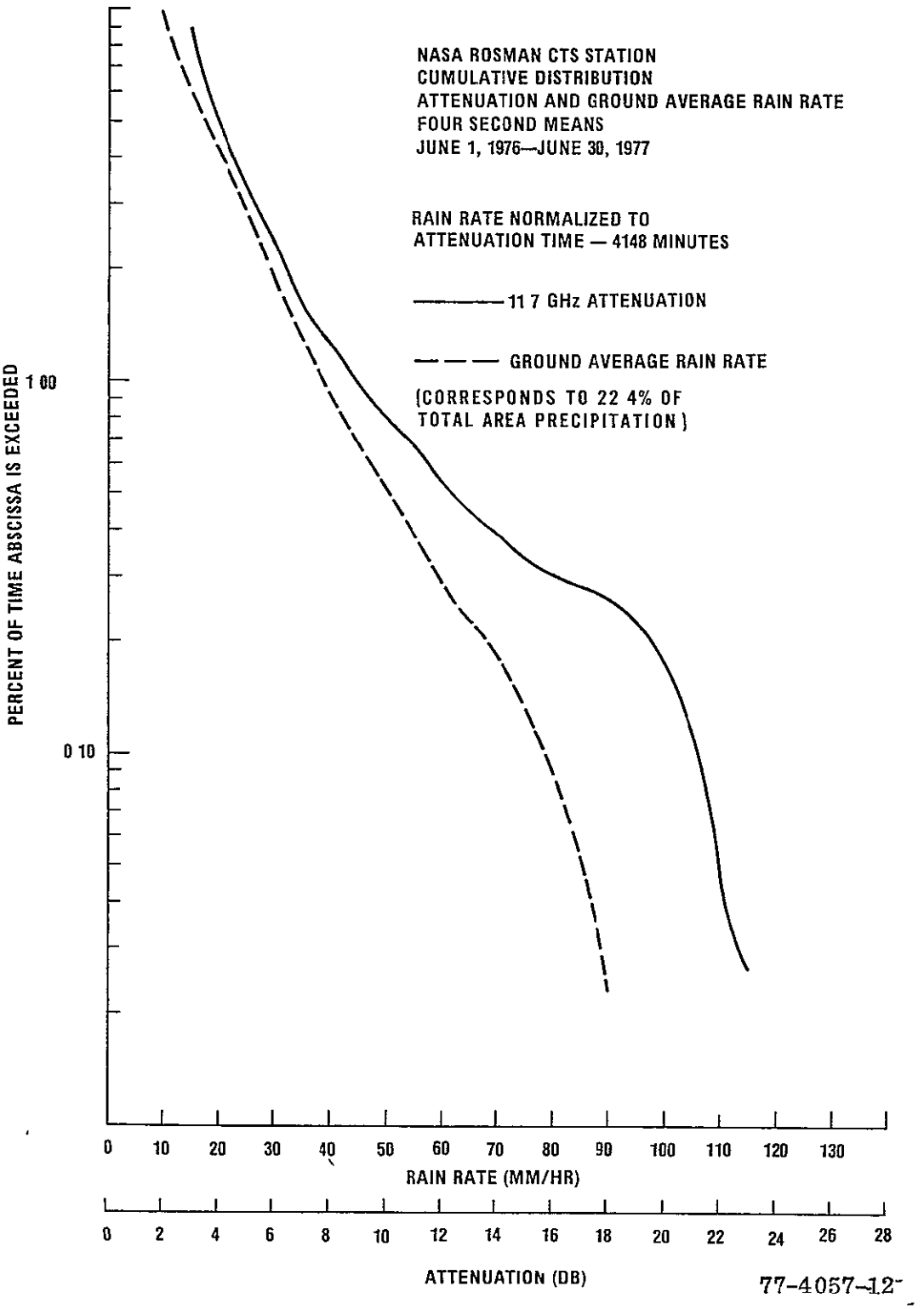

Figure 2-12. Long Term Rain Rate (GA) and Attenuation Distributions at the Rosman North Carolina Station

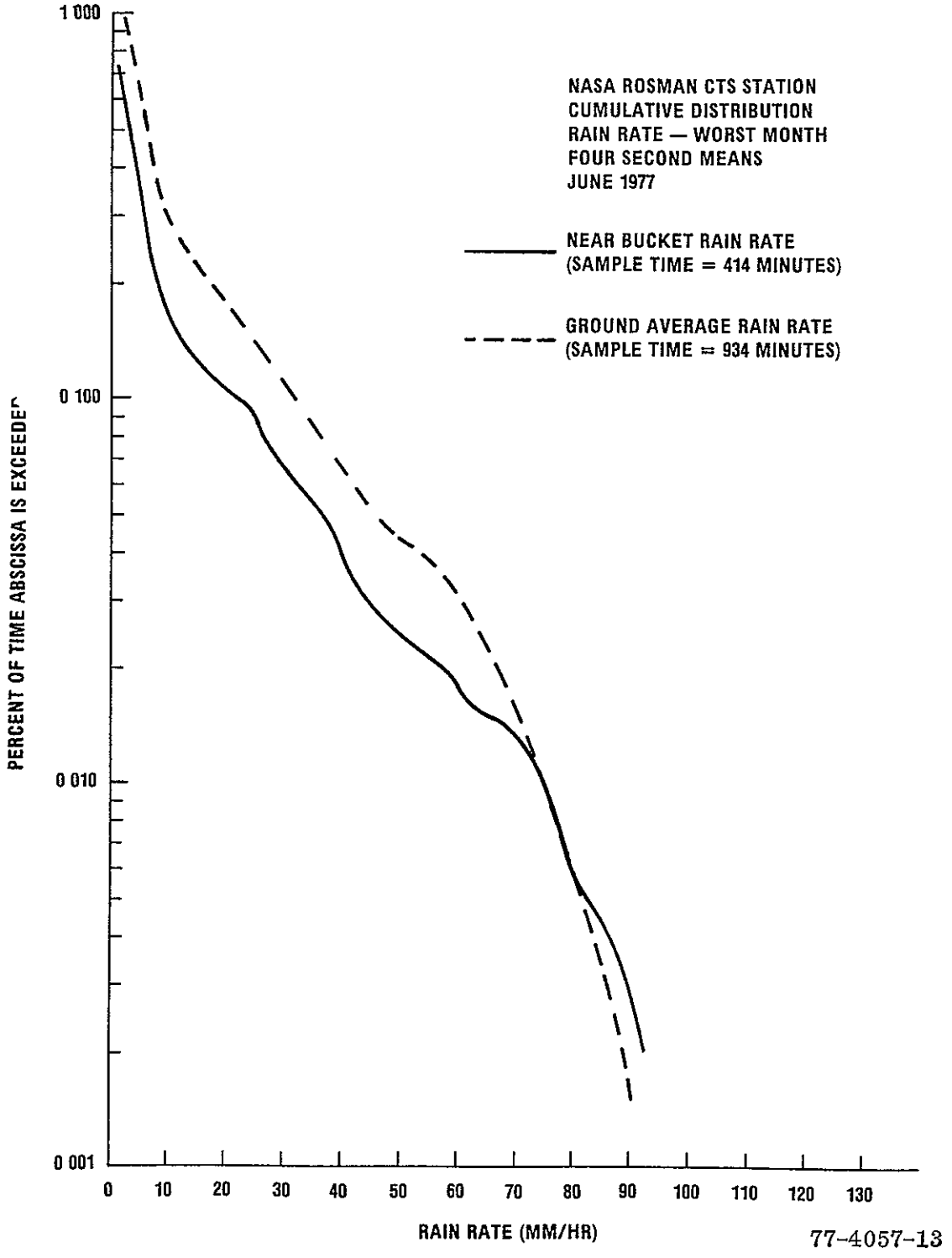

Figure 2-13. Worst Month Rain Rate Statistics in 1977 (June) for the Rosman, North Carolina Station

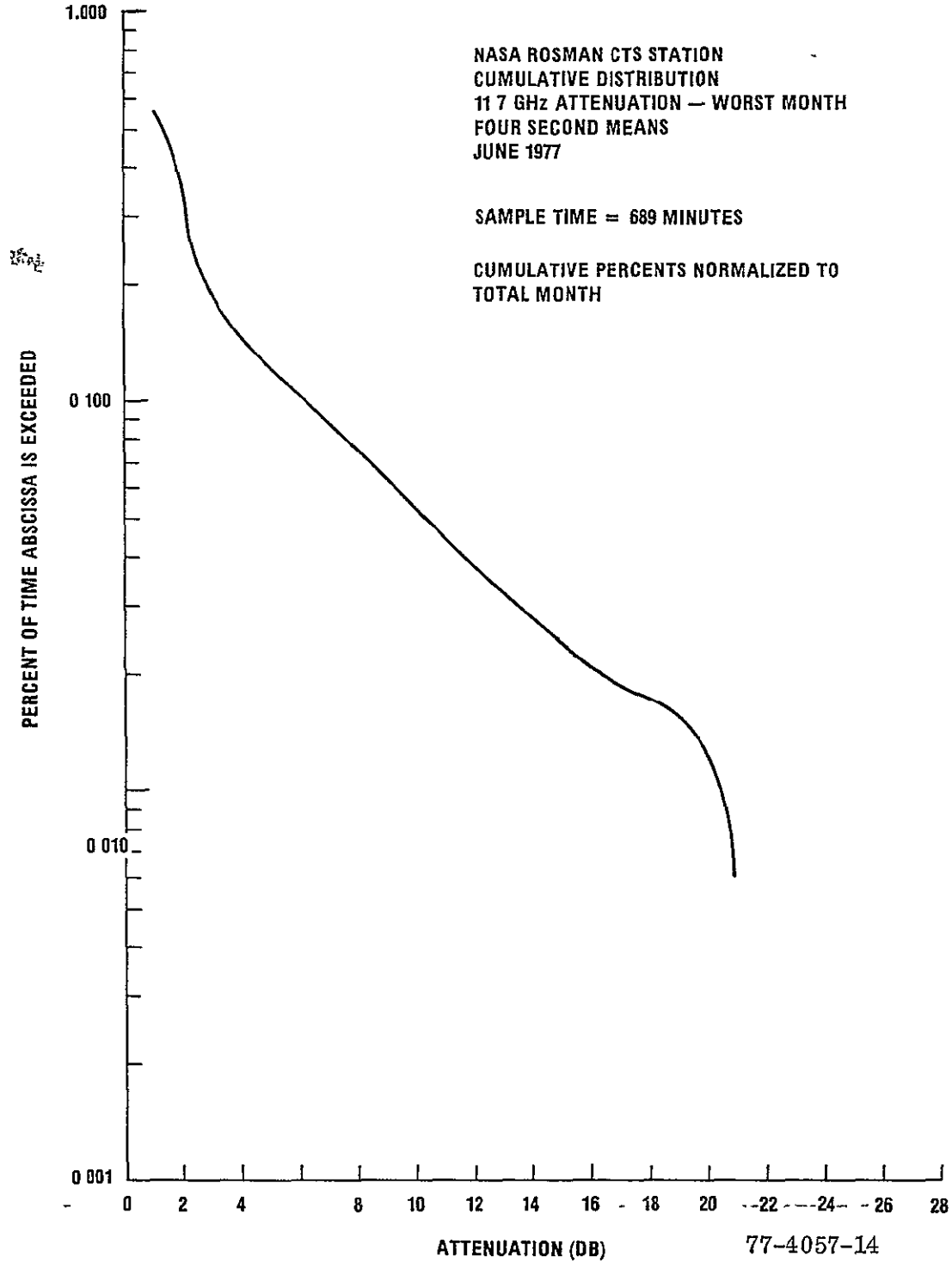

Figure 2-14. Worst Month Attenuation Statistics for 1977 (June) for the Rosman North Carolina Station

2.4 PROPAGATION DATA SUMMARY

A large amount of rain rate and attenuation data has been reduced for the general time period June 1976 through June 1977. A summary of this data is presented in Tables I and II for three representative percentage factors. The long term data collected at the Greenbelt station was 3.5 times greater than the data collected at Rosman. It is interesting to note that for the "worst month" statistics the collected data at Rosman was twice the data obtained at Greenbelt. It is also noticed that the 4 second averaging of the rain rate at Rosman drastically reduces the peak rain rate values relative to those obtained at Greenbelt which employs instantaneous values. This is due to the fact that high rain rate values involve the time between bucket tips that are on the order of a few seconds. Hence, averaging even over a few seconds can effect the rain rate values. This fact coupled with the previous statement that involves the resulting poor accuracy of measuring high rain rate values from strip charts moving at a relatively slow speed causes divergence of the high rain rate measurement from both stations.

The "worst" month statistics for both Greenbelt and Rosman is shown in Figure 2-15. Because Rosman utilizes a 4 second average and recorded data over a longer period of time (689 minutes versus 351 minutes) it is expected that the peak attenuation values below the 0.1% level would be higher for Rosman. If service times corresponding to percentage values greater than 0.01% are desired then the averaging time of the attenuation values must be specified since cumulative plots of different averaging times tend to diverge in these low regions.

As shown in Figure 2-7 the worst month (May 1977) statistics for Greenbelt greatly exceed the statistics for either June or August. However, in the determination of the most representative worst month statistics for a given locale, the occurence of the violent storm (May 6) that caused such a high measurable value of δ is a rare event that in the long term shouldn't be considered as representative of the general types of storms that occur in the region.

TABLE I

SUMMARY OF 11.7 GHz ATTENUTATION STATISTICS

	PERCENTAGE VALUES		
	0.1%	0.01%	0.005%
Rosman (4 Sec. Mean) Yearly = 4148 Minutes (Less than 22.4% of Total Precipitation*)	2.2 dB	8 dB	11.2 dB
Worst Month June 1977 689 Minutes	6.4 dB	20.2 dB	21 2 dB
Greenbelt (Minutely Mean) Yearly = 14647 Minutes (Within 96.7% of Total Precipitation*)	2 1 dB	10 dB	15 dB
Worst Month August 1976 351 Minutes	5 dB	15.6 dB	19.4 dB
Worst Month May 1977 227 Minutes	6.5 dB	>30 dB	

*Corresponds To Total Area Precipitation.

TABLE II

SUMMARY OF RAIN RATE STATISTICS

	PERCENTAGE VALUES					
	0.1%		0.01%		0.005%	
	NB (MM/HR)	GA (MM/HR)	NB (MM/HR)	GA (MM/HR)	NB (MM/HR)	GA (MM/HR)
Rosman (4 Sec. Mean) Yearly NB = 5012 Minutes GA = 6521 Minutes Corresponds to 22.4% of Total Precipitation*	11	12	49	41	65	54
Worst Month June 1977 NB = 414 Minutes GA = 934 Minutes	22	32	75	75	82	82
Greenbelt (Minutely Mean) Yearly 11587 Minutes Corresponds to 96.7% of Total Precipitation*	21		82		147	
Worst Month August 1976 597 Minutes	20		112.5		140	
Worst Month May 1977 178 Minutes	10		110			

*Corresponds To Total Area Precipitation.

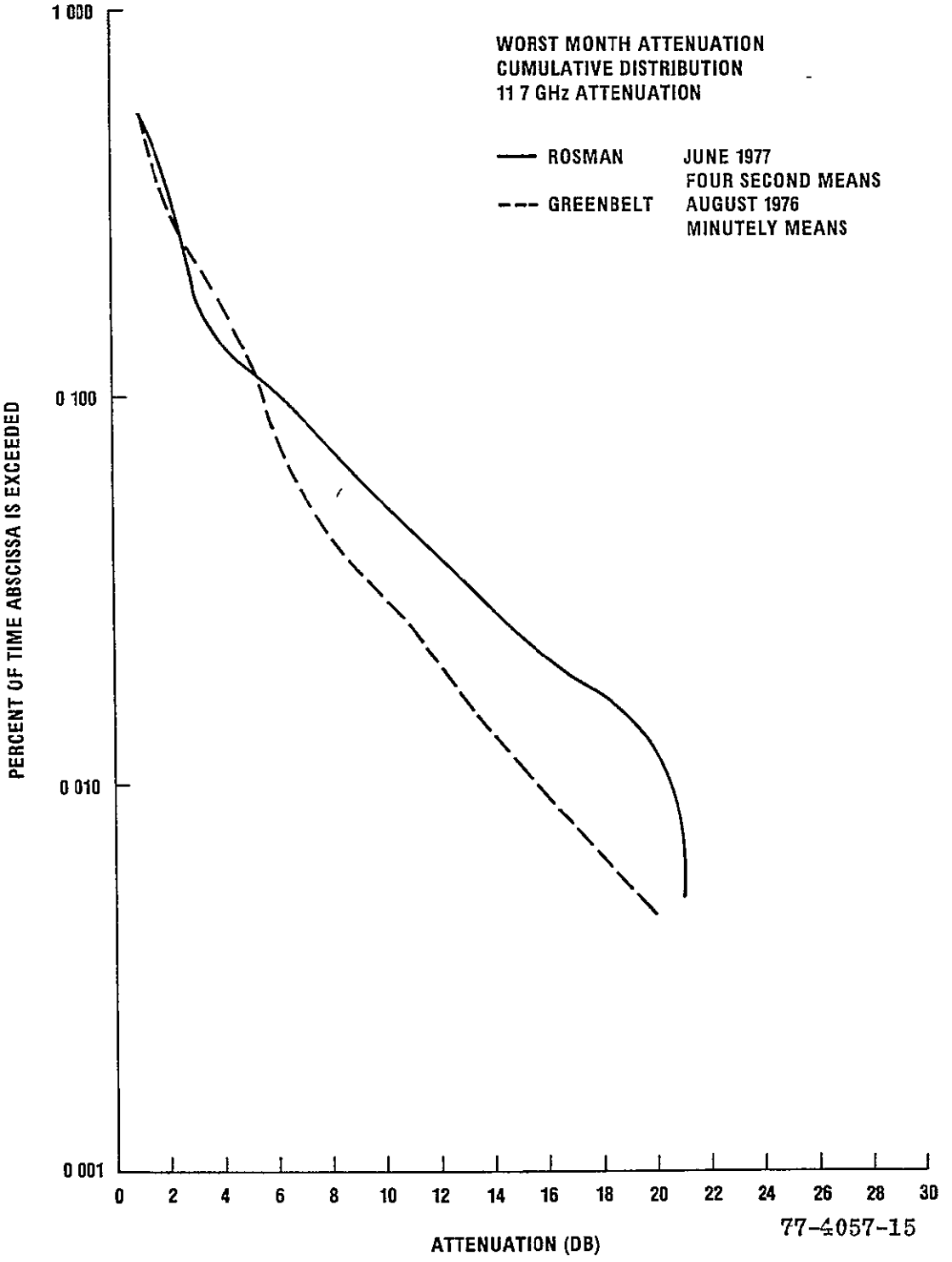

Figure 2-15. Worst Month Attenuation Cumulative Distribution 11.7 GHz Attenuation

2.5 METEOROLOGICAL PARAMETERS

In addition to the attenuation (δ) measurement at the Rosman station measurements of point rain rate, ground average rain rate and backscatter measurements from a multifrequency radar are performed concurrently. A description of the radar is given in section 5 and reference (7). One of the objectives of the experiment is to determine functional relationships between these meteorological parameters and the 11.7 GHz attenuation.

Figures 2-16 and 2-17 show scatter plots of 4 second mean values of the integrated radar reflectivity versus δ for the 3 GHz and 8.75 GHz frequencies. As shown a definite functional relationship exists up to a δ of about 4 dB. The leveling out and decrease in the radar return is caused by two effects: (1) As the δ increases returns are received by a greater number of range bins, because the range bin threshold level increases as the range to the bin increases, the returns from the higher range bins can be below their respective threshold values thus they would be eliminated in the integrating process (2) Since the elevated radio beam and the radar beam are not exactly coincident, the precipitation causing the attenuation may not be within both beams at the same time. It is believed that this latter factor is the reason for the non-functional relationship between parameters as will be shown. These plots illustrate the difficulty in attempting to independently measure the effects of the attenuation.

In Figures 2-18 and 2-19 the integrated radar return is plotted against the near bucket rain rate. The same type of leveling off is seen in these plots even though NB values exceeding 80 MM/HR were measured. It appears that the rain cell causing the attenuation must have been localized near the first rain bucket and its intensity rapidly decreased passed this general area. The large spread in the radar return for rain rate values less than 10 MM/HR is probably due to the fluctuation in the radar parameter over the time between bucket tips (For rain rate of 10 MM/HR, $\Delta t \approx 1.5$ minutes) necessary to measure rain rates less than 10 MM/HR.

In Figure 2-20 the near bucket rain rate (NB) is plotted against δ. A general trend between NB is noted at all δ values other than in the 8 dB region. In comparing this plot with the ground average rain rate (GA) versus δ plot shown in Figure 2-21, it is noticed that a definite decrease in GA occurs in the δ region of 8 dB. This result along with the plots shown in Figures 2-18 and 2-19 show that the main precipitation region was, in fact, located in close proximity to the NB. A measure

of the degree of non-homogeneousness of the rain environment can be obtained from the scatter plot of NB versus GA shown in Figure 2-22. The general trend of the points show that NB>GA so the conclusions stated above are also borne out by this plot. The plots shown in the Figures 2-16 through 2-22 are an excellent example of the difficulties involved in obtaining a quantitative estimate of the intensity of precipitation that is causing the attenuation on a test run basis. It could be concluded that a realistic functional relationship between δ and the meteorological parameters can only be obtained from sets of long term data compiled over a long period of time and encompassing different types and degrees of precipitation, such as the use of long term cumulative distributions to obtain rain rate and attenuation pairs.

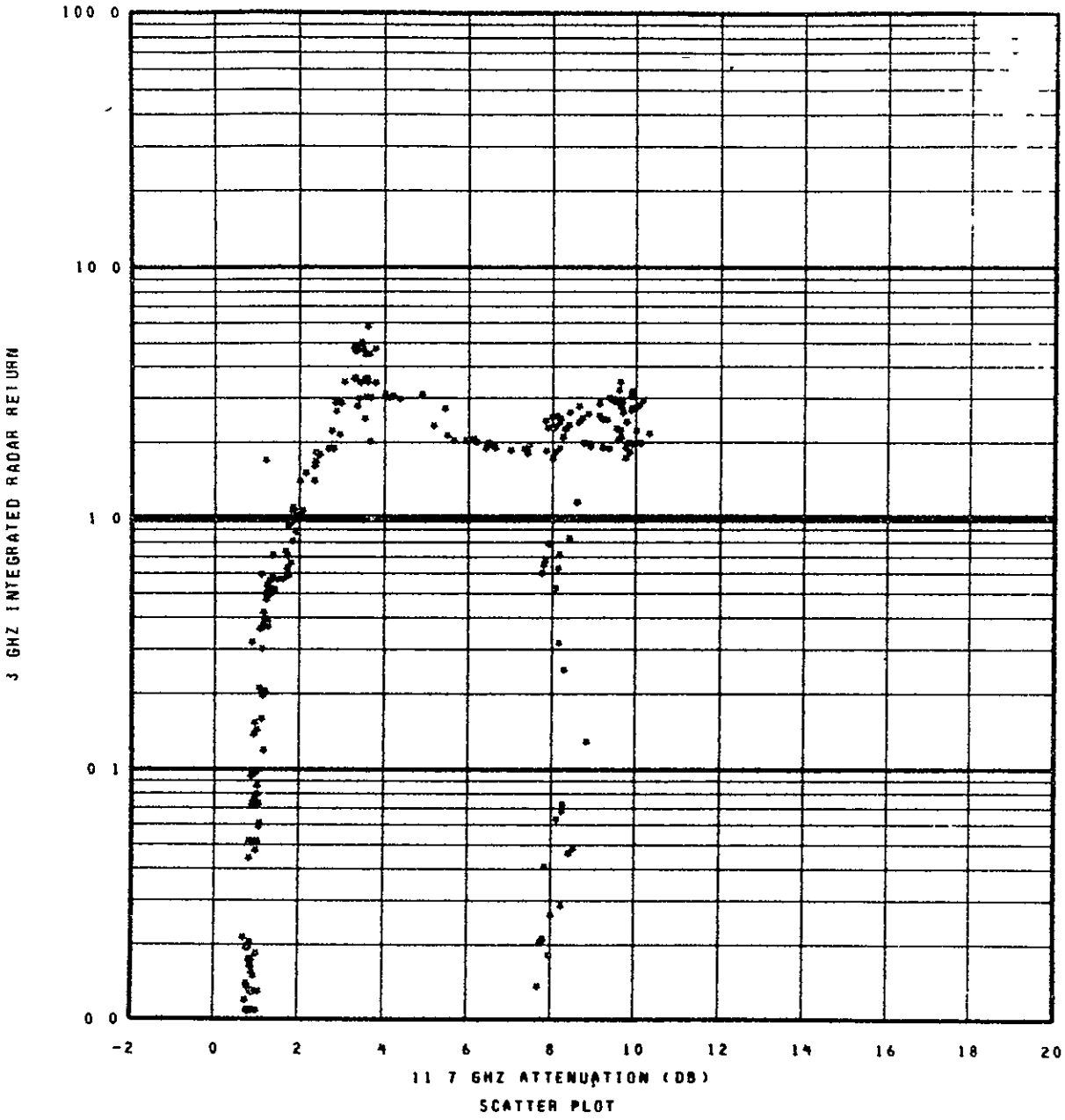

77-4057-16

START TIME		STOP TIME	
OUTER INTERVAL			
YEAR	= 1977	YEAR	= 1977
DAY	= 181	DAY	= 181
GMT	= 2311	GMT	= 2335
INNER INTERVAL			
DAY	= 181	DAY	= 181
GMT	= 2311	GMT	= 2335

Figure 2-16. 3 GHz Integrated Radar Return versus 11.7 GHz Attenuation

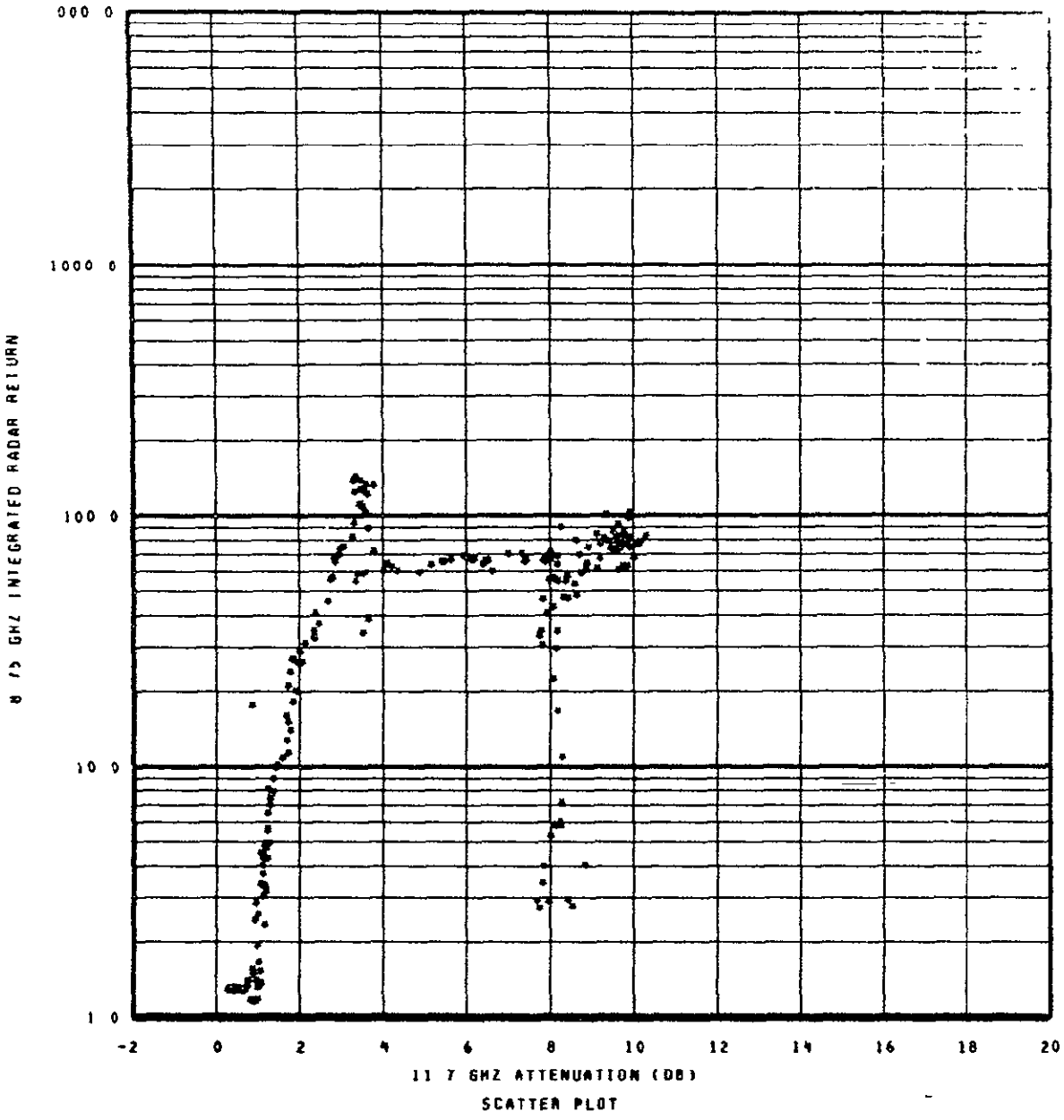

Figure 2-17. 8.75 GHz Integrated Radar Return versus 11.7 GHz Attenuation

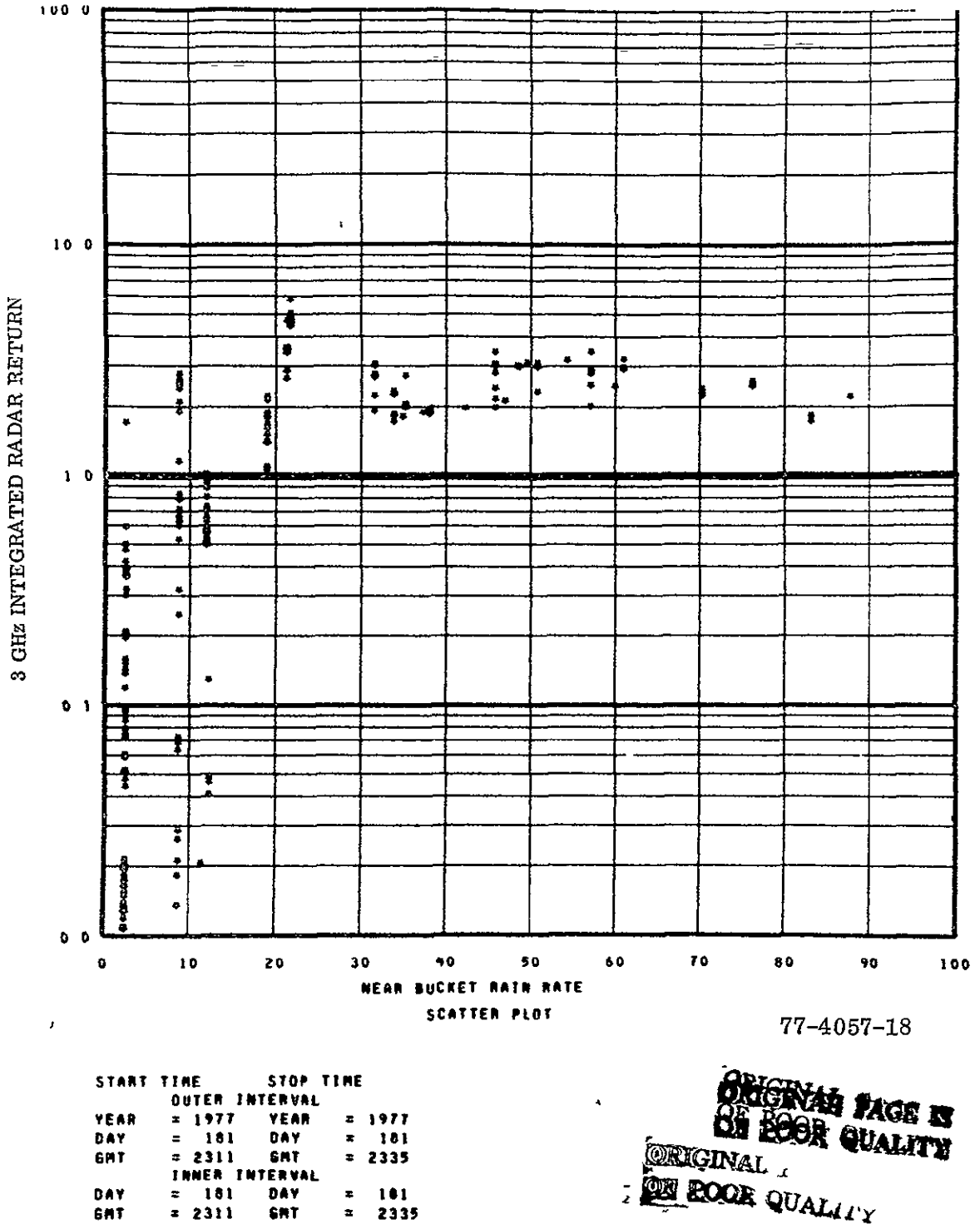

Figure 2-18. 3 GHz Integrated Radar Return versus Near Bucket Rain Rate

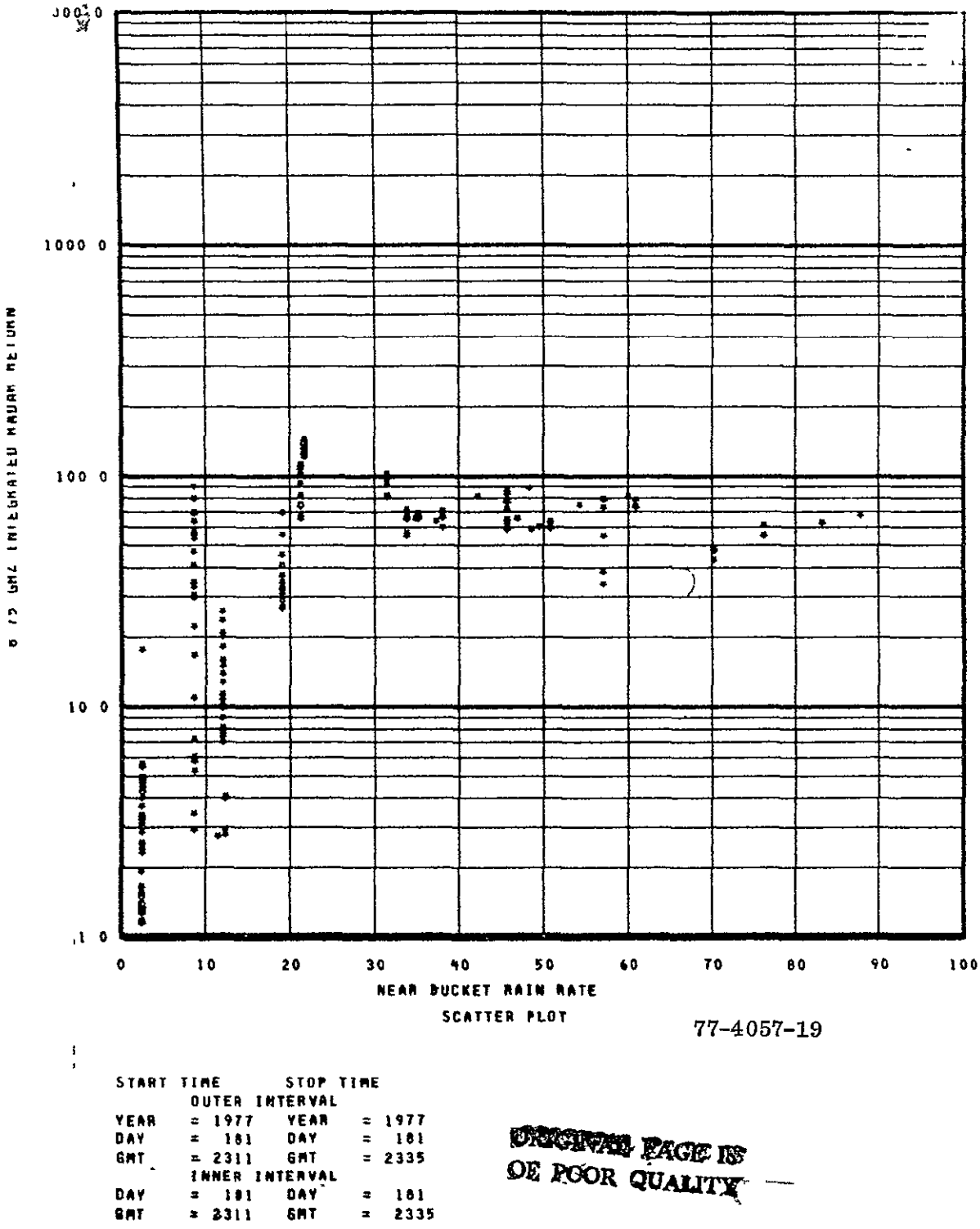

Figure 2-19. 8.76 GHz Integrated Radar Return versus Near Bucket Rain Rate

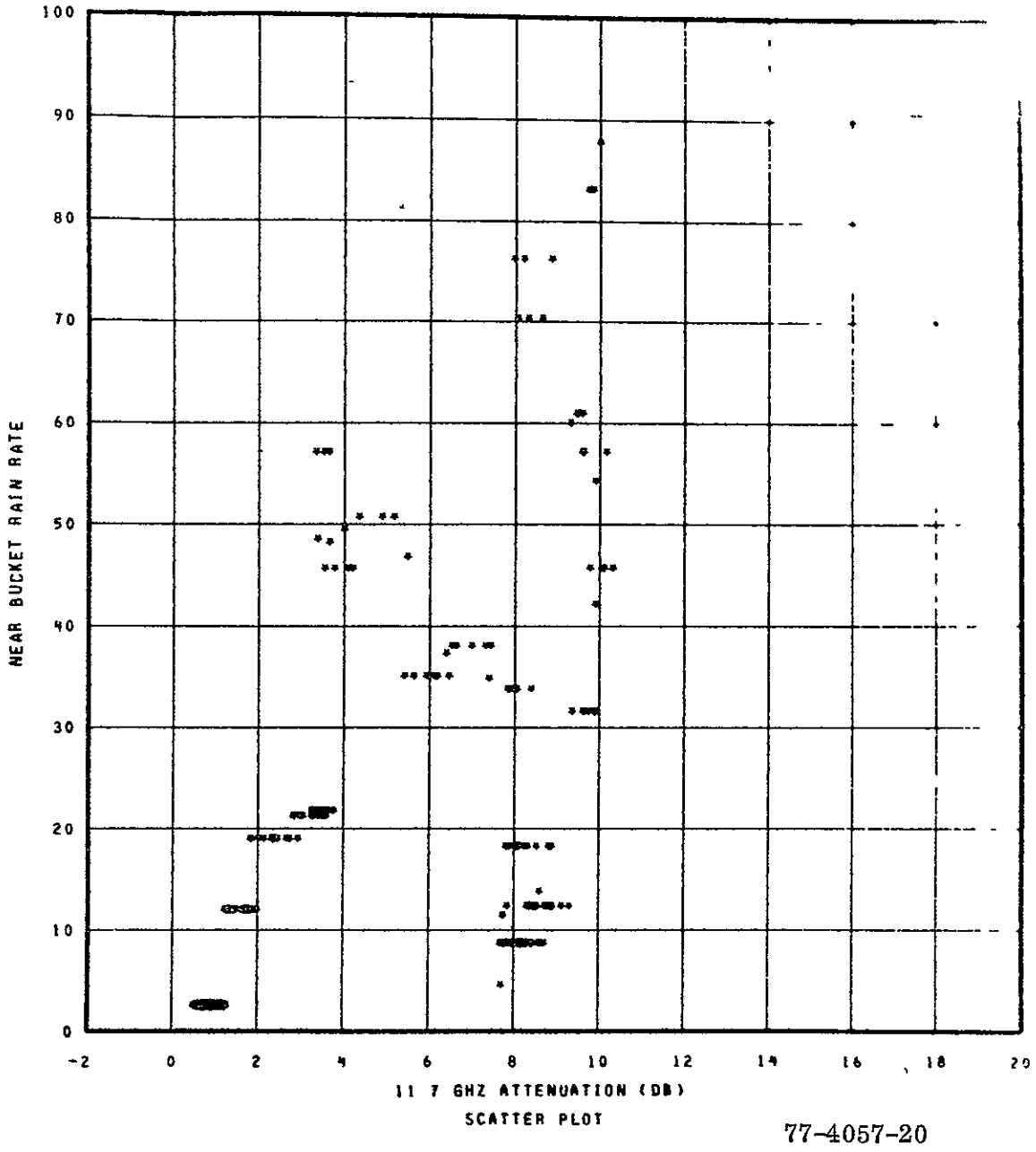

Figure 2-20. Near Bucket Rain Rate versus 11.7 GHz Attenuation (Four Second Means)

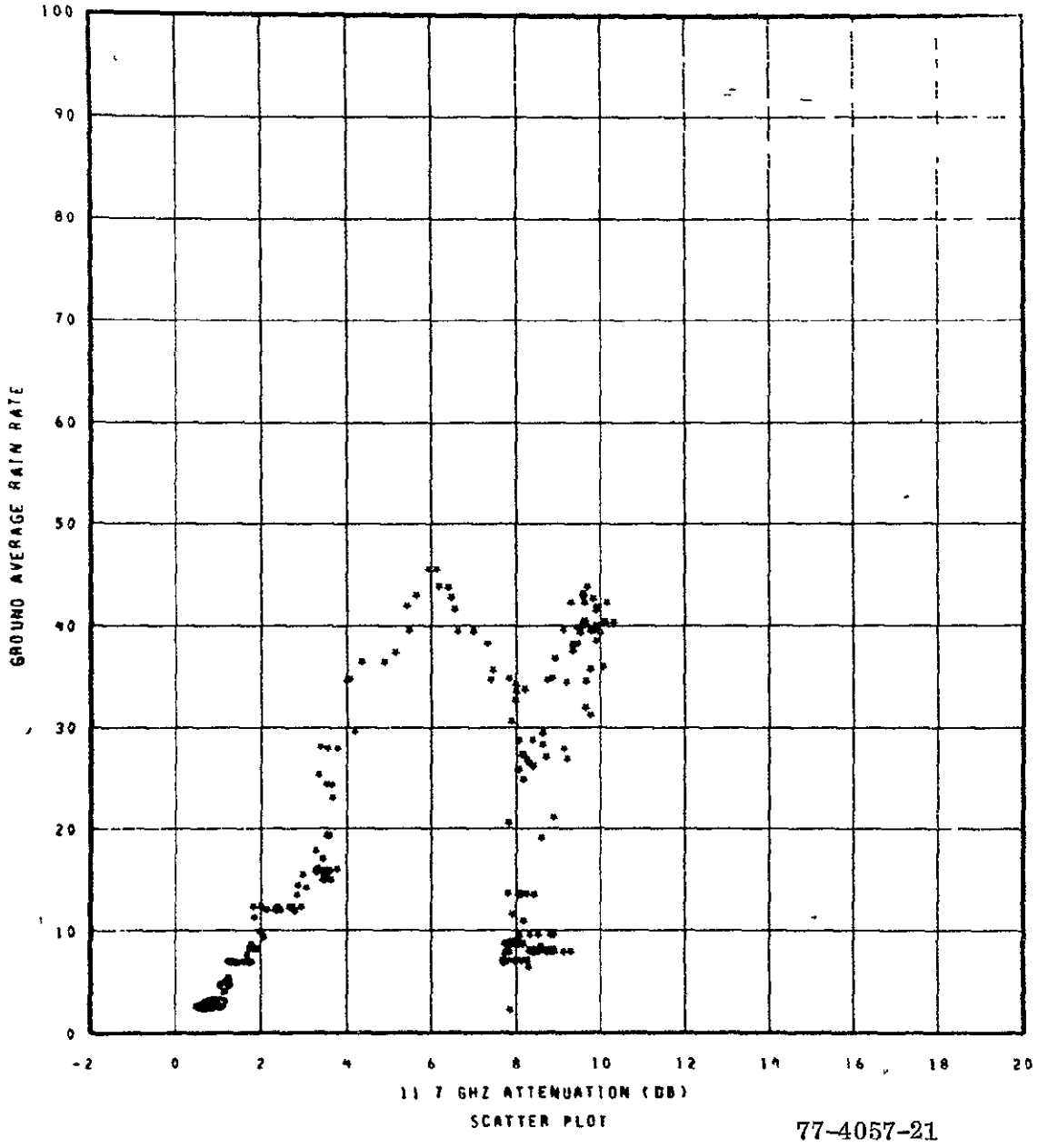

Figure 2-21. Ground Average Rain Rate versus 11.7 GHz Attenuation (Four Second Means)

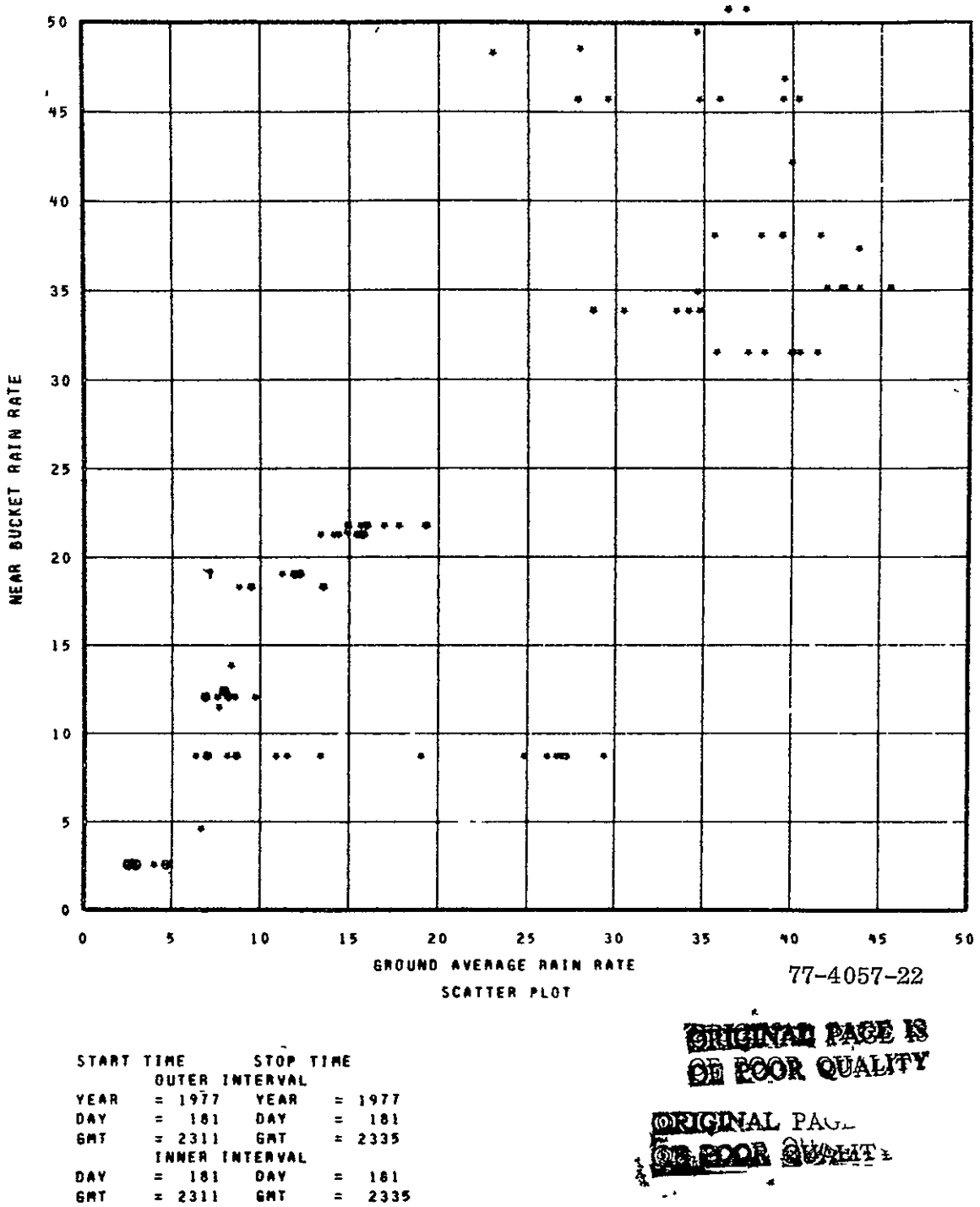

Figure 2-22. Near Bucket Rain Rate versus Ground Average Rain Rate

2.6 ATTENUATION PREDICTION FROM RAIN RATE

A method has been developed for predicting the cumulative distribution for attenuation (δ) from the cumulative distribution of the corresponding rain rate parameter. The method involves utilizing the cumulative percentages (for a given rain rate bin) computed from the rain rate distributions given in Figures (2-6), (2-8) and (2-13). The corresponding attenuation value is computed for each rain rate bin from the least mean square fit of the δ -rain rate pairs obtained from the long term rain rate and attenuation cumulative distributions as discussed in section 4. The resulting attenuation value is assumed to correspond to the actual percentage value of the rain rate distribution. For example, in the case of the worst month rain rate statistics for May of 1977 at the Greenbelt station (Figure (2-8)), in the first 5 MM/HR rain rate bin, the corresponding percentage is 0.406%. The midpoint of this bin, R = 2.5 MM/HR, is utilized for the rain rate and δ pair ($\text{Attn} = .5843R^{0.7863}$) to obtain a value of δ of 1.3 dB. This value is assumed to correspond to the 0.406% value. The resulting predicted cumulative distributions is shown in Figure (2-23). Reasonable correspondence is obtained with the actual measured distribution. The measured and predicted distribution for August of 1976 is shown in Figure (2-24). Also the above distributions for the NB and GA factors for the Rosman station is given in Figure (2-25). It is noticed that excellent correlation is obtained for the GA factor.

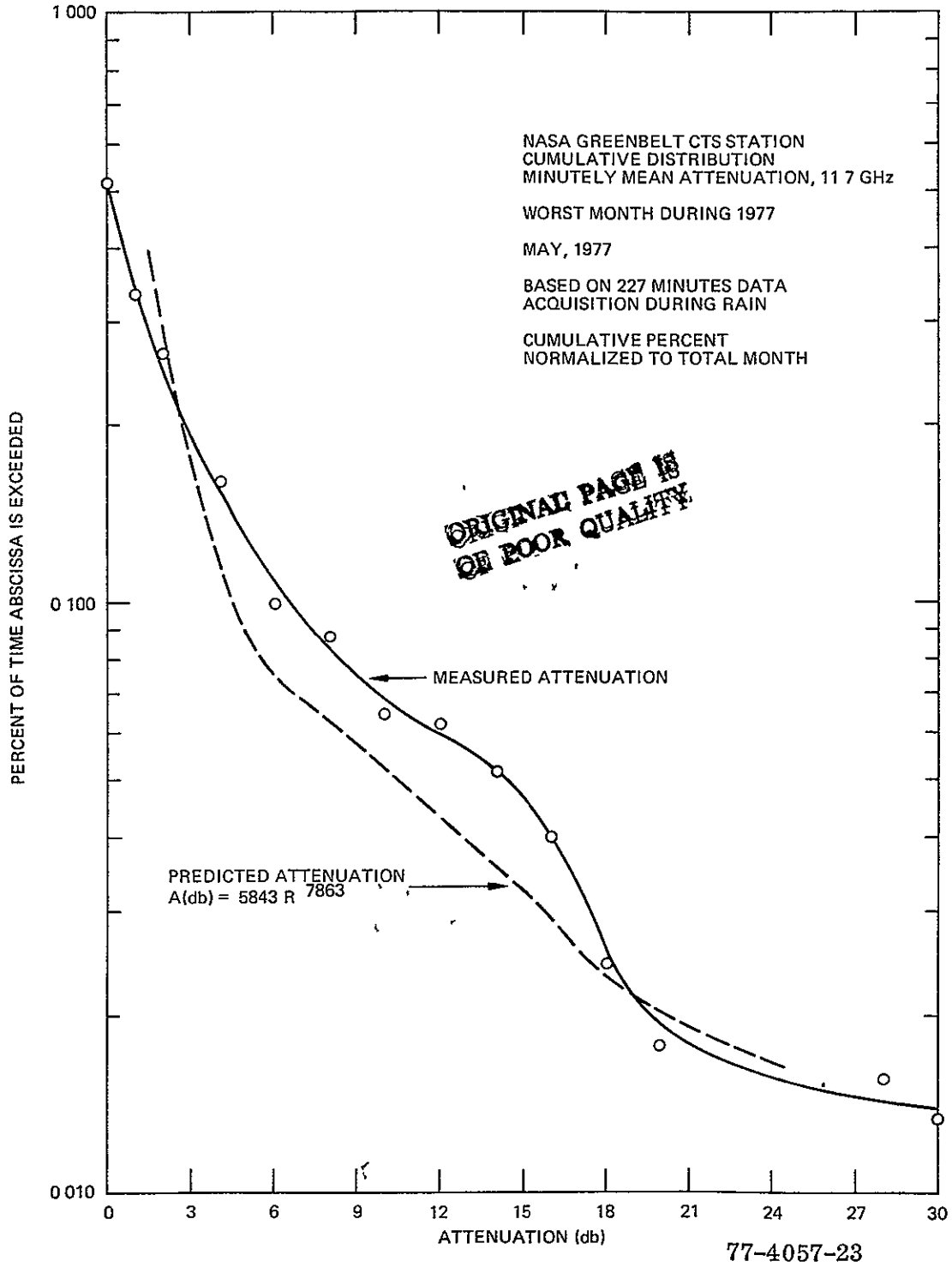

Figure 2-23. Predicted and Measured Cumulative Attenuation Distributions

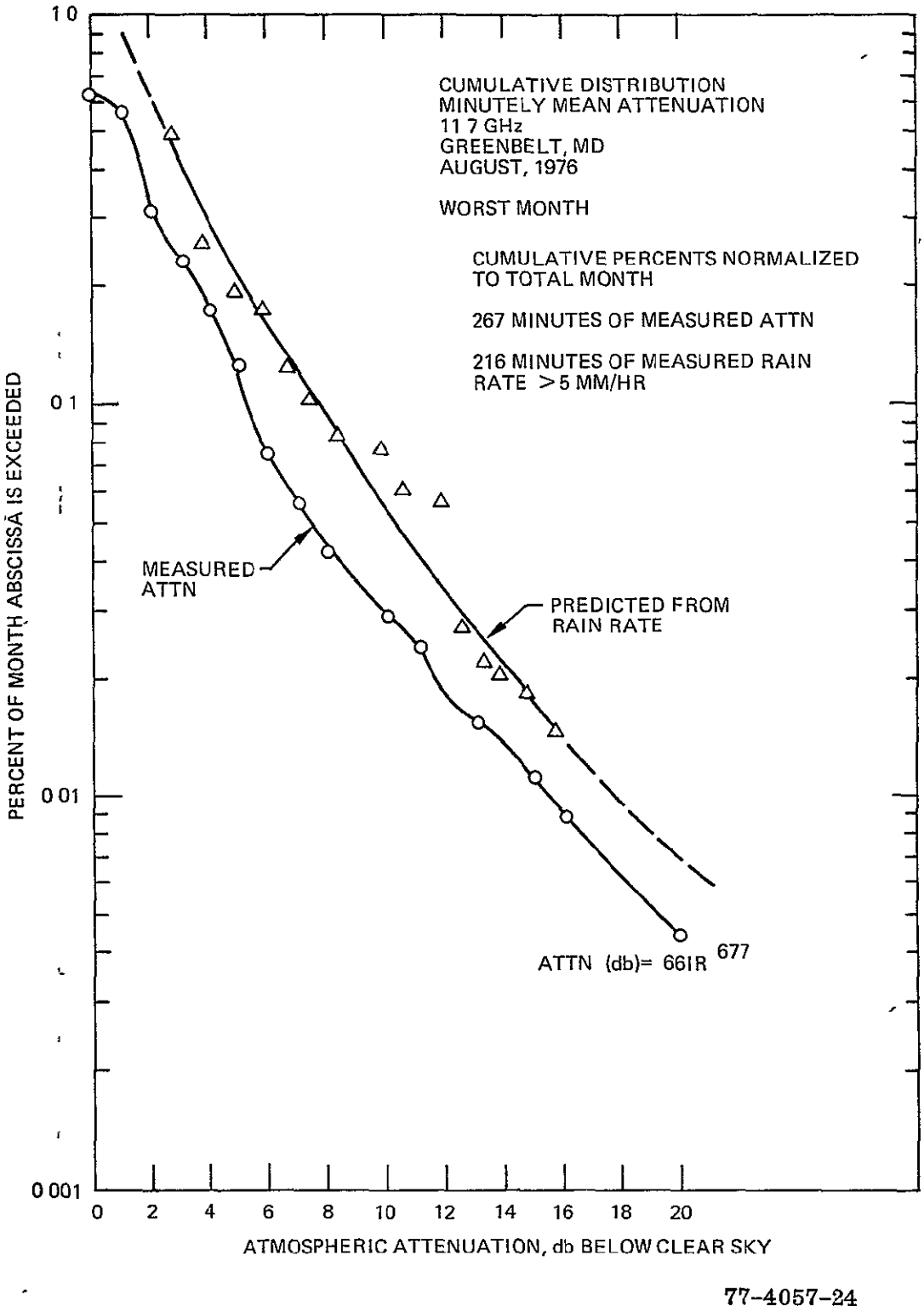

Figure 2-24. Measured and Predicted Cumulative Attenuation Distributions

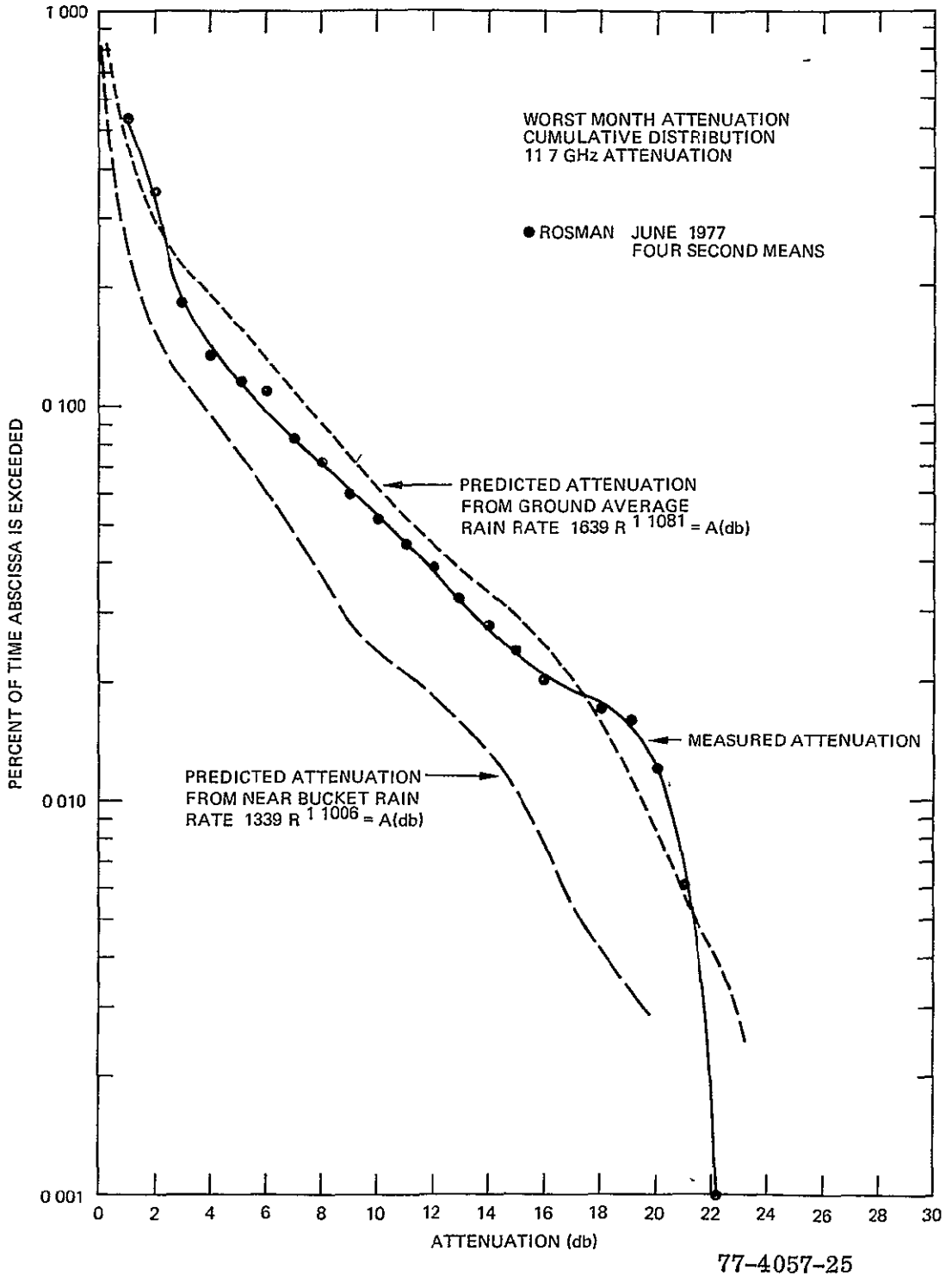

Figure 2-25. Measured and Predicted Cumulative Attenuation Distributions

SECTION 3
CTS VIDEO CHANNEL TESTS

3.1 INTRODUCTION

During scheduled CTS test periods, several tests were performed which help to characterize the overall ground/satellite/ground loop at the NASA Greenbelt PTF Station.

The results of these tests are presented in this section.

3.2 TEST DESCRIPTION

The following is a list of tests performed and a short description of each:

a. Satellite Transponder Linearity. For this test, the video carrier was transmitted from the ground station at various uplink power levels. The uplink levels ranged from that required to saturate the satellite transmitter down to the lowest level for which the resultant downlink signal was measurable. The satellite transmitter power (P_{ts}) was monitored at NASA Lewis by means of telemetry. The ground transmitter power (P_{tg}) is also monitored for each power level. P_{ts} was then plotted against P_{tg} to access the CTS transponder linearity, for the RB-1/TB-1 channel.

b. Two-Carrier Intermodulation. Two ground stations transmitted co-channel CW signals at various relative uplink levels. With the 40 MHz carrier spacing used, only third intermodulation products fall in band. These were measured relative to the higher power carrier which was held constant while the level of the other signal was decreased in successive steps down from equal satellite accessing power levels.

c. Two-Carrier Compression. For this test, two co-channel C.W. signals were transmitted, as in the two-carrier intermodulation test above. Starting at equal satellite accessing powers, one carrier was held at constant uplink power while the other was decreased successively in 3 dB steps. The level of each carrier was monitored in the ground receiver IF at each step.

d. C/N, Video TT/N. Carrier-to-noise ratio was measured in the ground receiver IF for various uplink levels. For each level, the carrier was FM modulated with a test tone and the test tone to noise at the video output was measured. C/N vs TT/N was then plotted.

e. Audio S/N. For various uplink power levels, the audio signal to noise was measured by FM modulating both the 5.36 MHz and 5.14 MHz audio subcarriers in turn, and measuring the audio signal to noise at the audio output terminals. This was done both in the presence and absense of a video signal, and also with both subcarriers on simultaneously.

f. Baseband Frequency Response. For this test, the video baseband was swept with a constant amplitude signal. This was a point by point test, and each baseband frequency deviated the RF carrier by a constant amount. The test was run in the spacecraft loop and the relative amplitude at each point in the receiver baseband was plotted.

3.3 DISCUSSION OF TEST RESULTS

a. Satellite Transponder Linearity. Figures 3-1 shows a plot of uplink versus downlink power. For P_{ts} 12 to 20 dBw, the P_{ts}/P_{tg}, follows a linear relation. Limiting due to saturation begins at a P_{ts} of approximately 18.5 dBw. In order to raise the P_{ts} 3 dB from 100 to 200 watts, an increase of 7 dB in uplink power is required. Once an absolute reference has been established a P_{ts} value can be obtained from the uplink/downlink characteristic for a given measured value of the ground transmit power. Satellite telemetry provides only a piece-wise continuous record of downlink power.

b. Two-Carrier Intermodulation. Figures 3-2 and 3-3 show the upper third order intermod level for various satellite accessing power ratios in RB-1/TB-1. In comparing the right-hand side of figure 3-3 with that of figure 3-2, higher third order intermods are seen in figure 3-2. This is expected, since the composite uplink and therefore the composite level at the satellite transmitter input is higher, driving the transmitter further into saturation. The effect of limiting is therefore more pronounced in figure 3-2 than in figure 3-3.

Figure 3-4 shows similar test results for RB-1/TB-2. Both the upper and lower third order intermods are shown in this figure. In comparing this channel with RB-1/TB-1, it is seen that the upper third order intermod level is some 10 dB higher in RB-2/TB-2. This is because of the effect of satellite limiting due to saturation being more pronounced in RB-2/TB-2 than in RB-1/TB-1.

c. Two-Carrier Compression. In order to assess the power sharing characteristics of two signals in the same channel, two-carrier compression tests were run in RB-1/TB-1 and RB-2/TB-2. The results are shown in figures 3-5 and 3-6, respectively. These figures are drawn so that the relative levels of each carrier can be seen, along with the composite downlink level, as determined from the spacecraft telemetry. Starting from the ordinate on figure 3-5, it is seen that both carriers were equal in level as seen in the ground receiver IF. The composite downlink transmitter power was 190 watts, as seen from the satellite telemetry. As one carrier is decreased in uplink power in 3 dB steps (C_2) it is seen that the other approaches a 4 dB increase in downlink level (C_1). The lower power carries decreases linearily until the sixth 3 dB step, after which the compression effect increases.

Transponder compression of C_2 by C_1 is defined as

$$\left(P_{o_1}\,(\text{dB}) - P_{i_1}\,(\text{dB})\right) - \left(P_{o_2}\,(\text{dB}) - P_{i_2}\,(\text{dB})\right)$$

where P_1 and P_2 are the relative carrier powers, and $P_1 > P_2$. The subscripts o and i refer to satellite transmitter output and input, respectively. P_{o_1} (dB), for example, is the satellite transmitted power of carrier 1 expressed in dB. The transponder compression for P_{ts} = 160 watts is 3 dB for all input level differentials less than 18 dB. Above 18 dB, the compression increases to 9 dB for a 21 dB difference in input level.

Figure 3-6 shows similar results for RB-2/TB-2. The compression here is 3 dB throughout.

d. Carrier-to-Noise, Test Tone-to-Noise. C/N and video TT/N were performed in both satellite channels. Figures 3-7 and 3-8 show the results for RB-1/TB-1 and RB-2/TB-2, respectively. The uplink power was varied to obtain a range of C/N values. At each value, the carrier was FM modulated with a 760 kHz signal at 10 MHz peak deviation. TT/N was measured at the video output, through a 4.5 MHz video L.P. filter.

The results in figures 3-7 and 3-8 show the expected trend of TT/N vs C/N, except in the region of higher values, where the TT/N shows an unexpected rate of increase with C/N. This effect is in the ground receiver, perhaps due to limiting in post detection circuitry. The last point on the right hand side of the curves represents the C/N corresponding to maximum downlink power.

Static threshold occurs at 9 dB in figure 3-7 and 10 dB in figure 8.

e. Receiver Baseband Frequency Response. Figure 3-9 shows the receiver baseband frequency response. The response is normalized to 1 kHz. The test was run in the spacecraft loop. The transmitter modulator was swept with a constant amplitude signal across the video band. The response therefore includes contributions from both the ground transmitter and receiver.

f. Receiver Audio Channel Frequency Response. Frequency responds were run on both the 5.14 and 5.36 MHz audio subcarrier channels, the results are shown in figure 3-10. Each shows the expected response. The passband is limited to 6 kHz, where the response is some 3 dB down.

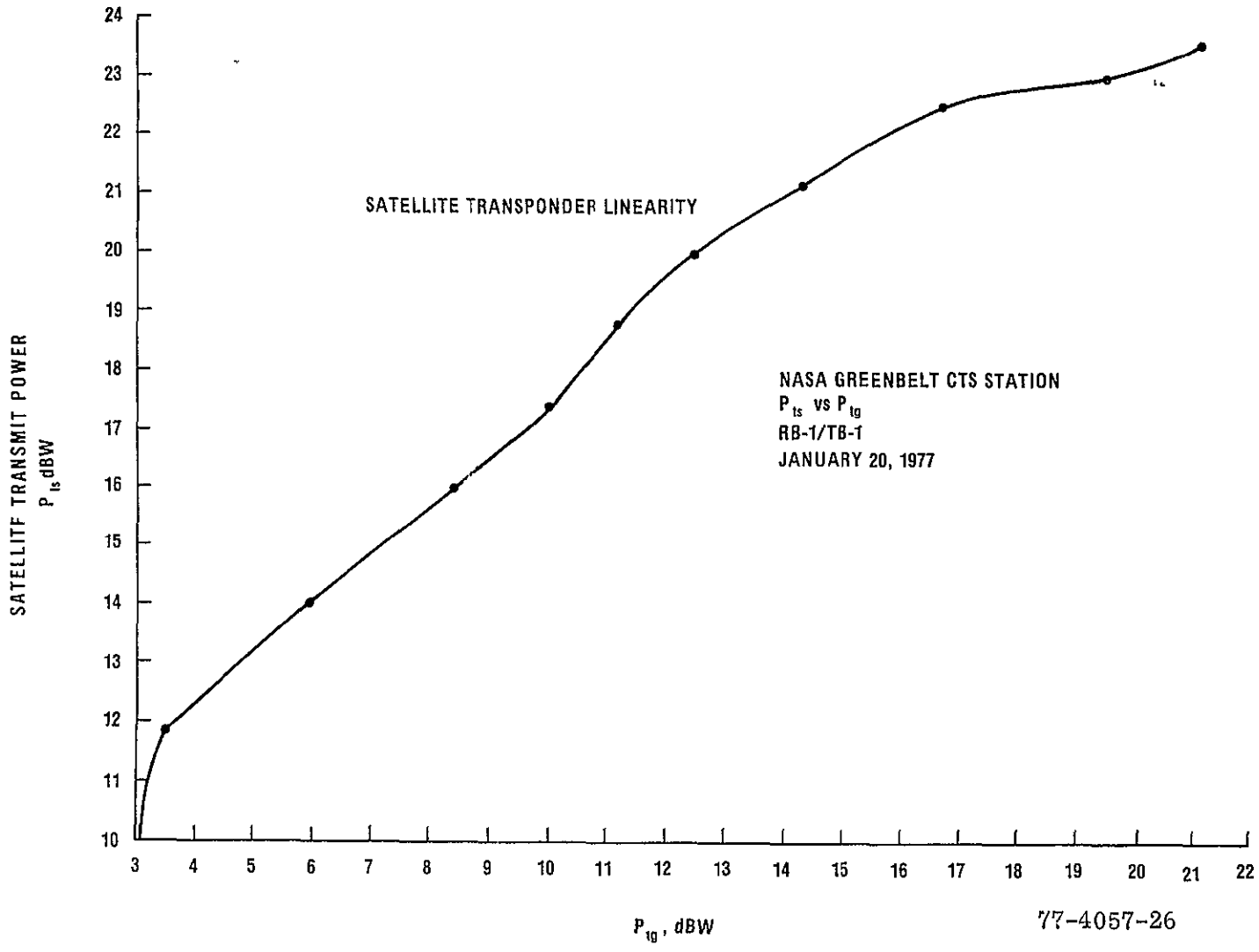

Figure 3-1. Satellite Transmit Power Versus Ground Transmit Power

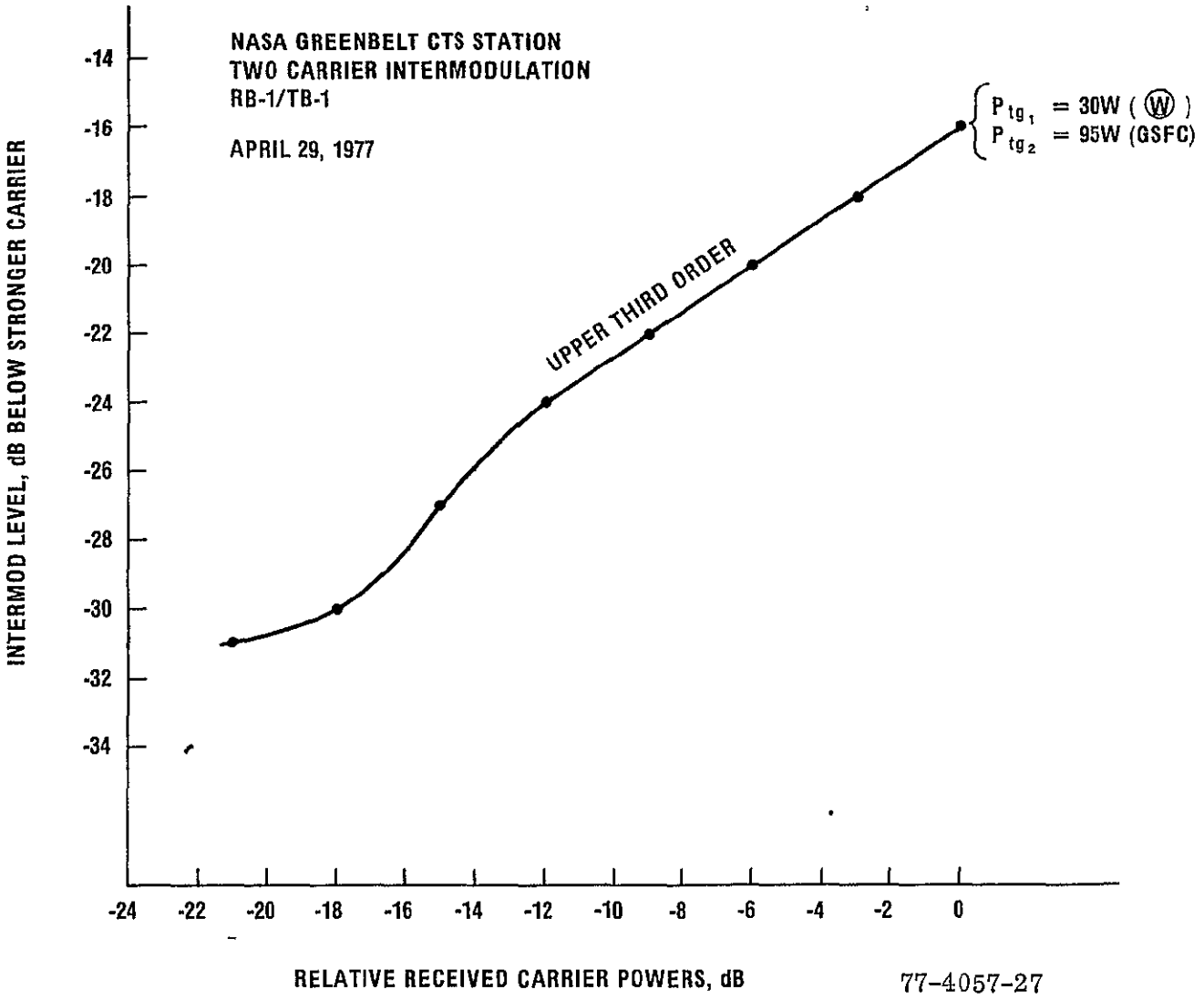

Figure 3-2. Intermodulation Levels Versus Ground Received Power (RB1/TB1)

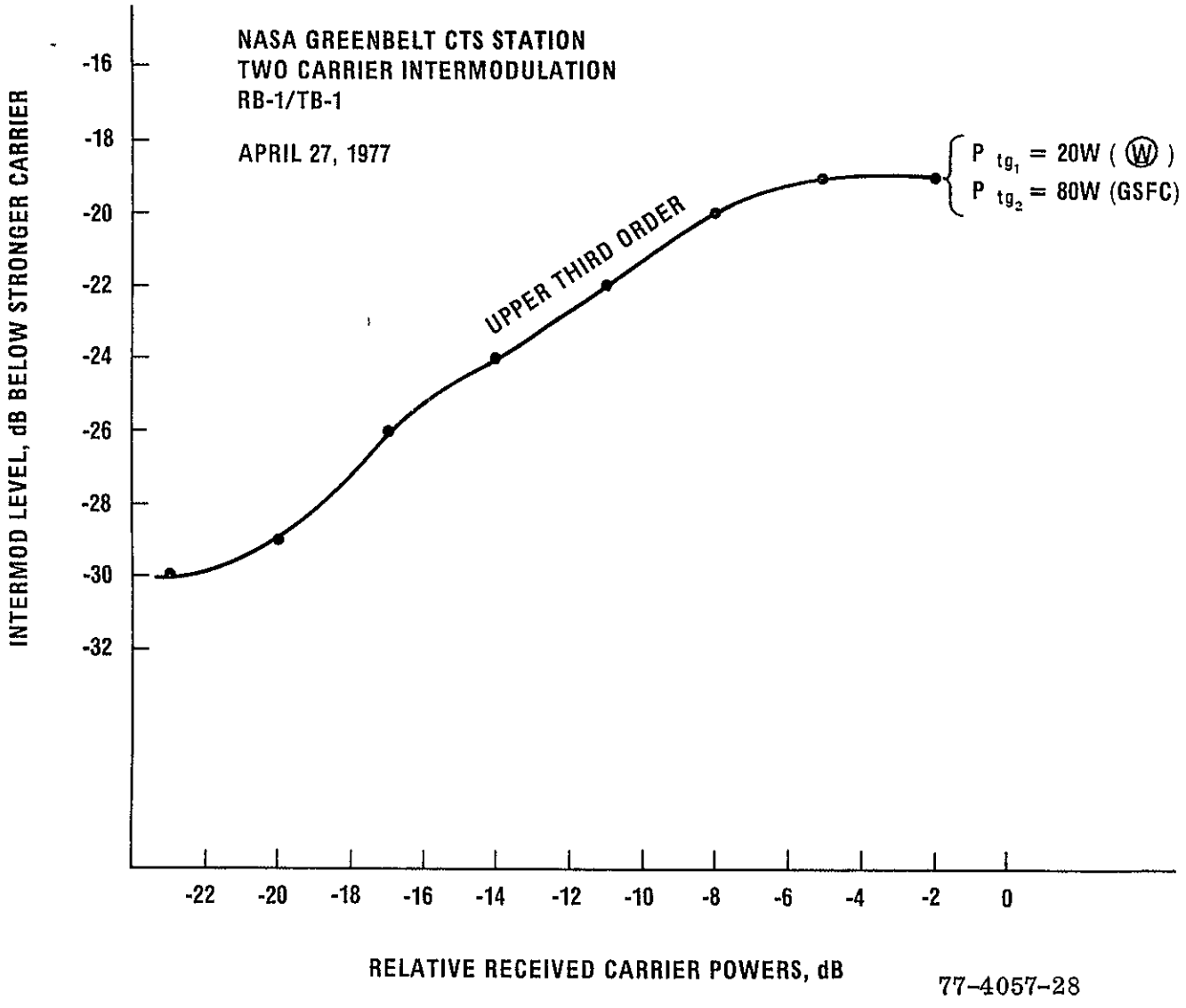

Figure 3-3. Intermodulation Levels Versus Ground Receiver Power (RB1/TB1)

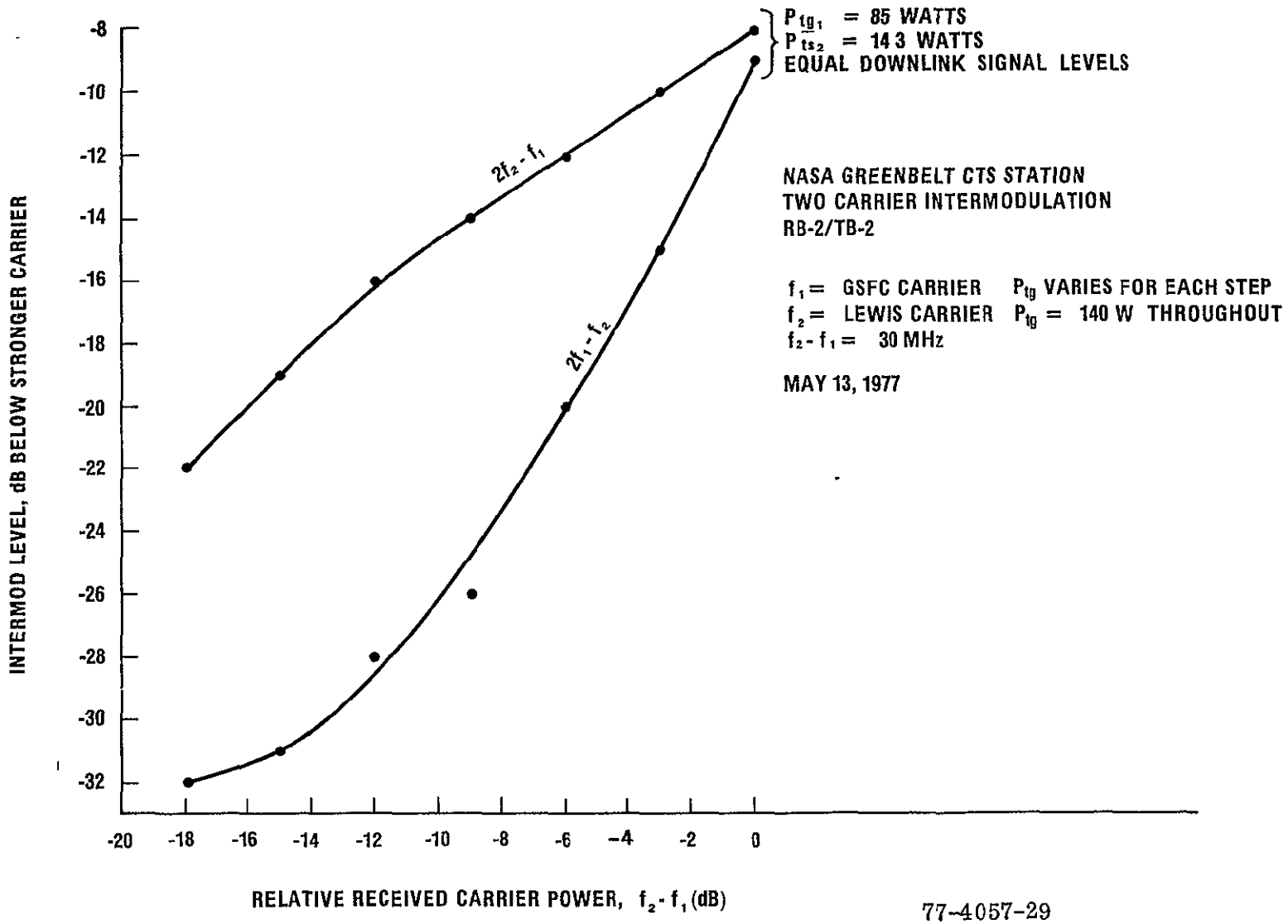

Figure 3-4. Intermodulation Levels Versus Ground Received Power (RB2/TB2)

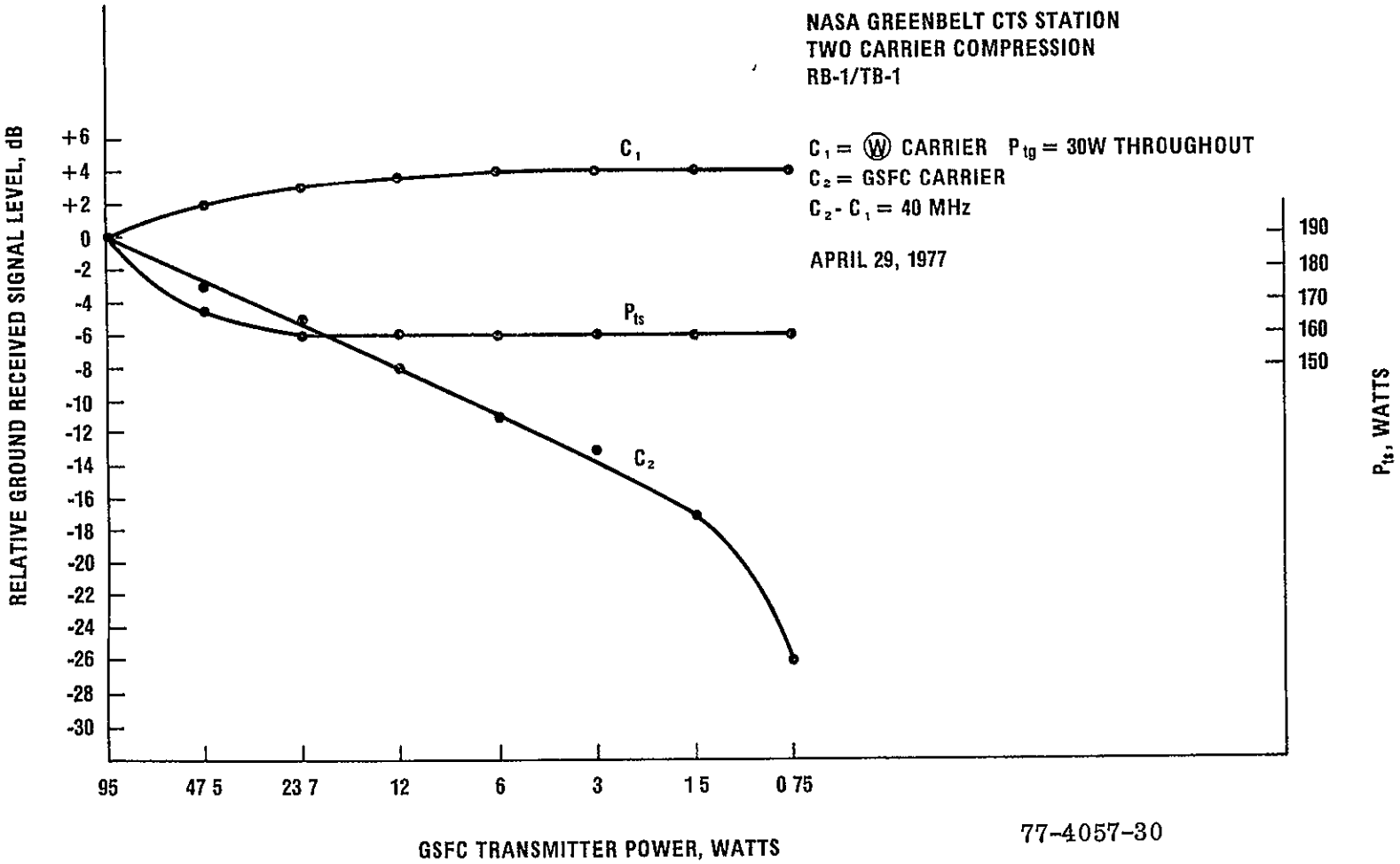

Figure 3-5. Received Carrier Compression Versus Ground Transmit Power

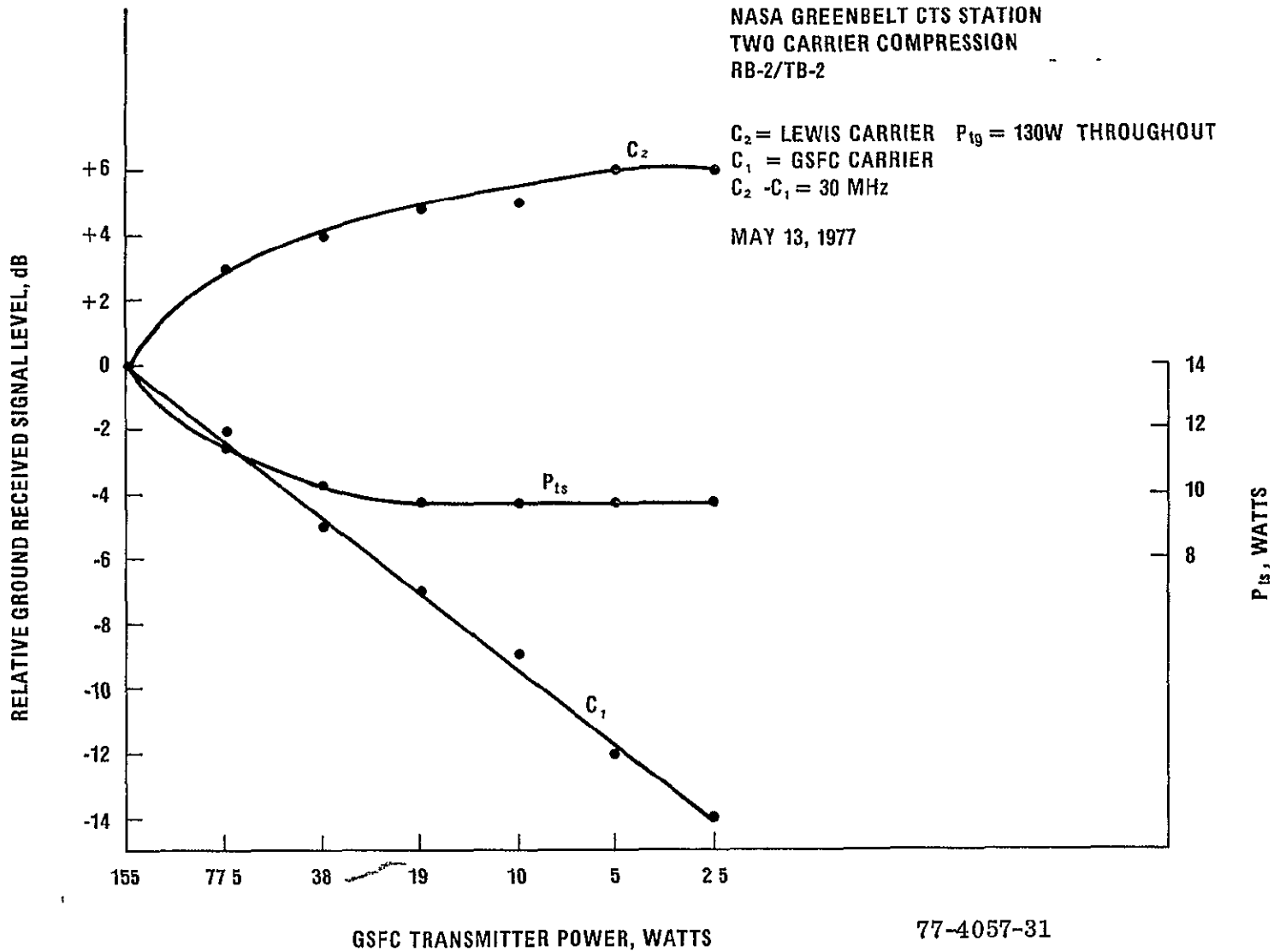

Figure 3-6. Received Carrier Compression Versus Ground Transmit Power

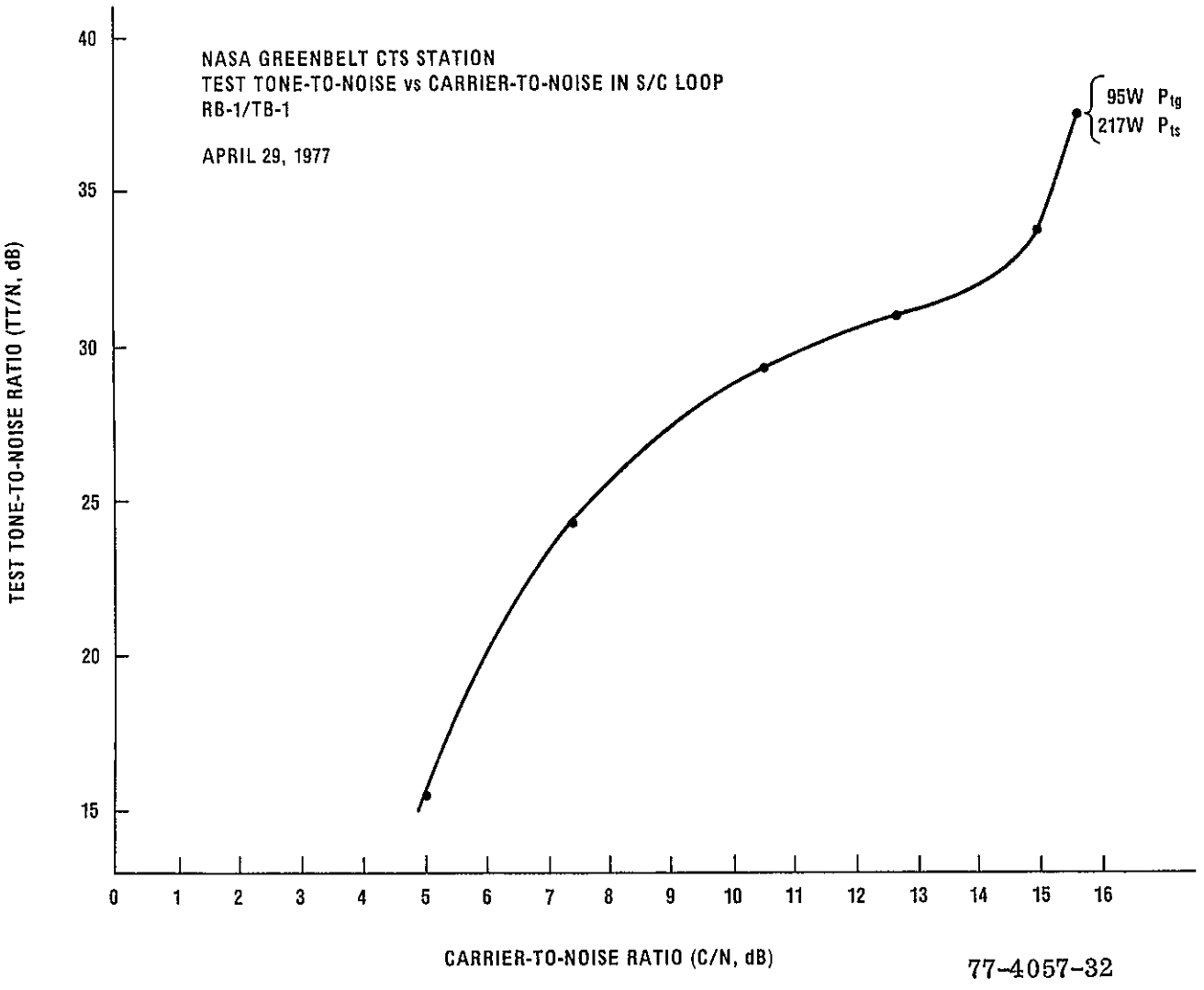

Figure 3-7. Baseband TT/N Versus Predetection C/N

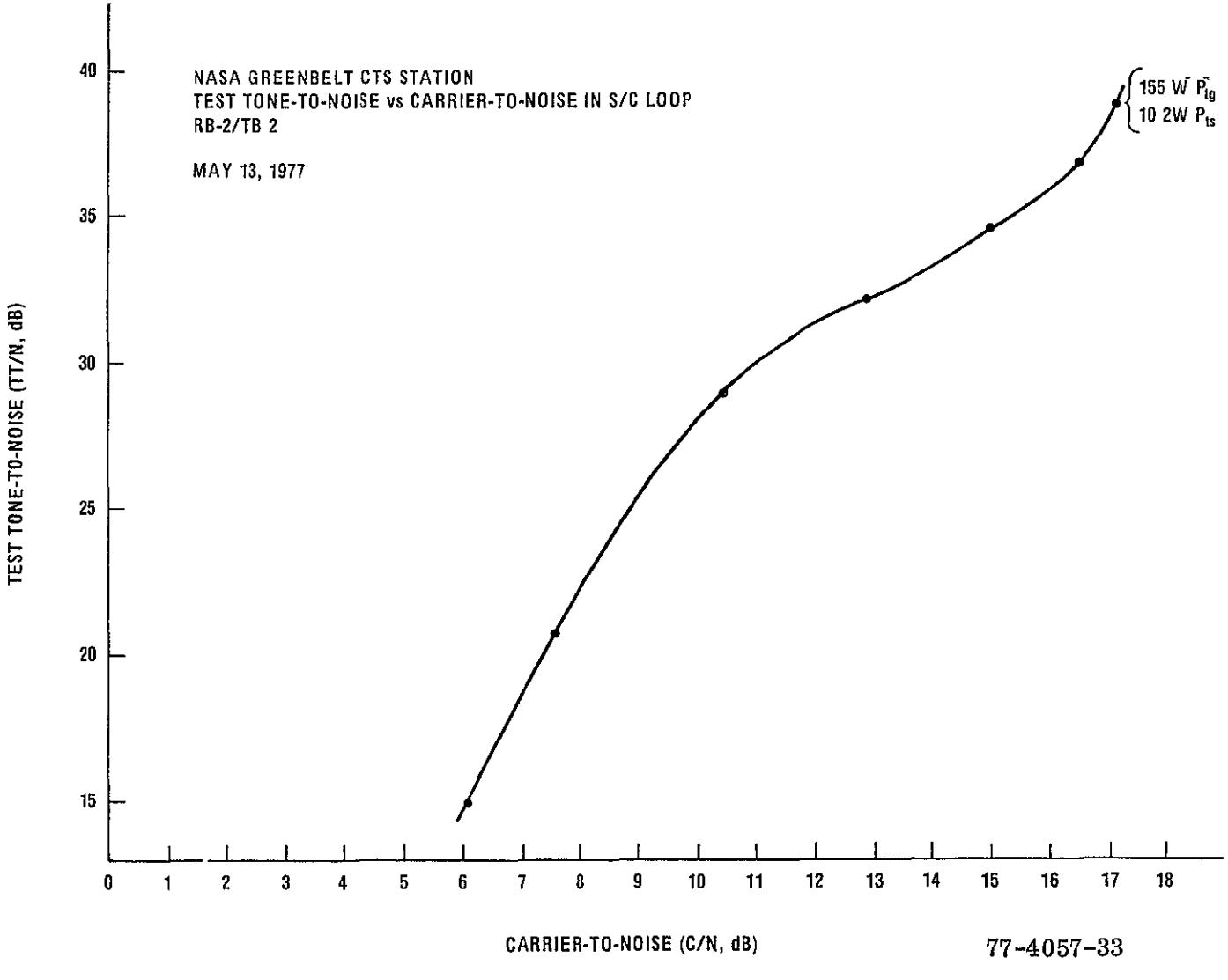

Figure 3-8. Baseband TT/N Versus Predetection C/N

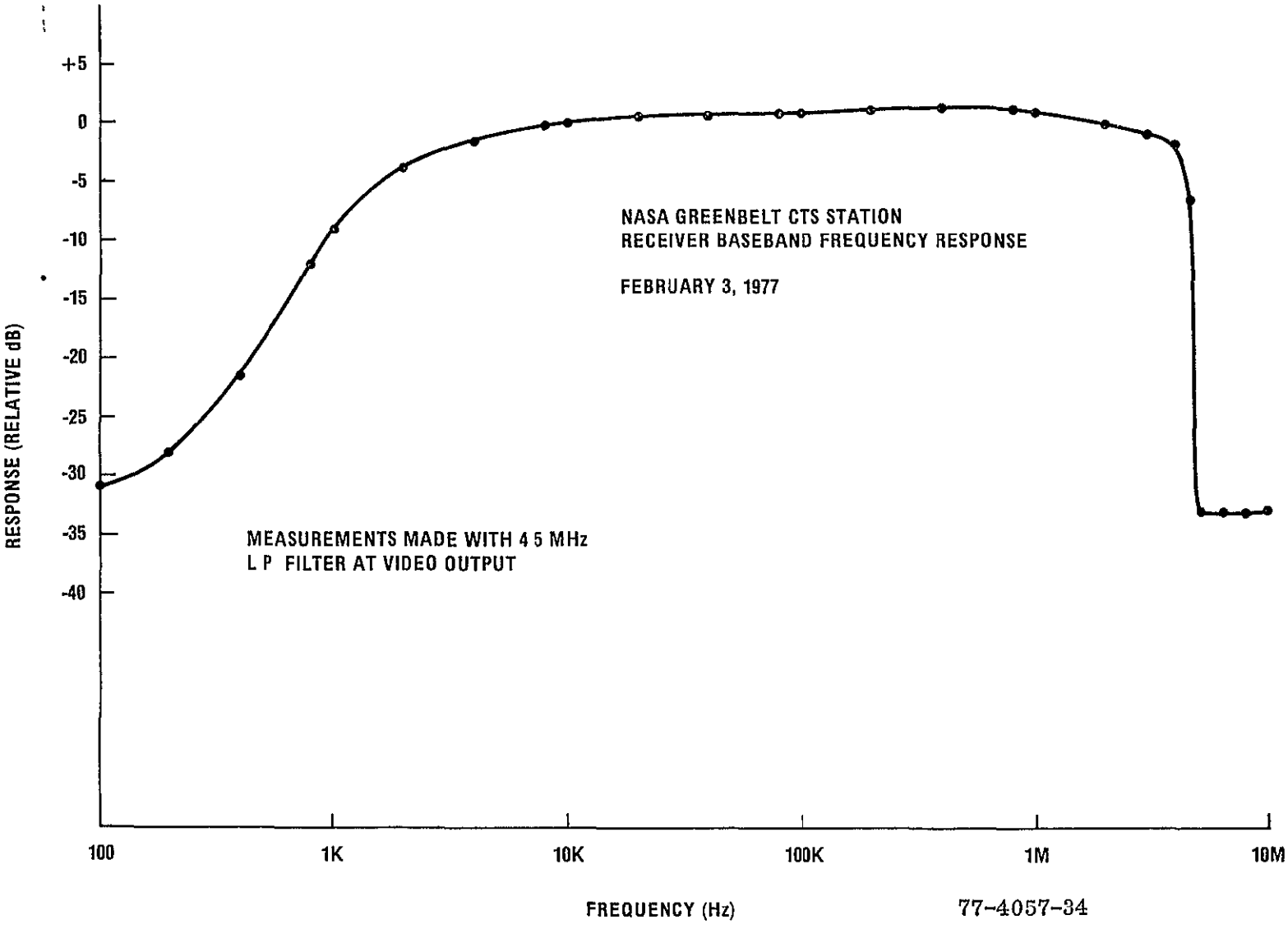

Figure 3-9. Receiver Baseband Frequency Response

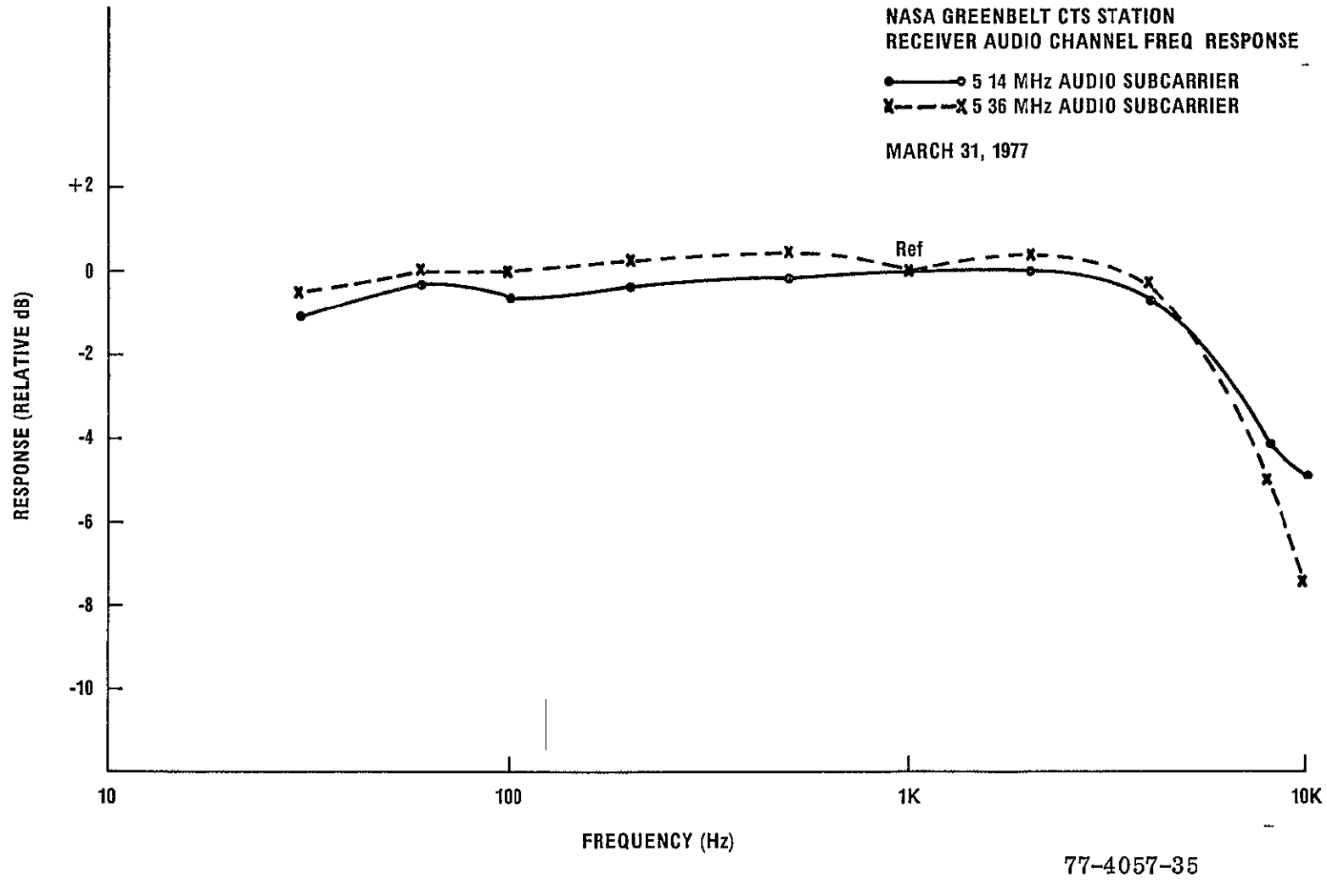

Figure 3-10 Audio Baseband Frequency Response

SECTION 4

PATH LENGTH ANALYSIS

4.1 INTRODUCTION

In order to predict the attenuation (δ) from measured values of rain rate over an elevated path some measure of the path length (L) through the storm must be determined. This is seen from the following empirical expression[2] that relates δ dB to rain rate, R.

$$\delta\,(\mathrm{dB}) = aR^{b}L \tag{1}$$

where

δ is the total path attenuation

R is the rainfall rate over the path length L, in kilometers.

The constraints in the above equation are developed from the Mie theory for spherical particles with a Laws and Parsons drop-size distribution assumed[3]. The constants a and b are a function of frequency and are listed in Appendix A for the frequencies of interest.

Because of the elevated path condition of an earth-to-spacecraft link the factor L is a function of the rain type, (geometrical aspects of rain environment), elevation angle and frequency of the transmitted signal. A method for obtaining some measure of the effective path length, L, was developed by Ippolito[4] that utilized the above equation and concurrent measurements of δ and R. It involved a least mean square fit of the above measurements to the function cR^{d}. Then equating the resulting function to the above equation.

$$cR^{d} = aR^{b}L \tag{2}$$

$$\frac{c}{a}R^{d-b} = L(R)$$

From Appendix A, it is shown that as the frequency increases, "a" tends to increase and b tends to decrease and approach unity at the upper frequency limit of 30 GHz. The values of c and d are obtained from a least mean square fit of the δ-rain rate pairs obtained from the long term cumulative distributions of the type shown in Figures 2-4 and 2-11. Generally, the d factor has been found to be less than unity. Therefore, as the frequency increases the (d-b) factor decreases thus causing L to be less dependent on rain rate over a wider range of rain rate values. The effect of L on elevation angle, θ, should also be considered since they would be inversely proportional. For a given rain environment characterized by a height h and a large horizontal extent, the change in L with respect to a change in elevation angle θ is,

$$\frac{dL}{d\theta} = - h \frac{\cos\theta}{\sin^2\theta} \tag{3}$$

As θ varies from 45° to 30° the rate factor varies from -1.414 h to -3.46h. A decrease in the elevation angle will cause L to increase and thus making the path length a more complicated function of both rain rate and θ. Fortunately, for satellite communications the elevation angle is generally $\geq$ 30°. For this high angle limit, the value of L tends to approach a limiting condition much faster as the rain rate increases.

4.2 PATH LENGTH DATA

The values of "c and d" were obtained from δ and rain rate cumulative distributions that were computed from data obtained over a period of one year. The pair values and the resulting c and d factors are shown in Appendix B for the 11.7 GHz frequency. These δ and rain rate pair values were obtained from the long term cumulative distributions given in Figures (2-4), (2-11) and (2-12). The values correspond to various constant percentage values obtained over the overall distribution. The r factor also listed in Appendix B is the correlation coefficient for the δ and rain rate variables. The overall data is summarized in Table III.

Limiting values of L (R) were computed assuming a rain rate of 120MM/HR which sufficiently high to assume a close approximation to the L (R) limit. As shown in Table III, a surprising result is that the L (R) limit over a wide range of conditions tends to approach a value of about 4 Km. The only deviation was the 15.3 GHz data which produced a limit of 1.55 Km. This data was not obtained by the constant percentage method previously described. In this case a direct point to point attenuation and rain rate pair values were obtained by noting these values at a given instant of time. However, at the lower rain rate values of 10 MM/HR the L (R) value tends to deviate between the two stations at the 11.7 GHz frequency. From the data obtained to data, it could be concluded that prediction of the L (R) value at high values of rain rate should be possible. However, at low values the prediction process could be a complicated function of frequency, elevation angle and locales from the standpoint of characteristic weather types.

Path length values for an R value of 120 MM/HR normalized to an elevation angle of 45° are presented in the last column of Table III. As shown, there appears to be a frequency dependence on these normalized values where a higher value occurs at the 11.7 GHz frequency relative to the values at 20 GHz and 30 GHz.

Future investigations will involve the use of the multifrequency radar for determining path length. In this case a direct measure of the path length can be obtained from the type of plots shown in Figure 5-10 of Section 5. Path length as a direct function of time will be obtained and long term statistical plots developed for comparison with the path length magnitudes, obtained from the attenuation and rain rate pair value techniques.

TABLE III

EFFECTIVE PATH LENGTH PARAMETERS

EXPERIMENT CONDITION	SATELLITE	NOMINAL ELEVATION ANGLE	ATTN. = cR^d cR^d	L (R)	L (R) R=120MM/HR (Km)	L (R) R=10MM/HR (Km)	NORMALIZED L (R) TO $\theta = 45°$ R=120MM/HR (Km)
ROSMAN							
15.3 GHz	ATS-5	42°	$2.365R^{0.3663}$	$67.57R^{-.7887}$	1.55	10.98	1.643
20 GHz	ATS-6	45°	$.763R^{0.885}$	$11.1R^{-.2154}$	3.96	6.76	3.96
30 GHz	ATS-6	45°	$1.389R^{0.9154}$	$8.423R^{-.1199}$	4.74	6.39	4.74
11.7 GHz (NB)	CTS	36°	$.1339R^{1.1006}$	$7.97R^{-.1244}$	4.4	5.98	5.28
11.7 GHz (GA)	CTS	36°	$.1639R^{1.1081}$	$9.76R^{-.1419}$	4.94	7.04	5.93
GREENBELT							
11.7 GHz	CTS	30°	$.5843R^{.7863}$	$34.8R^{-.4637}$	3.78	11.96	5.34

SECTION 5
WEATHER RADAR ANALYSIS

5.1 INTRODUCTION

The purpose of this section is to present the various technical problems and results obtained to data in employing the multifrequency weather radar for analyzing the rain environment and predicting the rain attenuation values. To date, it has been found that the factors of correct radar calibration and changes in the drop size distribution as a function of time have been the main deterrents in obtaining reasonable results when employing the radar return. A measure of predicting the effects of the rain environment from the radar return was determined by comparing the predicted results with the measured rain rate and attenuation values of the spacecraft-to-ground link when transmitting a 11.7 GHz beacon signal.

5.2 ANALYSIS OF RADAR EQUATION

The radar equation defines the received power ($\overline{P}_r$) that is obtained from a group of randomly distributed scatterers in a given volume. The signal is the sum of the signals scattered by each of the scatterers, with the phase of each signal taken into account. It has been found that $\overline{P}_r$ varies from one reflected pulse to the next because of the movement of the rain drops with respect to one another. The $\overline{P}_r$ factor is related to the radar parameters as follows:

$$\overline{P}_r = \frac{P_t G^2 B^2 \lambda^2 h}{L\, 512\, \pi^2\, (2 \ln 2)\, r^2} \sum_{\text{vol.}} \sigma_i \qquad (1)$$

where:

	3 GHz	8.75 GHz
P_t = Peak transmitted power	Measured	
G = Peak antenna gain	37.2 dB	38.7 dB
B = Antenna 3 dB beamwidth	2.3°	1.9°
λ = Operating wavelength in meters	0.1	.0343
h = Pulse length in meters	200	
r = Range in meters		
L = Two-way line loss		
2 ln 2 = Beam shape correction factor		
$\sum_{\text{vol.}} \sigma_i$ Operates within a unit illuminated volume		

The $\sum_{\text{vol.}} \sigma_i$ factor represents the summation of the total rain drop echoing areas of particles within a unit illuminated volume. This parameter is called the "radar reflectivity" and is designated by the symbol η expressed in units of mm^2/m^3.

For rain drop diameter, D, which satisfies the condition that $D/\lambda < .2$, the Rayleigh approximation[5] holds and

$$\sum_{\text{vol.}} \sigma_i = \frac{\pi^5}{\lambda^4} \left| \frac{\varepsilon - 1}{\varepsilon + 2} \right|^2 \sum D_i^6 \qquad (2)$$

where ε is the complex dielectric constant of water. For the 3 GHz radar λ = 100 mm, rain drops less than 20 mm satisfies the above condition. The D values of interest generally fall within an interval of 0.5 mm to about 6 mm. Therefore, the 3 GHz signal clearly meets the above condition. For the 8.75 GHz radar λ = 34.3 mm and the D limit in this case is 6.86 mm which still satisfies the Rayleigh limitation.

The summation factor relating to the distribution of rain drop sizes can be expressed as $\sum n_i D_i^6$ where n_i is the number of drops in discrete intervals of diameter. It is assumed that all particles within the interval are the same size. The above summation factor is defined as the reflectivity factor, Z. It is noted that Z is only a function of the drop size distribution.

Equation (1) can be expressed as

$$\overline{P_r} = \left[\frac{P_t G^2}{L} \left(\frac{B^2 \lambda^2 h}{1024\pi^2 \ln 2} \right) \right] \frac{\eta}{r^2} \qquad (3)$$

The expression within the bracket is defined as the radar constant (C). All factors can be measured and therefore known for determining C. The antenna gain G is taken as the peak value of this parameter. If this parameter is taken to be constant then it follows that the precipitation causing the backscatter is located at the optimum point of the antenna beam. This is obviously not true since the $\overline{P_r}$ value could have resulted from a small amount of precipitation located at low ranges or an intense pocket of precipitation located at longer ranges where in both cases the regions correspond to one of the sidelobes of the antenna pattern. As a result, it is often not possible to determine what part of the beam will contain sufficient power to give a detectable echo. For the case of a high Z, one might expect an echo to be received before the intense precipitation region enters the beam as it moves across the region. As a result the dimensions of the region would be exaggerated. For light precipitation the other extreme would be expected from the effects produced by the finite beamwidths of the antennas. Because of this phenomenon, the radar constant can also vary due to the two-way radiation pattern of the antenna. If the peak antenna gain is assumed then equation (3) reduces to,

8.75 GHz

$$\overline{P}_r = \left(2 \times 10^{-6} \frac{P_t}{L} \right) \frac{\eta}{r^2} \tag{4}$$

3 GHz

$$\overline{P}_r = \left(1.242 \times 10^{-5} \frac{P_t}{L} \right) \frac{\eta}{r^2} \tag{5}$$

The values of P_t and L are updated by periodic measurements and then included in the radar parameter expression.

By combining equations (2) and (3) the Z factor can be expressed as a function of $\overline{P}_r$. Utilizing equation (2) it can be shown that,

8.75 GHz

$$\eta \left(\frac{mm^2}{m^3} \right) = 1.913 \times 10^{-4} \, Z \left(\frac{mm^6}{m^3} \right) \tag{6}$$

3 GHz

$$\eta \left(\frac{mm^2}{m^3} \right) = 2.65 \times 10^{-6} \, Z \left(\frac{mm^6}{m^3} \right) \tag{7}$$

Also, from equations (4) and (5)

8.75 GHz

$$\eta = \left(\frac{5 \times 10^5 \, L}{P_t \, (mw)} \right) P_r \, (mw) \; r^2 \, (meters) \tag{8}$$

$$Z = 5.22 \times 10^3 \left(\frac{5 \times 10^5 \, L}{P_t \, (mw)} \right) P_r \, (mw) \; r^2 \tag{9}$$

3 GHz

$$\eta = \left(\frac{8.06 \times 10^4 \, L}{P_t \, (mw)} \right) P_r \, (mw) \; r^2 \tag{10}$$

$$Z = 3.77 \times 10^5 \left(\frac{8.06 \times 10^4 \, L}{P_t \, (mw)} \right) P_r \, (mw) \; r^2 \tag{11}$$

5.3 MEASURED PARAMETERS

In order to relate the radar return to the measured parameters of attenuation (δ) and rain rate (R) an empirical relationship was developed that related Z to R. It has been found that when the R-Z data points for a given experiment are plotted a considerable amount of scatter of points about a best fit line is observed. This indicates that for a given Z there may exist a number of R values. One of the major factors contributing to this spread is the variablity of rain drop distributions since it is possible for several distributions to produce a particular value of Z.

One of the methods that is usually employed to reduce the R-Z scatter is to define the R-Z expressions for various rain types. Typical rain type values that are employed (as developed by Joss[6]) are:

Drizzle	$Z = 140R^{1.5}$	(12)
Widespread Rain	$Z = 250R^{1.5}$	(13)
Thunderstorms	$Z = 500R^{1.5}$	(14)

As shown, the rain type constant, K, can vary from 140 to 500. The increase in K causes Z to increase for a given R. It could be concluded that a higher percentage of large drop sizes exist for thunderstorms than for widespread rain. Because $Z \sim D^6$ an increase in Z is realized.

If the drop size distribution is specified, the value of Z can be computed from the expression,

$$Z = \int_0^\infty N_D D^6 \, dD \tag{15}$$

For example, if the Marshall-Palmer distribution is assumed

$$N_D = N_o e^{-\Lambda D} \tag{16}$$

where

$$\Lambda = 41 R^{-0.21}$$

Λ (cm^{-1}) R (mm/Hr)

$N_o = .08 \text{ cm}^{-4}$

Combining (15) and (16)

$$Z = \frac{N_o\, 6!}{\Lambda^7} \tag{17}$$

Equation (15) reduces to

$$Z\left(\frac{mm^6}{m^3}\right) = 296\, R^{1.47} \tag{18}$$

5.4 RAIN RATE AND ATTENUATION PREDICTION

Rain rate and attenuation prediction utilizing the radar return can be realized from equations (9) and (11) and depending on the rain type constant K, (12), (13) or (14). For rain rate,

8.75 GHz

$$R^{1.5} = \frac{5.22 \times 10^3}{K} \overbrace{\left(\frac{5 \times 10^5 L}{P_t}\right)}^{C_8} P_r r^2 \qquad (19)$$

3 GHz

$$R^{1.5} = \frac{3.77 \times 10^5}{K} \overbrace{\left(\frac{8.06 \times 10^4 L}{P_t}\right)}^{C_3} P_r r^2 \qquad (20)$$

The above equations were employed in computing the rain rate for the first useable range bin that corresponds to the second rain bucket. The results are shown for 20 second averages in Figures 5-1 and 5-2. The radar constant was computed from the measured values listed in Section 5.2. For this run, a $200\ R^{1.6}$ relationship was employed. As shown, the radar computed rain rate over predicted the measured rain rate especially for the 3 GHz radar. Better correspondence can be obtained by decreasing the radar constant and/or increasing the rain type constant K. For the levels of the measured rain rate, a maximum value of 200 is reasonable. Therefore, on the basis of a least mean square fit of the measured and radar computed rain rates, the C_8 value should be decreased by a factor of 4.2 dB and the C_3 value by a factor of 8.1 dB.

For attenuation prediction, the following expressions are developed:

$$Z = KR^c$$

Attenuation rate (AR) in each 100 meter range bin = $a\ R^b$ dB/Km

Eliminating R

$$(AR) = a\left(\frac{1}{K}\right)^{b/c} Z^{b/c} \qquad (21)$$

Total attenuation δ over all useable range bins r

$$\delta\,(dB) = a\left(\frac{1}{K}\right)^{b/c} (.1) \sum_{i=1} Z_i^{b/c} \qquad (22)$$

For the frequency of interest, 11. 7 GHz

$$a = .0168 \quad b = 1.25 \quad \text{and} \quad c = 1.5 \tag{23}$$

$$\delta(\text{dB}) = .00168 \left(\frac{1}{K}\right)^{.833} \sum_{i=1}^{r} Z_i^{.833}$$

On day 95, 1977 very heavy precipitation was measured. Minutely mean time plots of δ and the integrated radar reflectivity for this storm event are shown in Figure 5-3. Peak secondly values of δ of 25 dB was measured before the receiver lost lock. As shown, good correlation is obtained between the minutely mean integrated η and δ values. Peaks in the η plot show the existence of signal attenuation (δ) due to rain. The magnitude of the η peaks are not directly proportional to the attenuation. However, the increase in η at the very high δ values shows that this parameter can be employed for indicating attenuation at these high levels.

Utilizing equation (22) with a c of 1.6 and a K of 200 the predicted δ values were computed as shown in Figure 5-4 with the corresponding measured δ values. The radar predicted values of δ were computed utilizing the original radar constant computed from the listed radar parameters. As shown reasonable correlation is obtained at the low measured values of δ but a gross over-prediction resulted at the high values of δ. An opposite result was obtained when the radar constant of the rain rate calibration method was employed. In this case a predicted δ of only 18 dB was obtained. It appears that in order to obtain realistic results from the radar prediction technique, a method must be devised so that good correlation is obtained at the low measurable values of δ so that the radar predicted high values of δ can be accepted as a reasonable estimate of the actual value of δ. In order to realize this end, the method must take into account both the change in G^2 and the rain type constant K as the rain cells of varying intensity moves through the elevated beam. For example, if at the deepest part of the fade a K value of 350 was employed, the predicted δ value would decrease to 45.2 dB which is a more resonable number. Also the use of a single rain bucket as a calibrating source for the radar constant does not appear to produce reasonable results when this constant is employed for predicting attenuation within the elevated beam. Since only one range bin (100 meters long) within the elevated beam is being sampled, this signal is not indicative of what is happening in the main portion of the beam. Another method of calibration which employs parameters that are a measure of the total phenomenon occurring in the beam and also takes into account changes in the weather constant should be developed.

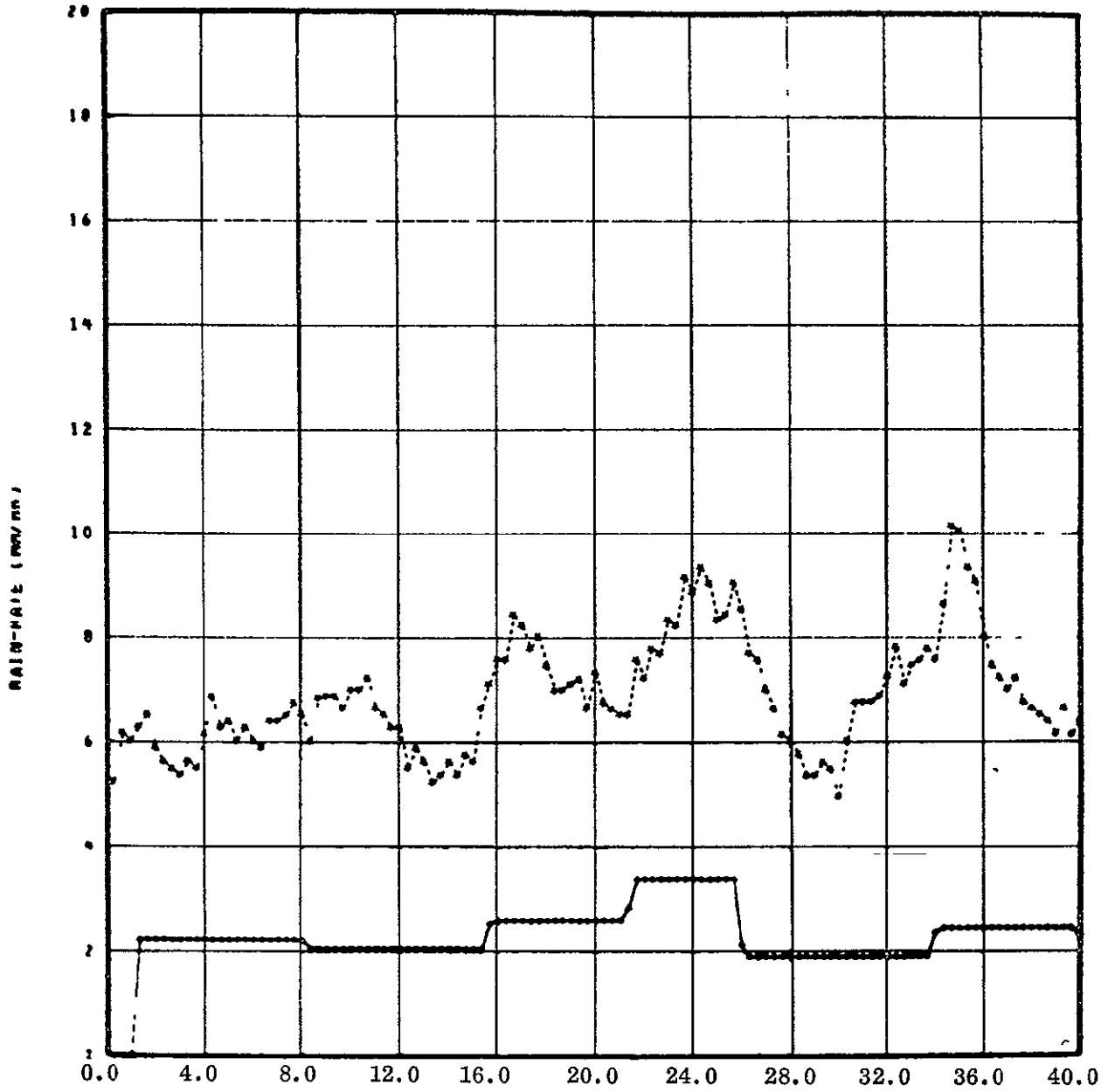

Figure 5-1. Measured and Computed Rain Rate Versus Time

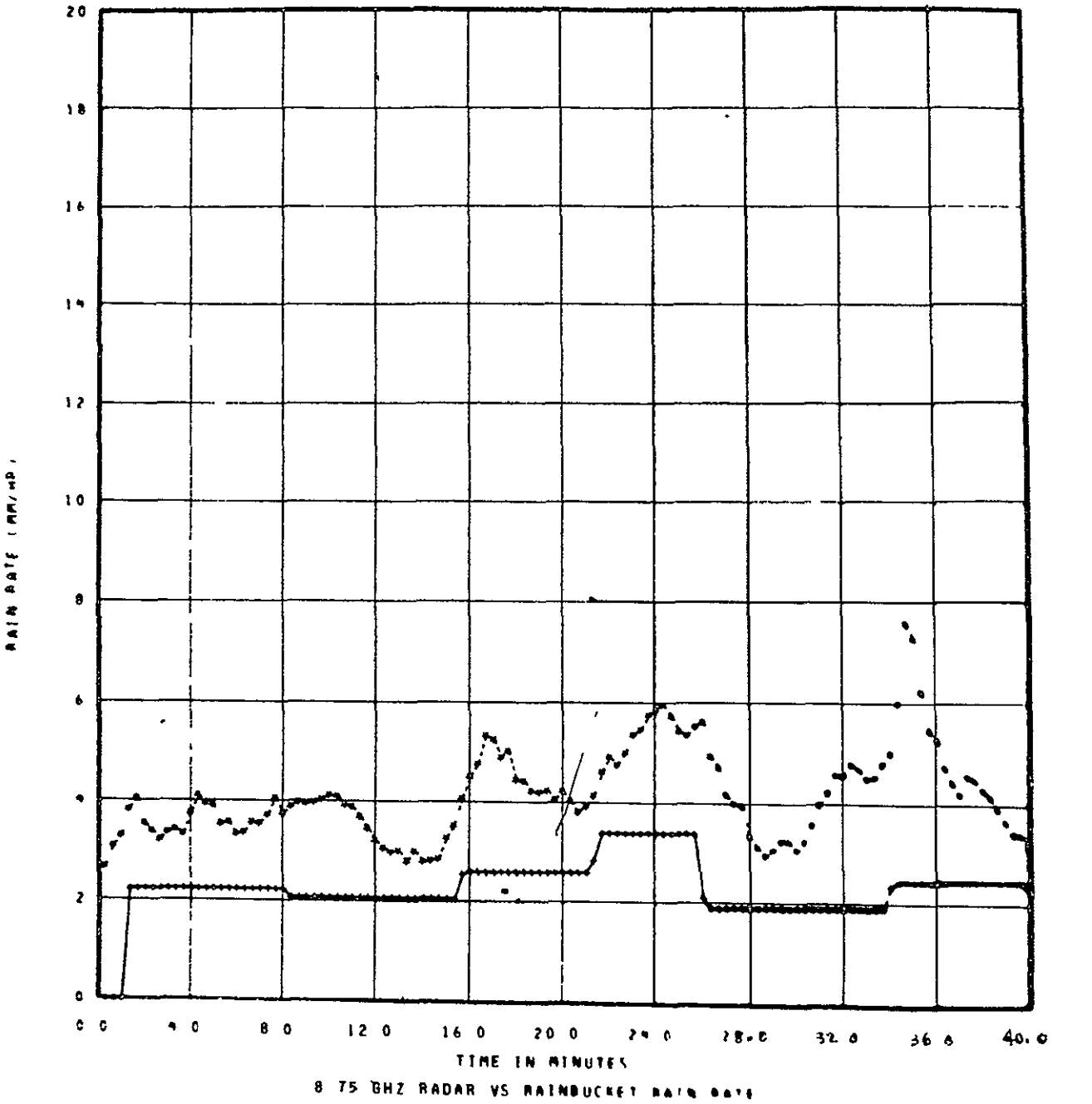

START TIME STOP TIME

YEAR	= 1976	YEAR	= 1976
DAY	= 258	DAY	= 258
GMT	= 1833	GMT	= 2000

80 SECS AVGD = 20
* RANGE BIN 1
* RAIN BUCKET 2

CONT RAIN(200)

76-4039A-47

Figure 5-2. Measured and Computed Rain Rate Versus Time

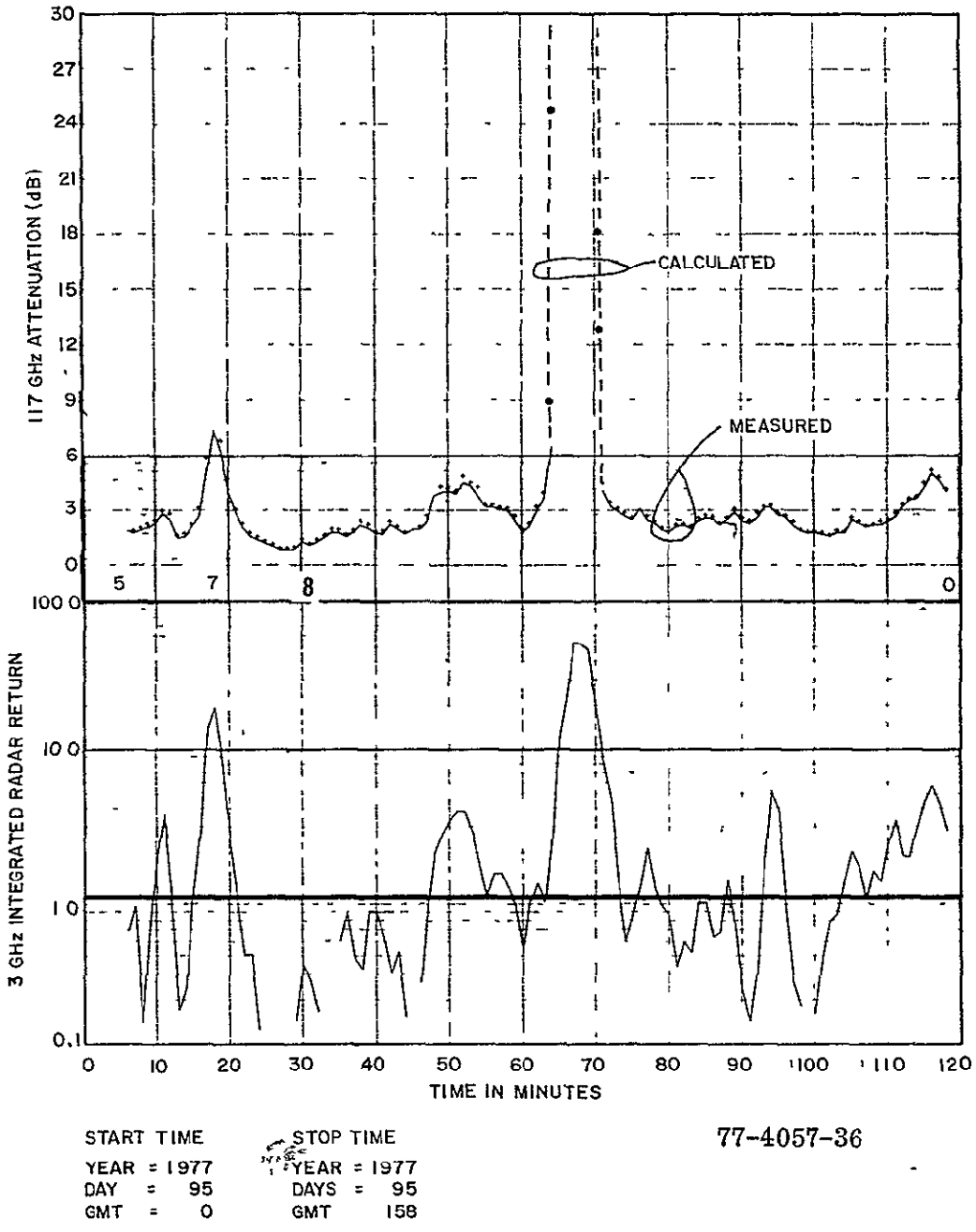

Figure 5-3. Attenuation and Radar Reflectivity, Rosman, N.C., Day 95, 1977

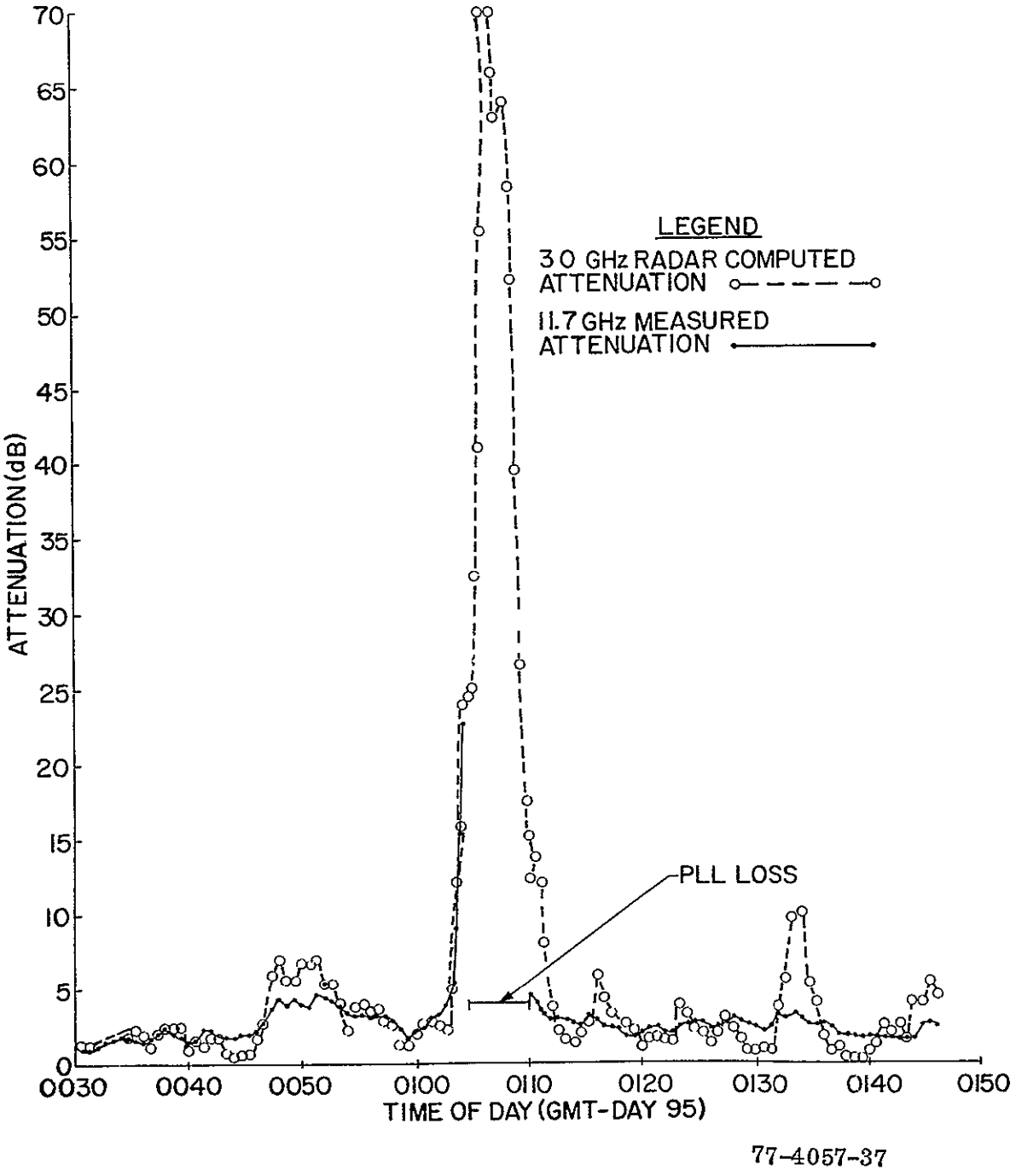

Figure 5-4. Radar Computed Attenuation, Rosman, N.C., April 4, 1977

5.5 RADAR RATIO CONCEPT

Since the radar and rain type constants vary as a function of time during the precipitation period, some measure of this variation for a particular storm must be obtained. Therefore, it was decided to alter equation (23) so that these two constants can be expressed as a ratio of radar constant to weather type constant. In utilizing equations (9) and (11) it can be shown,

8.75 GHz

$$\delta(\mathrm{dB}) = 2.1\left(\frac{C_8}{K}\right)^{.833} \sum_{i=1}^{255} (P_r r^2)^{.833} \tag{24}$$

3 GHz

$$\delta(\mathrm{dB}) = 74.2\left(\frac{C_3}{K}\right)^{.833} \sum_{i=1}^{255} (P_r r^2)^{.833} \tag{25}$$

Since δ , P_r and r can be measured for a test run, the ratio can be computed as a function of δ . Similarly, the ratio can be expressed as a function of rain rate,

$$\frac{C_8}{K} = \frac{1.91 \times 10^{-4} R^{1.5}}{P_r r^2} \tag{26}$$

$$\frac{C_3}{K} = \frac{2.65 \times 10^{-6} R^{1.5}}{P_r r^2} \tag{27}$$

It is reasoned that the radar ratio will vary as a function of the rain type. For light uniform rains, the value of the C parameter should decrease since G^2 is inversely proportional to the C_3 and C_8 parameters. This follows because the radar return from light rains should only exceed the threshold value within the regions where the peak antenna gain is located. The rain type constant K should also decrease for light rains as shown in equations (12) and (13). On the other hand for heavy rains which are heterogeneous in nature the G^2 factor should tend to decrease thus causing C to increase while the K factor will increase. It is hoped that the above trends will keep the radar ratio uniform over a range of varying precipitation conditions.

From equation (20),

$$C_3 = \frac{8.06 \times 10^4 \, L}{P_t}$$

For L = 4 (6 dB) P_{AVE} = 17 dBm P_t = 75178 MW.

$C_3 = 4.29$ For a K of 200

$$\frac{C_3}{K} = .02 \text{ (NOMINAL)}$$

For measured attenuation (δ) values obtained from the test run on day 95, a 30 second mean plot of C_3/K vs δ is shown in Figure 5-5. The ratio parameter (20 second mean) as a function of rain rate is plotted in Figure 5-6. In the latter figure the plots tends to approach a limiting value of about .005 as the rain rate increases past about 10 MM/Hr. A trend of decreasing ratio values as δ increases is shown in Figure 5-5. Unfortunately due to the limited sample size, the ratio values for the 30 second average attenuation values past 5 dB is limited. However, it appears that the ratio value should be below 0.1 and above about .003 for δ > 5 dB. A trend of increasing ratio values as δ decreases is mainly due to the threshold levels set on each range bin. This will be discussed later. As δ decreases (equation (25)), $P_r r^2$ factor will also decrease but because of the above level a larger decrease in the number of useable range bins could occur thus causing an increase in the ratio factor in order to obtain correspondence with δ .

A large spread in the ratio value for the case of low rain rates is shown in Figure 5-7. For rains rates lower than 5 MM/Hr the time between bucket tips is greater than 3 minutes. Since 20 second average values are plotted a relatively large fluctuations in the P_r factor of equation (27) can occur over the above time interval thus contributing to the large spread. For low rain rate values, an averaging time greater than 20 second is required before a realistic trend in the ratio parameter becomes obvious. It may be more reasonable to employ a variable averaging time for the radar return equal to the time between bucket tips. In this way a better comparison between measured rain rate and radar computed rain rate and the ratio factor can be obtained.

As shown in equation (25) the predicted value of δ is a sensitive function of the ratio parameter C_3/K. For example, decreasing the parameter by a factor 2 results in a δ reduction of 0.56. The peak δ computed in Figure 5-4 of 70 dB was for a ratio value of .02. If this ratio is reduced to .01 the resulting prediction is 39.2 dB. Of course, it could be argued that if the system margin is less than 39 dB it doesn't matter if the resulting δ is 39.2 or 70 dB. This is true from a magnitude standpoint but not from the standpoint of a time duration since a large fade should stay below the system margin for a longer period of time.

Figure 5-8 shows time plots of 20 second averages of the radar computed and measured attenuation values for the day 95 test run. As shown, the main receiver broke lock at about 178 minutes into the run. The C/K values was held constant at .005. The peak predicted value of δ was 30 dB during a time period in which the measured wind speed was on the order of 35 MPH. In the time interval in which receiver lock was broken a large amount of turbulence existed within the elevated beam. The last measured 20 second average δ value that was recorded before lock was broken was 18.2 dB. It appears that the peak 20 second δ value was probably on the order of 35 dB. In this case the most meaningful C/K value to employ would be .006. A 5 dB change in the value is realized by a 0.001 change in the ratio. This sensitive dependence of δ on the C/K factor could negate its use for prediction if a large spread in the ratio value is obtained for δ values greater than 5 dB. A clear indication of this spread is shown in Figure 5-9 where the ratio factor is plotted against δ while utilizing a linear scale. Values of the ratio less than the computed nominal value of 0.02 is indicated on this linear plot. If the antenna gain factor G^2 is assumed to be constant and the weather constant K varies from 140 to 500, the range of variation for the ratio factor is .03 to .008. Since the plots show values of C/K less than .008, the assumption of a constant G^2 factor isn't justified as previously stated.

As previously stated the two factors that mainly cause the discrepancy between the measured and predicted attenuation is the variation in the G^2 and rain type constant. The errors in G^2 result from the rain return obtained from the main sidelobes which are about -20 dB down from the peak of the main lobe. It is reasonable to assume that the area of the sidelobes, A_s, is about 5 times the area of the main lobe A_m or $A_s = 5 A_m$. Therefore, if a uniform precipitation pattern exists, then the power returned from the sidelobes is 5% of the power returned from the main lobe or approximately 5% of the total received power. Clearly in the case of uniform rain, a

small error exists in assuming the rain return only applies to the peak of the beam. However, in the case of a non-uniform rain where an intense cell is located in the sidelobe, a serious error in estimating the rain rate or attenuation can occur. For example, suppose an intense cell fills about 20% of the sidelobe area A_s then the corresponding P_r would be proportional to $20/100 \times 5\, Am \sum \sigma_i$. To obtain the same power in the main lobe,[5]

$$\overbrace{100\, Am\left(f\sum\sigma_i\right)}^{\text{MAIN LOBE}} = \overbrace{\frac{20}{100} \times 5\, Am\left(\sum\sigma_i\right)}^{\text{SIDE LOBE}} = Am\sum\sigma_i$$

or f = 1/100 which states that the apparent scattering cross - section in the mainlobe f, is .01 of that actually in 20% of the sidelobe. If

$$\sigma_i \sim (\text{Rain Rate})^{1.5}$$

Then assuming the precipitation is at the peak of the beam the apparent rate of rainfall is only 4.6% of the actual rate. Hence, for heterogeneous precipitation patterns serious errors can arise in predicting either rain rate or attenuation.

It has been stated that the drastic increase in the C/K ratio as note in Figure 5-9 for $\delta < 3$ dB is mainly due to the threshold levels set on the various range bins. A locus of these threshold values is shown in Figure 5-10 for the 3 GHz radar. From reference (1) the relation between rain rate, R and attenuation, δ, was obtained

$$\delta = .2476R^{.8583} \text{ and } L = 14.74R^{-.3917}$$

Therefore, for a given δ an equivalent R can be computed which in turn correspond to a given threshold range R_t obtained from Figure 5-10. The results of the computations are shown in Table IV.

TABLE IV

RANGE THRESHOLD EFFECTS

Attn (dB)	Equivalent Rain Rate	$Z = 200R^{1.6}$ dBZ	Threshold Path Length (Km)	Required Apparent Path Length (Km)
1	5.1	34.3	1.8	7.8
2	11.4	39.9	3.4	5.68
3	18.3	43.2	5.0	4.72
4	25.6	45.5	5.8	4.14
5	33	47.3	6.8	3.75

The path length required to obtain a δ for a given R was computed from the expression $L = 14.74\ R^{-.3917}$ and listed in the above table. For example, for a δ of 1 dB the required path length is 7.8 Km, however, the threshold path length restricts the returns to 1.8 Km. Therefore, in order to obtain correspondence with the measured δ, the C/K factor must be drastically increased. It is noticed that a δ of 3 dB the threshold range and the apparent path length are almost equal. Therefore, above a δ of 3 dB the range bin threshold values do not effect the value of C/K. It is noticed in Figure 5-9 that at a δ of about 3 dB the C/K values tends to flatten out. A better example is shown in Figure 5-11. In this test run the value of C/K abruptly increases at $\delta \leq 3$ dB and also tends to converge at higher values of δ. Therefore, for the present threshold characteristics of the radar receiver it is not possible to obtain a realistic measure of C/K at δ values less than 3 dB.

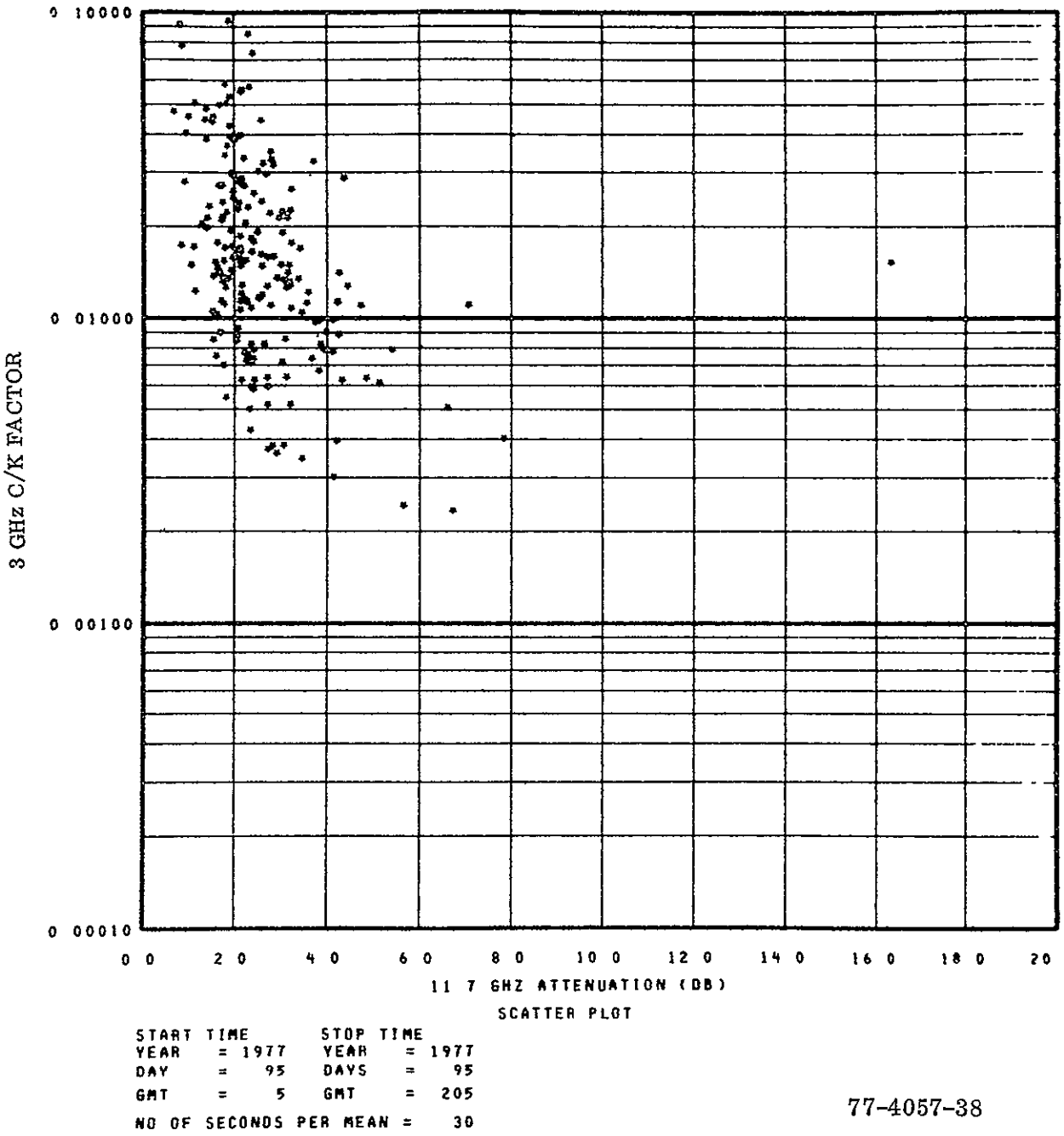

Figure 5-5. 3 GHz Radar Ratio Versus 11.7 GHz Attenuation

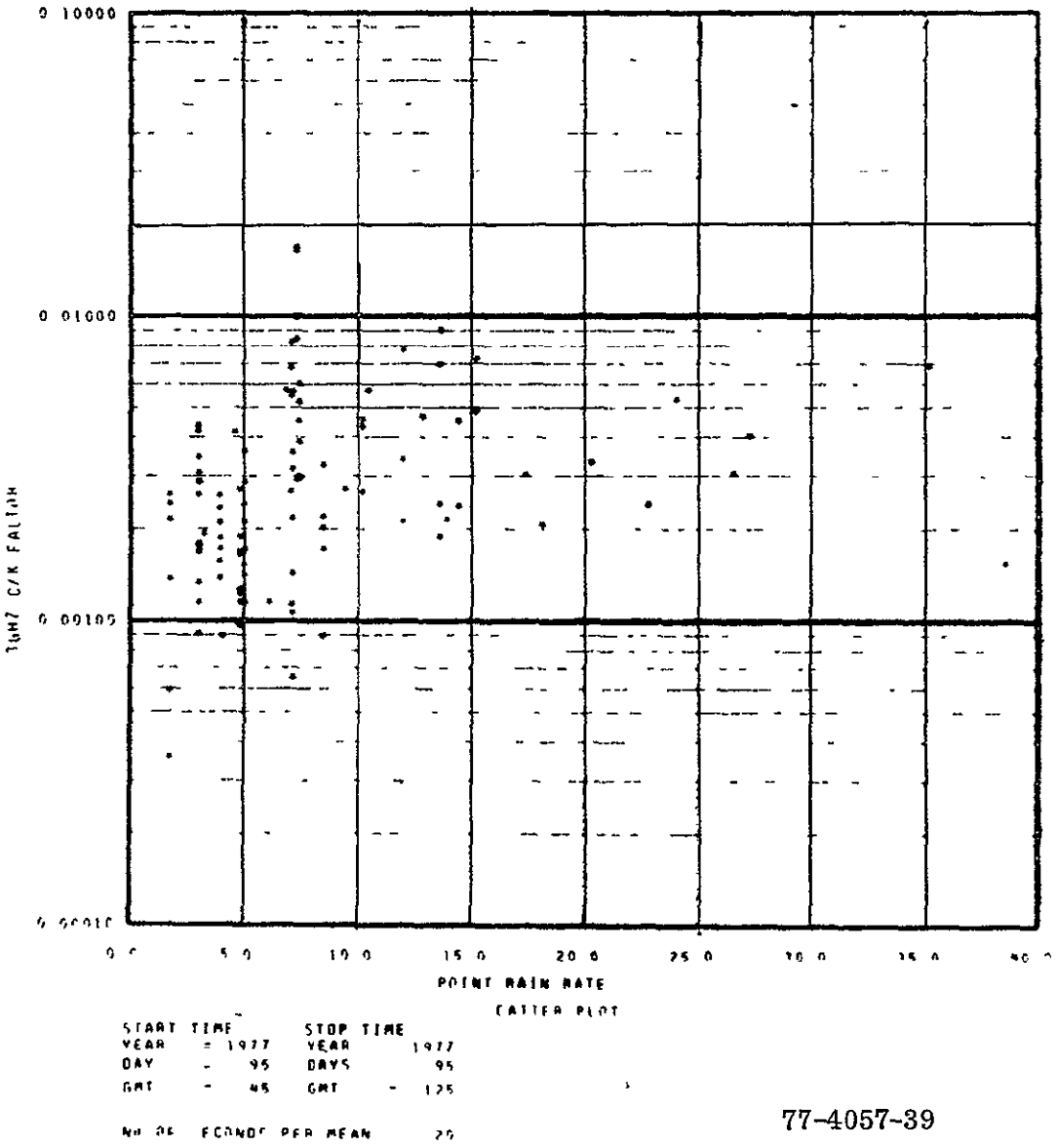

Figure 5-6. 3 GHz Radar Ratio Versus Rain Rate

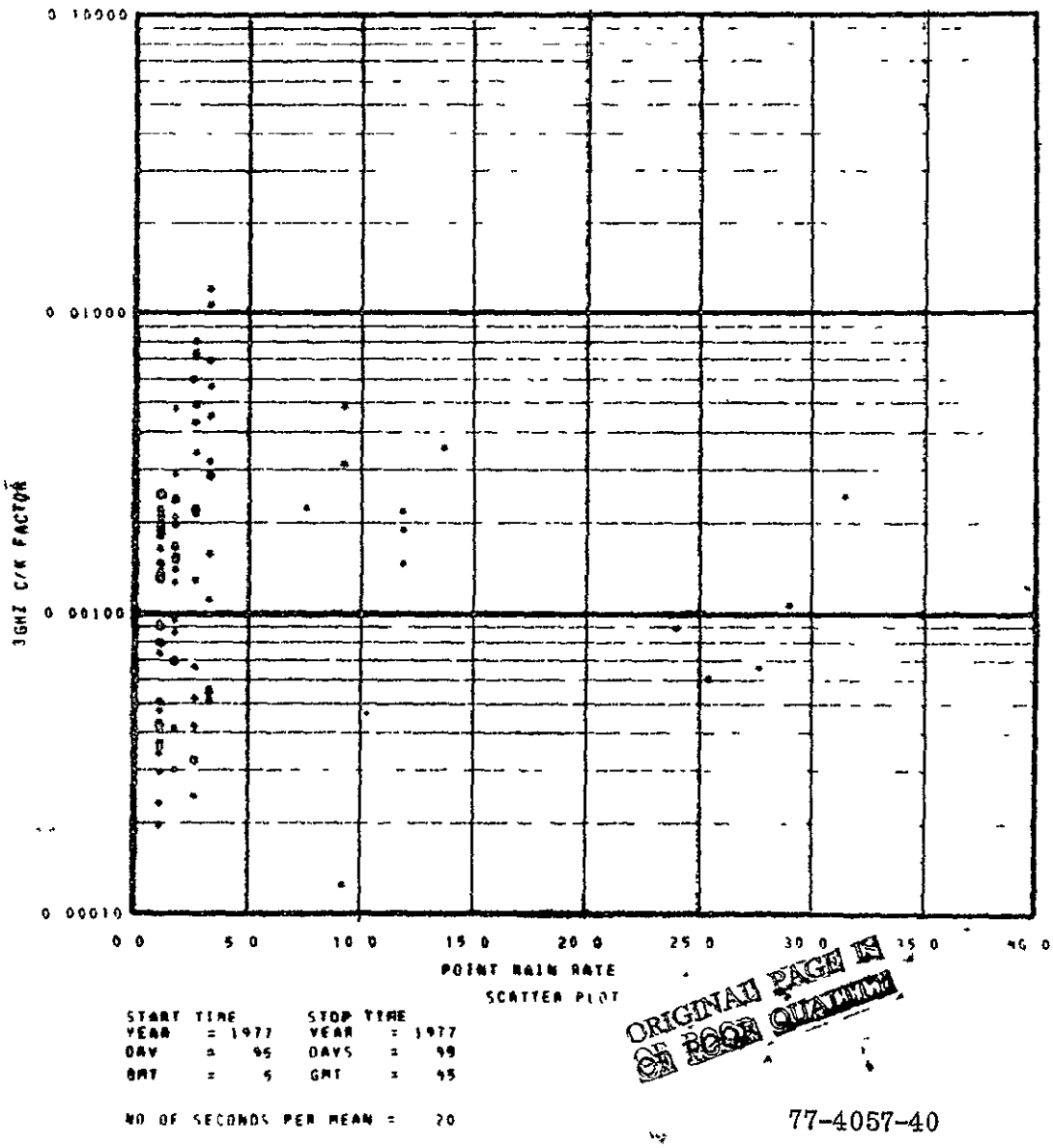

Figure 5-7. 3 GHz Radar Ratio Versus Rain Rate

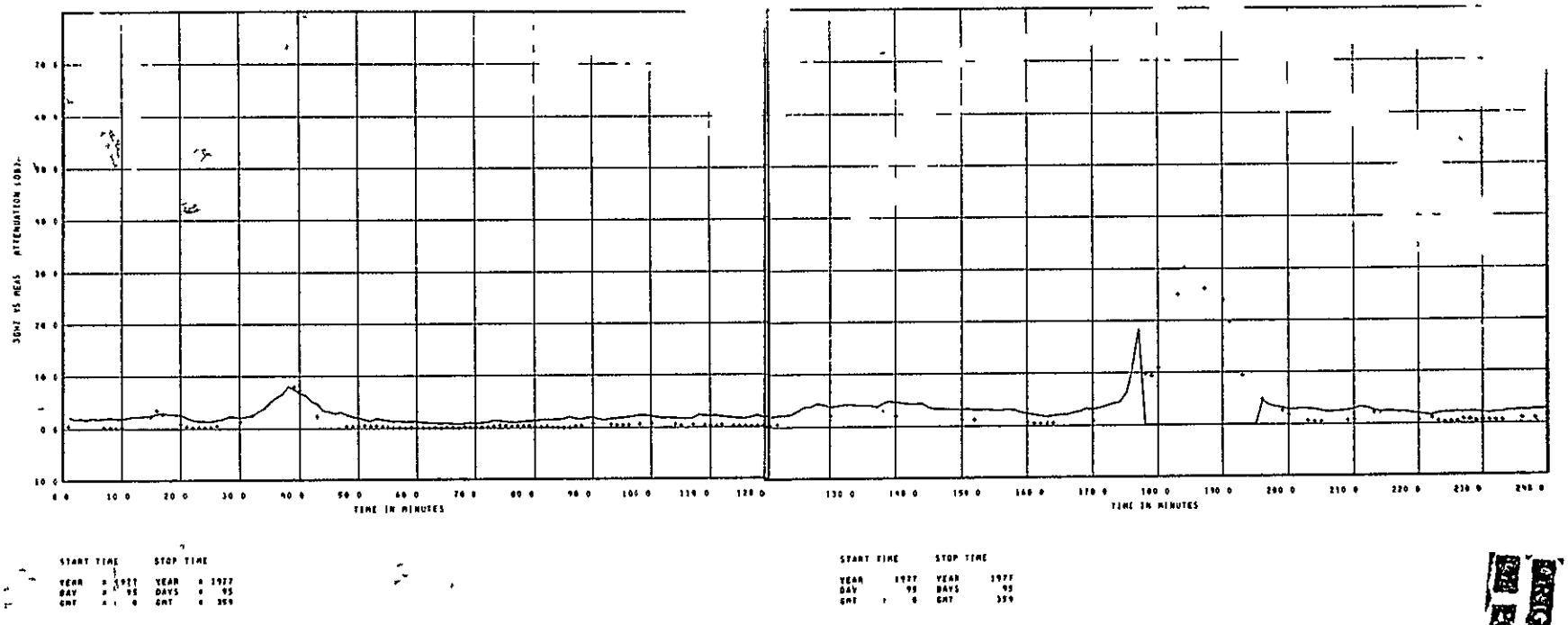

Figure 5-8. Measured and Computed Attenuation Versus Time

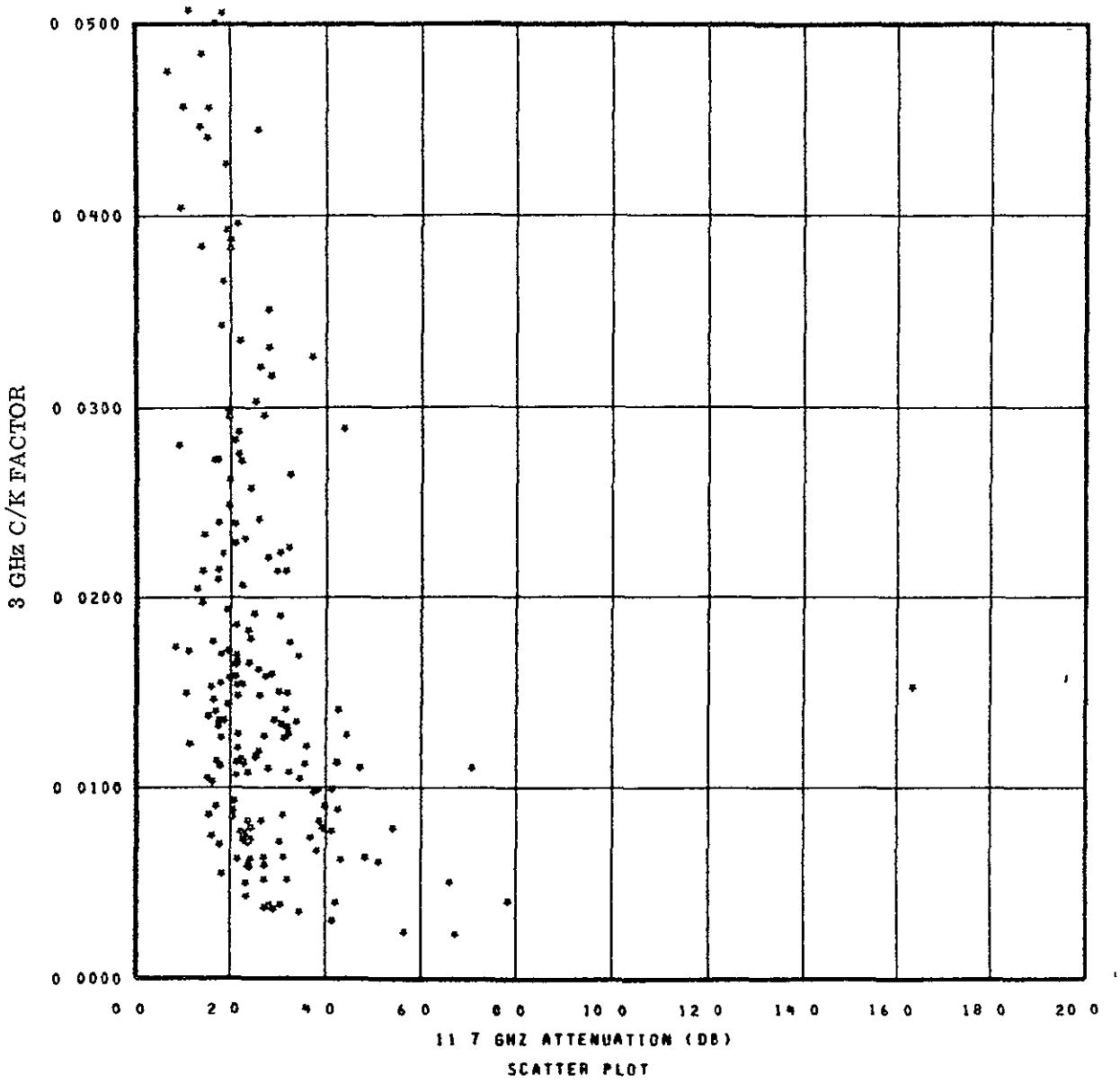

Figure 5-9. 3 GHz Radar Ratio Versus Attenuation (Linear Scale)

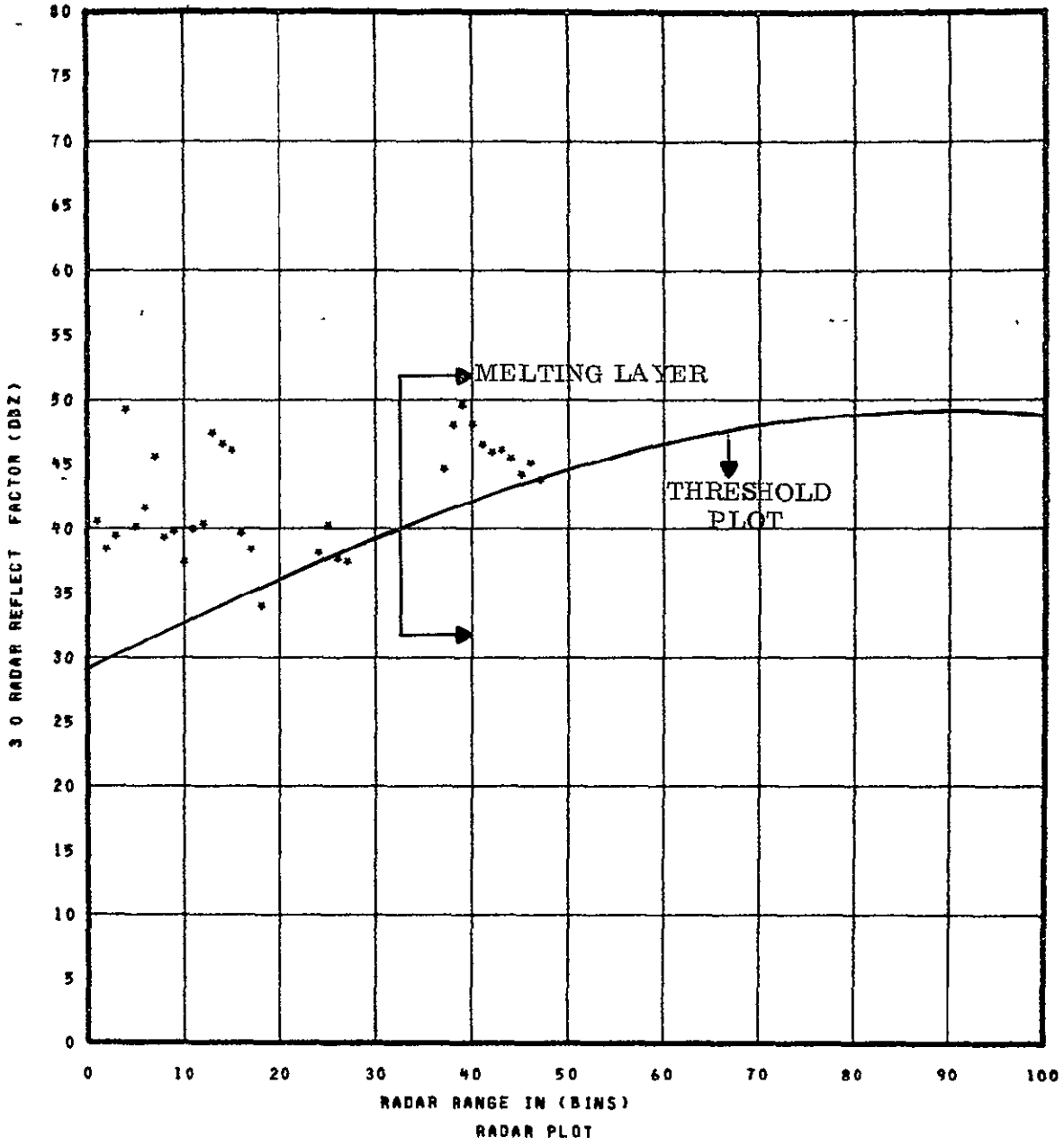

START TIME STOP TIME

YEAR	= 74	YEAR	= 74
DAY	= 171	DAY	= 171
GMT	= 1905	GMT	= 1920

TIME OF PLOT

GMT = 1907
SECS = 43

75-0005-VA-76

Figure 5-10. 3 GHz Radar Reflectivity Factor (dBZ) Versus Range

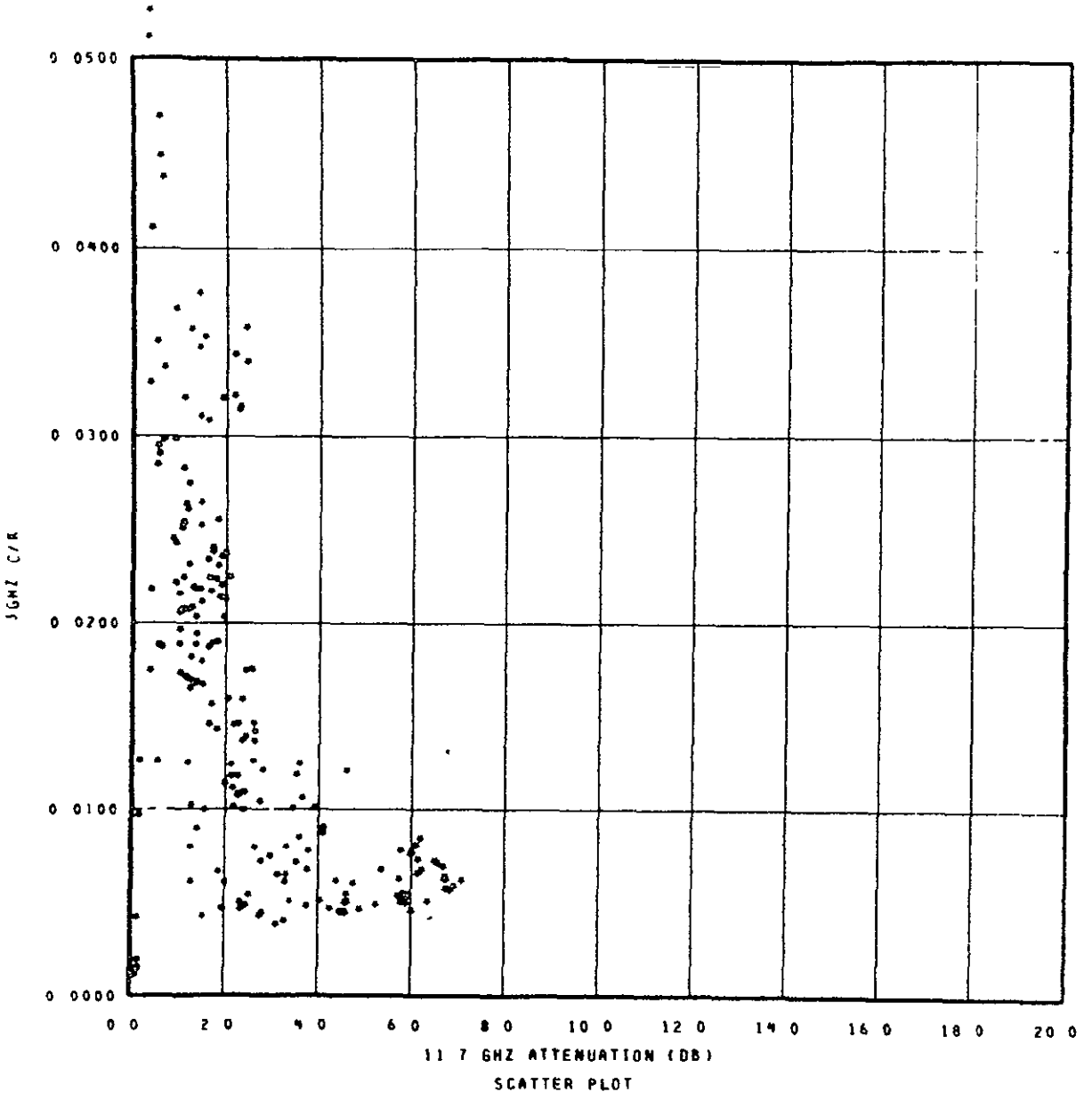

77-4057-43

START TIME		STOP TIME	
YEAR	= 1977	YEAR	= 1977
DAY	= 89	DAYS	= 89
GMT	= 500	GMT	= 700
NO OF SECONDS PER MEAN	= 30		

Figure 5-11. Radar Ratio Versus 11.7 GHz Attenuation

SECTION 6
SUMMARY AND CONCLUSIONS

Rain rate and attenuation data was measured over a 12 month period starting in June of 1976 to May of 1977 at the NASA Greenbelt station. Attenuation (δ) values exceeding 30 dB were measured at the 11.7 GHz frequency. Rain rate values exceeding 180 MM/Hr were also measured. These peak values resulted from a violent strom that occurred on May 6, 1977. A total of 14,647 minutes of δ data was recorded during the above time period. Also 11,587 minutes of rain rate data was also processed. The worst month statistics for 1976 corresponded in August and for 1977, June.

For the NASA Rosman station, the statistics are developed from the 4 second mean values of δ, near bucket rain rate and ground average rain rate. Data was processed over a 13 month period from June 1, 1976 to June 30, 1977. Peak δ values exceeding 20 dB were measured. Also 4 secondly average rain rate values exceeding 80 MM/Hr were measured. A total of 4148 minutes of δ data was obtained and 6521 minutes (GA), 5012 minutes (NB) rain rate data was measured. The only significant worst month statistics that was obtained during the above period was in June of 1977. A summary of the δ and rain rate statistics are shown below.

Utilizing the total precipitation that was measured by the weather bureau as a standard in both the Rosman and Greenbelt area, it was determined that the Greenbelt station measured 96.7% of the total area precipitation and Rosman measured only 22.4%. The large divergence in the Rosman data is due to the fact that automated (computer) rain rate measurements were only taken over an 8 hour daily working period between June 1, 1976 to March of 1977. From March until July of 1977, 24 hour coverage was obtained through the use of an automated initiation program that started the rain rate and attenuation measurements after a number of bucket tips were detected.

In addition to the δ measurements at the Rosman station measurements of point rain rate, ground average rain rate and backscatter measurements from a multi-frequency radar are performed concurrently. One of the objectives of the experiment is to determine functional relationships between these meteorological parameters and the 11.7 GHz attenuation. The difficulties of obtaining these relationships are made evident by determining the non-heterogenous nature of the rain environment that

SUMMARY OF 11,7 GHz ATTENUATION STATISTICS

	PERCENTAGE VALUES		
	0.1	0.01%	0.005%
Rosman (4 Sec. Mean) Yearly = 4148 Minutes Less than 22.4% of Precipitation*	2.2 dB	8 dB	11.2 dB
Worst Month June 1977 689 Minutes	6.4 dB	20.2 dB	21.2 dB
Greenbelt (Minutely Mean) Yearly = 14647 Minutes Corresponds to 96.7% of Precipitation*	2.1 dB	10 dB	15 dB
Worst Month August 1976 351 Minutes	5 dB	15.6 dB	19.4 dB
Worst Month May 1977 227 Minutes	6.5 dB	>30 dB	

*Corresponds To Total Area Precipitation.

SUMMARY OF RAIN RATE STATISTICS

	PERCENTAGE VALUES					
	0.1%		0.01%		0.005%	
	NB (MM/HR)	GA (MM/HR)	NB (MM/HR)	GA (MM/HR)	NB (MM/HR)	GA (MM/HR)
Rosman (4 Sec. Mean) Yearly NB = 5012 GA = 6521 Minutes 22.4% of total precipitation*	11	12	49	41	65	54
Worst Month June 1977 NB = 414 Minutes GA = 934 Minutes	22	32	75	75	82	82
Greenbelt (Minutely Mean) Yearly 11587 Minutes 96.7% of total precipitation*	21		82		147	
Worst Month August 1976 597 Minutes	20		112.5		140	
Worst Month May 1977 178 Minutes	10		110			

*Corresponds To Total Area Precipitation.

produces the high values of δ, near bucket (NB) rain rate and ground average (GA) rain rate. The scatter plots employed for this study are as follows:

(a) 3 GHz Integrated radar return versus δ (11.7 GHz).
(b) 8.75 GHz Integrated radar return versus δ.
(c) 3 GHz Integrated radar return versus NB.
(d) 8.75 GHz Integrated radar return versus NB.
(e) NB versus 11.7 GHz attenuation.
(f) GA versus 11.7 GHz attenuation.
(g) NB versus GA.

By utilizing the above plots for a storm that occurred on day 181 it was possible to determine that the main precipitation cell that caused the attenuation was located in close proximity to the near bucket area. Also, it was shown that since the elevated radio beam and the radar beam are not exactly coincident, the main rain cell was not present in both beams at the same time. It was concluded that a realistic functional relationship between δ and the meteorological parameters can only be obtained from sets of long term data compiled over a long period of time and encompassing different types and degrees of precipitation.

CTS video channel performance tests were performed at Greenbelt during the yearly test period. The tests performed were as follows:

(a) Satellite transponder linearity.
(b) Two-carrier intermodulation.
(c) Two-carrier compression.
(d) C/N, video TT/N.
(e) Audio TT/N.
(f) Baseband frequency response.

The results generally show that very satisfactory video and audio performance can be obtained from the CTS video channel.

The results of a continuing study of determining path length (L) as a function of rain rate for an elevated radio path are presented. Long term rain rate and δ pair values are employed in determining this functional relationship. From the data obtained, to data, it could be concluded that prediction of L at high values of rain rate should be possible.

However, at low values the prediction process could be a complicated function of frequency, elevation angle and locales from the standpoint of characteristic weather types. Also the results of the data show that the L limit at high values of rain rate tends to approach a value of about 4 Km. For low values of rain rate (R less than about 10 MM/Hr) the corresponding attenuation values would be in the range of about 1 dB to 4 dB. At the high values of rain rate (R 100 MM/Hr) where a constant value path length is obtained, attenaution values on the order of 20 dB would be obtained.

In order to obtain a more efficient means of predicting attenuation from the radar backscatter signals the radar ratio concept was developed. This ratio is equal to the radar constant over the weather type constant. It was reasoned that the above ratio should stay essentially constant over a wide range of δ values. From the limited data obtained to data a limiting value seems to occur at $\delta > 3$dB. Below 3 dB a drastic increase in the ratio was obtained. However, it was shown that this increase is mainly due to the range bin threshold values set by the noise characteristics of the radar receiver. For the present radar, the prediction process would only apply to δ values greater than 3 dB.

Rain rate and attenuation measurements are being continued at the Greenbelt station. The above measurements plus the measurement of radar backscatter will be taken at the Rosman station up to the end of October 1977. With the past and future measurements of attenuation and rain rate more representative long term statistics will be obtained as well as more accurate seasonal and worst month statistics. The elevated path length analysis will be continued with the inclusion of the radar data to obtain a direct measure of the path length. By utilizing this measure of path length and correlating this value with the actual measurement of rain rate, a functional relationship can be obtained between the radar measured path length and measured rain rate. This functional relationship will be compared with the function obtained from the attenuation measurements.

A study of the radar return for predicting attenuation by utilizing the radar ratio concept will continue. It is hoped that a meaningful amount of attenuation data greater than 10 dB will be obtained so that the usefullness of the radar technique can be determined.

A technique has been developed to predict the attenuation cumulative distribution from a measured rain rate cumulative distribution and a best fit estimate that relates attenuation to rain rate. In utilizing this technique reasonable estimates of the actual measured attenuation distribution has been obtained.

REFERENCES

1. CTS Communications Link Characterization Experiment, Technical Data Report Volume 2, April 1977, National Aeronautics and Space Administration, Goddard Space Flight Center, Greenbelt, Maryland.

2. Gunn, L.L. and East, T.W.R. "The Microwave Properties of Precipitation Particles, Journal of the Royal Meteorological Society, Vol. 80, 1954.

3. Laws, J.O. and Parsons, T.A. "The Relation of Raindrop Size to Intensity", Transactions American Geophysical Union Hydrologue, 1943.

4. Ippolito, L.J. "Summary and Evaluation of Results from the ATS Millimeter Wave Experiment", May 1972, NASA X-75-1-72-208, Goddard Space Flight Center, Greenbelt, Maryland.

5. Harrold, T.W., Estimation of Rainfall Using Radar - A Critical Review, Meteorological Office, Scientific Paper No. 21, London, 1965.

6. Joss J. Thomas, J.C. Waldvogel A (1968) "The Variations of Raindrop Size Distributions at Lorcano", Proceedings of the International Conference on Cloud Physics, August 26-30, Toronto Canada, pgs., 369-372.

7. ATS-6 Millimeter Wave Propagation Experiment - Final Data Analysis Report - National Aeronautics and Space Administration, Goddard Space Flight Center, Greenbelt, Maryland, September, 1975.

APPENDIX A

Power Curve Best Fit Coefficients For Medhurst Calculated Attenuation Factors (Laws & Parsons Drop Size Distribution)

Consider Table V of Medhurst (1965). Assume

$$A\ (dB/km) = a\ R^b,\ R \text{ in } \frac{mm}{hr}$$

Then, using power curve regression fit (HP65, STAT 1-24A), the a & b coefficients are found. r^2, the coefficient of determination, is also listed.

Freq (GHz)	λ(cm)	a	b	r^2
5.45	5.5	0.0012	1.2294	
6	5	0.0018	1.2485	0.9945
7.5	4	0.0035	1.3020	0.9975
10	3	0.0094	1.2791	0.9997
15	2	0.0328	1.1710	0.9988
20	1.5	0.0687	1.1004	0.9993
30	1	0.1649	1.0353	0.9989
60	.5	0.6050	0.8554	0.9981
100	.3	0.9395	0.7886	0.9954
11	2.73	0.0159	1.25	
12	2.5	0.0168	1.25	
14	2.14	0.0265	1.19	
15.3	1.96	0.035	1.15	
31.65	0.95	.185	1.00	

APPENDIX B

$\delta = cr^d$

GREENBELT STATION NEAR BUCKET		ROSMAN NEAR BUCKET		ROSMAN GROUND AVERAGE	
δ	RR	δ	RR	δ	RR
2.25	5	3	13	3	12
3	7.5	4	22	4	18
4	11	5	28	5	23
5	17.5	6	34	6	27
7	27.5	7	42	7	32
8.5	37.5	8	46	8	35
12.5	55.3	9	52	9	40
15.5	66.3	10	56	10	42
18.5	72.5	11	61	11	45
21.5	78.	12	65	12	50
		13	70	13	52
		14	72	14	55
		15	75	15	57
		17	77	16	60
		19	78	19	65
		20	83	20	70
		21	84	21	78
		22	91	22	86
		23	92	23	89
r = .9901		.9738		.9937	
d = .7863		1.1006		1.1081	
c = .5843		.1339		.1639	